Strong Emission Line H II Galaxies in the Sloan Digital Sky Survey. I. Catalog of DR1 Objects with Oxygen Abundances from T_e Measurements

Alexei Y. Kniazev[1,2,3], Simon A. Pustilnik[2,3], Eva K. Grebel[1,4], Henry Lee[1,5], and Alexander G. Pramskij[2,3]

kniazev@mpia.de, sap@sao.ru, grebel@astro.unibas.ch, hlee@astro.umn.edu, pramsky@sao.ru

ABSTRACT

We present the first edition of the **S**DSS **H**II-galaxies with **O**xygen abundances **C**atalog (SHOC), which is a listing of strong emission-line galaxies (ELGs) from the Sloan Digital Sky Survey (SDSS). Oxygen abundances have been obtained with the classic T_e-method. We describe the method exploiting the SDSS database to construct this sample. The selection procedures are described and discussed in detail, as well as some problems encountered in the process of deriving reliable emission line parameters. The method was applied to the SDSS Data Release 1 (DR1). We present 612 SDSS emission-line galaxies (624 separate SDSS targets in total), for which the oxygen abundances 12+log(O/H) have r.m.s. uncertainties ≤ 0.20 dex. The subsample of 263 ELGs (272 separate SDSS targets) have an uncertainty ≤ 0.10 dex, while 459 ELGs (470 separate SDSS targets) have an uncertainty $\leq$0.15 dex. The catalog includes the main parameters of all selected ELGs, the intensities and equivalent widths of hydrogen and oxygen emission lines, as well as oxygen abundances with their uncertainties. The information on the presence of Wolf-Rayet blue and/or red bumps in 109 galaxies is also included. With the use of combined g, r, i SDSS images we performed

[1]Max-Planck-Institut für Astronomie, Königstuhl 17, D-69117 Heidelberg, Germany

[2]Special Astrophysical Observatory, Nizhnij Arkhyz, Karachai-Circassia, 369167, Russia

[3]Isaac Newton Institute of Chile, SAO Branch

[4]Present address: Astronomisches Institut der Universität Basel, Venusstrasse 7, CH-4102 Binningen, Switzerland.

[5]Present address: Dept. of Astronomy, Univ. of Minnesota, 116 Church St. S.E., Minneapolis, MN, 55455 USA.

visual morphological classification of all SHOC galaxies. 461 galaxies (∼75%) are classified as confident or probable blue compact galaxies (BCG/BCG?), 78 as irregular ones, 20 as low surface brightness galaxies (LSBG), 10 as obviously interacting and 43 as spiral galaxies. In creating the catalog, 30 narrow line AGN and 69 LINERs were also identified; these are also presented apart of the main catalog. We outline briefly the content of the catalog, and the prospects of its use for statistical studies of the star formation and chemical evolution issues. Some of these studies will be presented in the forthcoming paper. Finally, we show that the method presented by Kniazev et al. (2003) for calculating O^+/H^+ using intensities of the [O II] λ7320,7330 Å lines for SDSS emission-line spectra in the absence of [O II] λ3727 Å line appears to yield reliable results over a wide range of studied oxygen abundances: $7.10 < 12 + \log(O/H) < 8.5$.

Subject headings: catalogs: – galaxies: abundances – galaxies: starburst – galaxies: dwarf – stars: Wolf-Rayet

1. Introduction

The heavy element abundances of gas-rich galaxies and their gas-mass fractions are the main parameters characterizing their global evolution (e.g., Pagel 1997; Matteucci 2001). These can be related to both the global properties of galaxies (e.g., Dalcanton, Spergel, & Summers 1997; Grebel, Gallagher & Harbeck 2003) and the membership of galaxies in various elements of large-scale structure (e.g., Popescu et al. 1996; Grogin & Geller 2000; Pustilnik et al. 2002b; Vilchez & Iglesias-Páramo 2003; Lee, McCall, & Richer 2003). The knowledge of the metallicity for large homogeneously selected galaxy samples would allow us to address various issues of galaxy chemical evolution on a good statistical basis. In particular, the possible difference in the chemical evolution rate in the various types of galaxy environments can be systematically examined. Having metallicities for galaxy samples at redshifts of, e.g., $z \sim 0.3$ and in the nearby Universe, one can directly probe the chemical evolution of gas-rich galaxies over timescales of several Gyr. In addition, estimates of stellar mass from galaxy photometry and of neutral gas mass from HI measurements bring new opportunities to confront the predictions of modern chemical evolution models with the observed properties of a large sample of galaxies.

To address the question of metallicity distributions in gas-rich galaxies and to understand possible relations between metallicity and other galaxy parameters, one can use several large ELG samples such as the results of University of Michigan (UM), Tololo and Calan-Tololo (Smith, Aguirre, & Zemelman 1976; McAlpine Smith & Lewis 1977; Salzer,

McAlpine, & Boroson 1989), Case (Pesch & Sanduleak 1983; Salzer et al. 1995; Ugryumov et al. 1998), Second Byurakan Survey (SBS; Markarian, Lipovetsky, & Stepanian 1983; Izotov et al. 1993), Heidelberg Void (Popescu et al. 1996), KPNO International Spectral Survey (KISS; Salzer et al. 2000; Melbourne & Salzer 2002), Hamburg/SAO Survey for Emission-Line Galaxies (HSS-ELG; Ugryumov et al. 1999; Pustilnik et al. 1999) and Hamburg/SAO Survey for Low Metallicity Galaxies (HSS-LM; Ugryumov et al. 2003).

Of special interest for such samples are HII galaxies and their most prominent representatives – Blue Compact Galaxies (BCGs). BCGs are gas-rich objects with typical total masses lower than 10^{10} $M_{\odot}$, have low metallicities in the range $1/15 \leq$ Z/Z$_{\odot}$ $\leq 1/3$, and form stars at noticeably non-stationary rates. Previously, samples of HII galaxies with reliably known metallicities (i.e., derived with the $T_{\rm e}$ method) were obtained through high S/N spectroscopy of strong-line ELGs, selected from the surveys cited above. However, well-selected gas-rich galaxy samples with reliable metallicity determinations are still quite small. Currently, it is possible to estimate that we have no more than ∼200 galaxies selected from the different samples with measured classic $T_{\rm e}$ method oxygen abundances with an accuracy better than 0.1 dex. This is related to the weakness of the key temperature-sensitive line [O III]λ4363, used in the classic $T_{\rm e}$ method to derive oxygen abundances with r.m.s. uncertainties of 0.01–0.1 dex. As well, many galaxies from these samples often have poor photometry, and, apart from the KISS survey, selection criteria are not well-defined in terms of apparent magnitude. Nevertheless, the accumulated data on low-mass galaxies give important clues about the metallicity distribution and indicate correlations with other galaxy global parameters.

In particular, these surveys have uncovered a significant number of extremely metal-poor galaxies (XMPGs)[1] with $Z \leq 1/20\ Z_{\odot}$. Some XMPGs are similar to the well-known I Zw 18 (Searle & Sargent 1972) and SBS 0335–052 (Izotov et al. 1990), which are candidates for young galaxies in the nearby Universe. These are probably the best local analogs of young low-mass galaxies which formed at high redshifts. Despite the paucity of such galaxies their systematic study can advance significantly the understanding of the details of galaxy formation and their early evolution. Therefore, it is important to have an effective means of enlarging substantially the number of XMPGs.

Besides the great interest in understanding the details of star formation, massive-star (including Wolf-Rayet stars) evolution and their interaction with the interstellar medium at very low metallicities, there are several other important directions related to the studies of HII/BCG metallicities in general. For example, with a larger ELG sample with abundances measured by the classic $T_{\rm e}$ method we can improve the calibration of the empirical methods

[1] Another name for these galaxies is extremely metal-deficient galaxies (XMDs).

(e.g., Pagel et al. 1979; McGaugh 1991; Pilyugin 2001, 2003; Denicoló, Terlevich, & Terlevich 2002), which provide a broad picture about the range of oxygen abundances for ELGs in general.

Therefore, it is natural to look for new opportunities offered by the Sloan Digital Sky Survey (SDSS; York et al. 2000). Owing to its homogeneity, area coverage, spectral resolution, and depth, the SDSS provides an excellent means of creating a large flux-limited sample of HII galaxies with heavy element abundances derived with the classic T_e method.

The SDSS consists of an imaging survey in five photometric bands (Fukugita et al. 1996; Gunn et al. 1998; Hogg et al. 2001), as well as a follow-up spectroscopic survey of a magnitude-limited sample of galaxies (mainly field galaxies brighter than $r = 17\overset{m}{.}77$; Strauss et al. 2002) and a color-selected sample of quasars (Richards et al. 2002). An automated image-processing system detects astronomical sources and measures their photometric and astrometric properties (Lupton et al. 2001; Stoughton et al. 2002; Smith et al. 2002; Pier et al. 2003) and identifies candidate galaxies and quasars for multi-fibre spectroscopy. The samples of galaxy and quasar candidates include a substantial number of emission-line galaxies. The spectra are automatically reduced and wavelength- and flux-calibrated (Stoughton et al. 2002; Abazajian et al. 2003).

The SDSS spectral data have already been used in a number of galaxy studies (e.g., Bernardi 2003; Eisenstein et al. 2003; Goto et al. 2003; Kauffmann et al. 2003; Kniazev et al. 2003; Stasinska & Izotov 2003). The paper presented here will extend the possibilities of using SDSS ELG spectra for the statistical studies of galaxy metallicities.

In this paper we describe the method used to extract from the SDSS database strong-line ELGs, which are suitable for determining oxygen abundances with the classic T_e method, i.e., the temperature-sensitive [O III] λ4363 Å line. The original galaxy sample is obtained from the SDSS DR1, which is briefly described in Section 2. The application of the developed pipeline yields the list of ELGs with HII-type spectra. In the same section the procedure of the ELG selection is described in detail. The method used to estimate the physical conditions in HII regions of the galaxies studied and their element abundances is described in Section 3. In the same section we outline a number of problems encountered while using the SDSS spectral data and the ways to resolve them. In Section 4 we check the quality of the oxygen abundance determination. The catalog of all selected ELGs along with their main parameters, emission line data, and the derived oxygen abundances is presented in Section 5. The results are presented in Section 6. We conclude with the key results of this paper in Section 7. We adopt here the Hubble constant $H_0 = 75$ km s^{-1} Mpc^{-1}.

2. Sample selection

2.1. DR1 spectral data

The SDSS uses two fiber-fed double-spectrographs to measure spectra of objects in the range from 3800 Å to 9200 Å with spectral resolution $R \sim 1800$. Each spectrograph handles 320 fibers (which we call a half-plate), and the two halves are reduced independently. For a single pointing, each observed plate contains 640 fibers, yielding 608 spectra of galaxies, quasars, and stars, and 32 sky spectra (Blanton et al. 2003). The fibers have a diameter of 3″. The instrumental resolution and pixel scale are close to constant in logarithmic wavelength rather than linear wavelength. The flux calibration procedure is summarized in Stoughton et al. (2002, Sections 3.3 & 4.10.1) and will be fully described by Schlegel et al. (in preparation). The flux calibration is imposed on each plate by a set of eight spectrophotometric standard stars, chosen by color to be F-subdwarf stars.

For our work we used the reduced spectra from the DR1 (Abazajian et al. 2003) database which cover a total area on the sky of ∼1360 deg^2. All these spectra have been copied from the official DR1 web-site (see `http://www.sdss.org/dr1/` for details) as two-dimensional FITS-files; one file for each spectral plate contains one spectrum per row. Also, the FITS file containing photometric and some spectral information for 133,996 DR1 galaxies with observed spectra was copied and used as a primary database in our work.

2.2. Measurement of lines

For the analysis of the SDSS spectra we used our own software for emission-line data, created for the HSS-ELG and for HSS-LM projects (Ugryumov et al. 2001, 2003). This software is based on the MIDAS[2] Command Language programs and was adapted especially for the requirements of the SDSS spectral data. The programs dealing with the fitting of emission/absorption line parameters are based on the MIDAS programs SET/FIT, FIT/IMAGE, COMPUTE/FIT and SAVE/FIT from the `FIT` package (MIDAS Users Guide 1998). The line fitting was based on the Corrected Gauss-Newton method. Every line in the reference list was fitted as a single Gaussian superimposed on the continuum-subtracted spectrum. Some lines were fitted simultaneously as a blend of two or more Gaussians features. For the current work, Gaussian blends were obtained for the Hα 6563 Å and [N II] $\lambda\lambda$6548,6584 Å lines, [S II] $\lambda\lambda$6716,6731 Å lines, and [O II] $\lambda\lambda$7320,7330 Å lines.

---

[2]MIDAS is an acronym for the Munich Image Data Analysis System, which is a package developed for the European Southern Observatory.

The continuum was determined with the help of the algorithm described in detail by Shergin, Kniazev, & Lipovetsky (1996). This algorithm initially had been developed in the Special Astrophysical Observatory of the Russian Academy of Sciences for the reduction package of one-dimensional radio data aimed at the detection of weak sources. It was also successfully used in the reduction of KISS data (Kniazev 1997), where it showed very robust results even for the objective prism spectra with the total length of only forty points. The clipping procedure of the algorithm deals with the noise level of a spectrum that in the general case changes from point to point; the noise level is thus defined as a function $\sigma(\lambda)$. By the definition of the algorithm, the fitted continuum also has an uncertainty $\sigma(\lambda)$ which is added to the uncertainty of the measured line intensity of the studied spectrum. Our continuum fit algorithm does not produce a continuum noise estimate. For the latter, we used the Absolute Median Deviation (AMD) estimator, $med(|x - \overline{x}|)$, where $\overline{x}$ is the mean of the input distribution (Korn & Korn 1968). If $\sigma_{\rm n}$ is the standard deviation for a normal distribution, then the standard deviation of the AMD estimator is $\sigma_{\rm AMD} \approx 0.674\,\sigma_{\rm n}$. Thus, the final noise estimate, σ, should be corrected as $\sigma = \sigma_{\rm AMD}/0.674$. The AMD algorithm is a fairly fast robust procedure and has been used for the stream data reduction system of observations with the RATAN–600 radiotelescope (Erukhimov 1988). Analysis of the algorithm, performed for Gaussian noise plus noise spikes with Poisson distribution, showed good stability of this estimator: the estimated value does not depend on the intensity of noise spikes. This was a reason to use this estimator for spectra with strong emission lines.

The quoted errors in the line intensities $\sigma_{\rm tot}$ include two components. First, $\sigma_{\rm f}$ is the fitting error from the MIDAS program `FIT/IMAGE` and is related to Poisson statistics of line photon flux. Second, $\sigma_{\rm c}$ is the error resulting from the creation of the underlying continuum (calculated using the AMD estimator), which is the largest error contributor for faint lines. So, the final error is calculated as:

$$\sigma_{\rm tot} = \sqrt{\sigma_{\rm f}^2 + \sigma_{\rm c}^2} \qquad (1)$$

2.3. Selection steps

To simplify the work with the entire sample of ∼134,000 spectra, we divided our selection procedure into two steps:

1. Fast measurements of the equivalent widths (EWs) of the strongest emission Balmer lines Hα, Hβ and Hγ for all objects allowed us to preselect a subsample with the strongest emission lines. With this step, we chose the Balmer lines instead of the [O III] λ4959,5007 Å lines. The reason is related to the steps described below, in which we plan to use the complete

subsample of H II galaxies limited by the value of EW(Hβ), since the latter can serve as an indicator of the age of the starburst (e.g., Schaerer & Vacca 1998).

We found that either the SDSS pipeline for the DR1 data truncated some fraction of the strongest emission lines in the galaxy spectra, or that the lines themselves were saturated. In Fig. 1 we show, as an example, the plot of EW(Hα) versus EW(Hβ) for our sample. For those data points that are located in this Figure below the "main sequence", the Hα line was truncated during the pipeline reduction or/and was saturated in the observations. We found that this problem can be overcome at the primary selection step, if we use simultaneously the three strongest Balmer lines (Hα, Hβ and Hγ) to preselect objects with the strongest oxygen emission. That is, the galaxy was considered to pass the preliminary selection procedure if one of the following EW thresholds was observed:

$$\mathrm{EW}(H\gamma) \geq 6\ \text{Å} \,||\, \mathrm{EW}(H\beta) \geq 20\ \text{Å} \,||\, \mathrm{EW}(H\alpha) \geq 50\ \text{Å} \tag{2}$$

Altogether, $\sim$5000 spectra were preselected with these criteria. The principal parameter of the imposed selection criteria is based on the threshold value of EW(Hβ). The two other thresholds are related to the former approximately through the theoretical Balmer decrement. The threshold value of the EW(Hβ) selection criterion was motivated by the requirement to have the measurable weak [O III] λ4363 Å emission line, necessary for a direct calculation of the electron temperature, T_e. This line normally is fainter than the [O III] λ5007 Å line by a factor of 200 to 40 in the $T_{\rm e}$ range 10,000 K to 20,000 K (Aller 1984). The intensities of [O III] λ5007 Å and Hβ in H II galaxies statistically have an average ratio [O III]/Hβ of approximately 4 ± 1 (e.g., Ugryumov et al. 2003). This translates to a Hβ/[O III] λ4363 Å intensity ratio of 50 to 10. Since the faintest measurable [OIII] λ4363 Å lines in the spectra of the SDSS ELGs are found to have the EW $\sim$0.4 Å, this implies that the primary selection criterion for the related Hβ-line should be EW(Hβ)$\gtrsim$20 Å. The standard Balmer ratio I($H\alpha$)/I($H\beta$) is 2.88 at 10,000 K. The observed value will be larger, if any extinction is present. The standard Balmer ratio I($H\gamma$)/I($H\beta$) is 0.47 at 10,000 K. Thus, our imposed selection criteria for the EW(Hα) and EW($H\gamma$) are somewhat softer relative to that for EW(Hβ).

With the models of Veilleux & Osterbrock (1987) and Baldwin, Phillips, & Terlevich (1981) we selected 99 narrow-line active galactic nuclei (AGN) and low-ionization nuclear emission-line region galaxies (LINERs; Heckman 1980). AGNs and LINERs are ionized by a non-thermal power law continuum and/or shock heating; thus, these galaxies were removed from the list. A diagram used for the classification and selection is shown in Fig. 2.

2. We measured all emission line intensities and calculated the chemical abundances for all objects in the preselected subsample. The method used for the calculations is described

in Section 3.1. Altogether, 638 spectra were finally selected by imposing the criterion of the accuracy of the oxygen abundance ≤ 0.2 dex. We found that among these 638 spectra, 28 belonged to 14 SDSS targets which were observed twice. EW(Hβ) distributions for the preselected and final samples are shown in Fig. 3. The main parameters of the galaxies from the final selected sample are summarized in Table 1 and measured lines for selected galaxies are shown in Tables 2 and 3. A complete description of these Tables is presented in Section 5.

3. Physical conditions and heavy element abundances

3.1. The Method

The measured emission line intensities $F(\lambda)$ were corrected both for reddening and for the effects of underlying stellar absorption following the procedure described in detail by Izotov, Thuan, & Lipovetsky (1994). We have adopted an iterative procedure to derive simultaneously both the extinction coefficient C(Hβ) and the absorption equivalent width for the hydrogen lines from the equation (Izotov, Thuan, & Lipovetsky 1994):

$$\frac{I(\lambda)}{I(\mathrm{H}\beta)} = \frac{\mathrm{EW}_e(\lambda)+\mathrm{EW}_a(\lambda)}{\mathrm{EW}_e(\lambda)} \frac{\mathrm{EW}_e(\mathrm{H}\beta)}{\mathrm{EW}_e(\mathrm{H}\beta)+\mathrm{EW}_a(\mathrm{H}\beta)} \cdot \frac{F(\lambda)}{F(\mathrm{H}\beta)} \exp\left[C(\mathrm{H}\beta) f(\lambda)\right], \tag{3}$$

where I(λ) is the intrinsic line flux and F(λ) is the observed line flux corrected for atmospheric extinction. $\mathrm{EW}_e(\lambda)$ and $\mathrm{EW}_a(\lambda)$ are the equivalent widths of the observed emission line and of the underlying absorption line, respectively. $f(\lambda)$ is the reddening function, normalized at Hβ. The theoretical ratios from Brocklehurst (1971) for the intrinsic hydrogen line intensity ratios for estimated electron temperature were used. For lines other than hydrogen $\mathrm{EW}_a(\lambda)$=0 and equation (3) reduces to

$$\frac{I(\lambda)}{I(\mathrm{H}\beta)} = \frac{F(\lambda)}{F(\mathrm{H}\beta)} \exp\left[C(\mathrm{H}\beta) f(\lambda)\right]. \tag{4}$$

To derive element abundances of oxygen, we use the standard two-zone model and the method from Aller (1984), and also follow the procedure described by Izotov, Thuan, & Lipovetsky (1994); Thuan, Izotov, & Lipovetsky (1995); Izotov, Thuan, & Lipovetsky (1997), and Izotov & Thuan (1999). The electron temperature $\mathrm{T_e}$ is known to be different in high- and low-ionization H II regions (Stasinska 1990). The procedure determines $\mathrm{T_e}$(O III) from the [O III]λ4363/(λ4959+λ5007) ratio using the five-level atom model (Aller 1984) and the electron density $\mathrm{N_e}$(S II) from the [S II]λ6717/λ6731 ratio. The minimum value of $\mathrm{N_e}$(S II) was set to be 10 cm^{-3}. To derive the $\mathrm{O^+}$ electron temperature, the relation between

T_e(O II) and T_e(O III) from a fit by Izotov, Thuan, & Lipovetsky (1994) to photoionized HII models by Stasinska (1990) was used:

$$t_e(\text{O II}) = 0.243 + t_e(\text{O III})\,[1.031 - 0.184\,t_e(\text{O III})]\,, \tag{5}$$

where $t_e = T_e/10^4$.

For oxygen, the following expression for the total abundance was used:

$$\frac{\text{O}}{\text{H}} = \frac{\text{O}^+ + \text{O}^{++}}{\text{H}^+}. \tag{6}$$

All uncertainties in the measurements of line intensities, continuum level, extinction coefficients, and Balmer absorption equivalent widths have been propagated in the calculations of oxygen abundance, and are accounted for in the accuracies of the presented element abundances. This is detailed in the algorithm steps shown below:
(1). All measured line intensities with the uncertainties specified with equation (1) were read and recalculated relative to the intensity of the Hβ line $\text{I}(\lambda)_1 = \text{I}(\lambda)/\text{I}(\text{H}\beta)$. New errors were calculated as

$$\sigma(\lambda)_1 = \text{I}(\lambda)_1 \cdot \sqrt{\left(\frac{\sigma(\lambda)}{\text{I}(\lambda)}\right)^2 + \left(\frac{\sigma(\text{H}\beta)}{\text{I}(\text{H}\beta)}\right)^2}, \tag{7}$$

(2). Using the system of equations (3) for hydrogen lines, the extinction coefficient $\text{C(H}\beta)\pm\delta\text{C(H}\beta)$ and the equivalent width of underlying absorption in Balmer hydrogen lines $\text{EW(abs)}\pm\delta\text{EW(abs)}$ were calculated.
(3). New relative intensities $\text{I}(\lambda)_2$ for hydrogen lines were calculated using EW(abs) from step (2) so that: $\text{I}(\lambda)_2 = \text{I}(\lambda)_1 \cdot (\text{EW}(\lambda) + \text{EW(abs)})/\text{EW}(\lambda)$. The errors $\sigma(\lambda)_2$ for these lines were recalculated using the determined δEW(abs).
(4). New relative intensities $\text{I}(\lambda)_3$ for all lines were calculated with equation (4) using the C(Hβ) value determined and the reddening function $f(\lambda)$ from Whitford (1958). Izotov, Thuan, & Lipovetsky (1994) gave an approximate reddening function in the entire spectral region as

$$f(\lambda) = 3.15854 \cdot 10^{-1.02109\lambda} - 1, \tag{8}$$

where λ is expressed in units of μm. Final errors $\sigma(\lambda)_3$ were recalculated using determined δC(Hβ) values[3]. All these relative intensities with their errors are presented in Table 3 and are used for calculation of temperatures, densities and oxygen abundances. Calculated oxygen abundances for selected galaxies are presented in Table 4.

[3]Because the theoretical ratios for the hydrogen lines used in equations (3) depend on the electron temperature T_e, which can be determined only after step 4 has finished, steps 2 through 4 were performed iteratively until the results converged, after which the final errors were calculated.

3.2. [O II] λ3727 Å detection problem

Since the SDSS spectra are acquired in the range $3800-9000$ Å, the line [O II] λ3727 Å is out of the range (or is very close to the edge) for objects with redshifts $\lesssim$ 0.024–0.025. Therefore, for such galaxies the determination of the O^+/H^+ abundance by the standard method, for which the intensity of [O II] λ3727 Å is used, is impossible. However, for most of the SDSS spectra of HII galaxies this problem can be overcome by a small modification of the standard method. As shown by Aller (1984, p.130), the value of O^+/H^+ can be equally well calculated from the intensities of the auroral lines [O II] λ7320,7330 Å. The necessary auxiliary quantities for the auroral lines (L_A), as well as those for the nebular ones (L_N), used in the respective formula for the calculation of ionic concentrations, are tabulated in Table 5-5b of Aller (1984). Both methods should give the same value of O^+/H^+ (see, Aller 1984, for all details), but since the total intensities of the [O II] λ7320,7330 Å lines are many times lower than that of the [O II] λ3727 Å line, application of the auroral line method is restricted to SDSS spectra with sufficiently high signal-to-noise ratio. This method was first employed by Kniazev et al. (2003)[4]. We show in Section 4 that this method gives reliable results over the entire range of abundances studied here.

3.3. Strong lines truncation

One of the problems, already mentioned in Section 2.3, was a significant truncation of the line emission for e.g., Hα, Hβ, [O III]$\lambda\lambda$4959,5007 Å, in a fraction of spectra obtained. Hereafter we assume that a studied line *1* with flux I_1 is truncated if the measured flux ratio of lines *1* and *2* satisfy the condition: I_1/I_2 is lower than the standard value of this ratio by more than $5\sigma_{\rm ratio}$. $\sigma_{\rm ratio}$ is calculated as:

$$\sigma_{\rm ratio} = \frac{I_1}{I_2} \cdot \sqrt{\left(\frac{\sigma_1}{I_1}\right)^2 + \left(\frac{\sigma_2}{I_2}\right)^2}, \tag{9}$$

where σ_1 and σ_2 are observational uncertainties of I_1 and I_2. The objects most likely affected are those that yield the most accurate element abundances, because their HII regions often have the strongest lines. There are two possible explanations for the truncation: (1) saturation of the strong emission lines, and (2) problems with the standard SDSS pipeline. The latter may result from the procedure used to clean images of cosmic ray contamination. The fraction of truncated spectra in the DR1 database is significantly reduced in comparison to

[4]In this work [O II] λ7320,7330 Å lines were used only if the line [OII] λ3727 Å was not detected in the spectra.

the Early Data Release. For example, the 17 selected spectra from the EDR database with truncated Hα line emission all appeared unaffected in the DR1 database, which supports the second suggestion about pipeline problems.

The truncation problem was overcome in the process of creating the SHOC catalog. First, in the preselection phase, we extended our selection criteria; see Section 2.3 for details. Second, in the process of computing oxygen abundances, most of the truncated emission lines were restored, based on "a priori" information about line intensity ratios. In particular, the intensities of the lines [O III] λ5007 and 4959 Å were restored to the adopted ratio of three. The latter was derived as the mean ratio I([O III] λ5007)/I([O III] λ4959) over all galaxies of the catalog with unaffected lines [O III] λ5007 and 4959 Å. The mean ratio is equal to 3.011 $\pm$ 0.017. Depending on whether the measured ratio [O III] λ5007/[O III] λ4959 was higher or lower than three, the intensity of either of the two lines was corrected. As is evident in Fig. 4, either line can appear truncated in the SDSS spectral data. Of course, it is difficult to exclude the possibility that both the [O III] λ5007 and 4959 Å lines were truncated. For this reason, we have indicated objects with truncated lines in Column 7 of Table 1. But in reality we found only one such spectrum SDSS J081447.52+490400.8 where both the [O III] λ5007 and 4959 Å lines were truncated (see notes to Table 1 for more details).

Spectra with truncated Hα and/or Hβ emission were more difficult to treat. The relation between I(Hα)/I(Hβ) and I(Hγ)/I(Hβ) is shown in Fig. 5. Only region "IV" is the correct region for the two Balmer line intensity ratios, whose theoretical values for $T_{\rm e}$ = 5,000, 10,000 and 20,000 K are shown by horizontal and vertical lines. Points located in regions "I" and "II" of the plot correspond to the truncation of the Hα line. Points located in regions "II" and "III" of the plot correspond to the truncation of the Hβ line. In region "II" of the plot, both Hα and Hβ are truncated. The Hβ line truncation is most severe for our procedure of the abundance calculation (see Section 3.1 for details), since all relative intensities I(line)/I(Hβ) are affected. The truncation of the Hα line will affect only the calculation of the extinction coefficient. However, since this coefficient is calculated by using all detected Balmer lines (up to eight), the overall effect of Hα line truncation can be rather small.

3.4. Atmospheric dispersion effects

The SDSS does not use an atmospheric refraction corrector, so the effective fiber position on the sky shifts slightly as a function of wavelength resulting from atmospheric dispersion (Fillipenko 1982). Fixed 3″ apertures and the presence of brightness gradients for galaxies create errors in measured fluxes. This is corrected in the SDSS by referring broadband spectrophotometry to 5.5″ × 9″ aperture "smear" exposures (Abazajian et al. 2003). These

problems are also reduced for compact objects similar to H II regions in our target galaxies. As well, the SDSS spectra presented here were taken at airmasses of 1.22 with r.m.s. 0.10, which further reduces dispersion effects. If the effect of atmospheric dispersion on our O/H data remained, we would expect increased data scatter with larger airmass. However, our data do not show any trend in the dependence of the error in oxygen abundance against the airmass of the observed galaxy. Finally, we obtain excellent agreement between our measured parameters and previously published values for already known HII galaxies recovered from the SDSS data (see Section 4.3 below). From this we conclude that the combination of relatively low airmass and applied 'smear' corrections help to reduce significantly the atmospheric dispersion effect for the sample. The limit is presumably the value that we currently can check via comparison of SDSS derived O/H and measurements from high S/N data in the literature.

4. Quality of the oxygen abundance determination

Comparing the quality of the oxygen abundance determination for SDSS ELGs with oxygen abundances from T_e measurements was first done by Kniazev et al. (2003), but only for oxygen abundances in the range $7.10 \leq 12+\log(O/H) \leq 7.65$. With our data it is possible to extend the analysis over a much larger abundance range.

4.1. Repeatibility

The comparison of several independent SDSS measurements for the same object allows a check of the repeatability of our method. Two independent measurements were available for 14 ELGs. The results of the comparison are shown in Fig. 6, where the differences Δ (First$-$Second) are plotted versus the value of 12+log(O/H) with the lower r.m.s. uncertainty. The latter we name as the 'First'. Where independent measurements exist for a given object, the more accurate value of the oxygen abundance is shown in the catalog. The shown error bars correspond to the errors of the differences, taken as a square root of the sum of the errors squared. The weighted mean of the difference Δ (First$-$Second) is -0.01 ± 0.01 dex with r.m.s. 0.05 dex. For seven of the 14 objects, [OII] λ3727 Å was not detected and [O II] λ7320,7330 Å were used to compute O^+/H^+. These objects are shown with filled circles in Fig. 6. For the seven objects with no [OII] λ3727 Å, the weighted mean of the difference Δ (First$-$Second) is 0.02 ± 0.03 dex with r.m.s. 0.07 dex. These comparisons show that for all repeated observations the oxygen abundances agree to within the cited uncertainties.

4.2. Oxygen Abundances with [O II] 3727,3729 Å and [O II] 7320,7330 Å

Another type of check can be performed based solely on SDSS spectra. For many objects with redshifts ≥ 0.024, the ionic O^+ abundance can be derived from [OII] λ3727 Å and [O II] λ7320,7330 Å lines. A comparison for 51 galaxies with an accuracy of the oxygen abundance $\leq$ 0.05 dex and for 159 galaxies with an accuracy of the oxygen abundance $\leq$ 0.1 dex is shown in Fig. 7. The weighted mean of the difference $\log(O/H)_{3727}$ – $\log(O/H)_{7320,7330}$ was found to be 0.002±0.002 dex with r.m.s. 0.02 dex in both cases, where $\log(O/H)_{3727}$ is the total oxygen abundance derived using [OII] λ3727 Å, and $\log(O/H)_{7320,7330}$ is the total oxygen abundance derived using [O II] λ7320,7330 Å. We concluded finally that the scatter between abundances derived with the [OII] λ3727 Å and with the [O II] λ7320,7330 Å lines is within the cited uncertainties as expected from Aller (1984).

4.3. The SDSS abundances versus the data from the literature

A fraction of the strong-line ELGs presented in the SHOC catalog is found also in earlier surveys, e.g., UM, First Byurakan Survey (FBS or Markarian galaxies – MRK), SBS, and HSS-ELG. For galaxies with sufficiently strong [OIII] λ4363 Å emission, independent spectrophotometry and oxygen abundances are published (see notes to Table 5 for references). These abundances can be used to estimate how reliable our own abundance determinations are. A comparison of 22 independent measurements of 15 strong-line ELGs is shown in Table 5. We added also some galaxies from Kniazev et al. (2003) since their abundances were calculated with the same method. For all but one of the SDSS spectra, oxygen abundances were calculated using the intensities of [OII] λ7320,7330 Å lines. We show these abundances in column 6 along with the information about truncated lines, restored for the abundance calculations. The weighted mean difference in log(O/H) is 0.02±0.01 dex with r.m.s 0.04 dex. We found that our oxygen abundances derived with the [OII] λ7320,7330 Å lines are consistent within the cited uncertainties with published abundances in the literature derived with [OII] λ3727 Å only. The results are illustrated in Fig. 8. Accounting for probable differences in the centers and sizes of the regions sampled by SDSS spectra and those used for comparison, the differences found in oxygen abundances are satisfactorily small.

5. Results

5.1. Description of Catalog

The main criterion for including a galaxy into the SHOC catalog was a small r.m.s. uncertainty of the oxygen abundance. We set the threshold r.m.s. value of 0.20 dex, corresponding to ∼58% of the oxygen abundance. This yielded 612 objects in the catalog with a number of objects with multiple HII regions (624 separate SDSS targets in total). 263 SHOC objects (272 separate SDSS targets) have uncertainties ≤0.10 dex, while 186 objects (198 separate SDSS targets) have intermediate uncertainties between 0.10 and 0.15 dex. In other words, ELGs with oxygen abundances having uncertainties ≤0.15 dex make up 75% of the entire catalog. In Fig. 9 we show representative spectra of four SHOC objects.

In Table 1 we present the SDSS parameters of all Catalog galaxies in the following format. *Column 1* lists internal numbers of objects in the catalog. The suffixes "a", "b", and so on represent different star-forming knots in the same galaxy (sorted by RA). Entries without an internal number correspond to a repeat spectrum of the same object. *Column 2* lists the SDSS name according to the coordinates of the spectral observations and how they exist in the DR1 database. *Column 3* lists the plate number, MJD (Mean Julian Date), and fiber number for spectral observations. *Column 4* lists the SDSS r-band Petrosian magnitudes. In many cases these magnitudes relate to the observed H II regions, but not to the whole galaxy due to problems in the pipeline which identify incorrectly an extended galaxy with a multiple number of some knots or H II regions (shredding, see, e.g., Abazajian et al. 2003; Kniazev et al. 2004). We strongly recommend using these cited magnitudes as preliminary measures. For further analysis we plan to check them with the SDSS database or/and with the photometry software of Kniazev et al. (2004). *Column 5* lists the derived galaxy redshift. *Column 6* is the Wolf-Rayet (WR) galaxy flag. "1", "2", or "3" mean that either only the "blue" bump, or only the "red" bump, or both bumps are detected. Nine previously known or suspected WR galaxies are shown as asterisks or crosses, respectively. *Column 7* lists the Truncation flag. If "1" is in any of the four positions, this indicates that the intensity of Hβ, λ4959, λ5007 or Hα, respectively, was corrected; see Section 3.3 for details. *Column 8* lists the morphological class, as assigned by the authors, with consultation with the NED database; see details in Section 5.2. *Column 9* lists alternative names for each galaxy, if available, according to NED. Only names from large surveys for AGN and actively star-forming galaxies were taken, as well as names from the catalogs of bright galaxies (UGC, NGC and CGCG).

Observed emission-line fluxes relative to the Hβ emission line, the Hβ flux, and the Hβ equivalent width in emission are presented in Table 2. In the current work we present only

those emission lines, that were used for oxygen abundance calculations. Relative emission-line intensities $I(\lambda)$ corrected for interstellar extinction and underlying stellar absorption are presented in Table 3. The calculated absorption Balmer hydrogen lines equivalent widths EW(abs) and the extinction coefficient $C(\mathrm{H}\beta)$ are also shown in Table 3. Derived oxygen abundances and their errors are presented in Table 4, together with calculated electron temperatures T_{e}(O [III]), T_{e}([O II]), electron density N_{e}([S II]), and the ionic abundances $\mathrm{O}^+/\mathrm{H}^+$ and $\mathrm{O}^{++}/\mathrm{H}^+$. $\mathrm{O}^+/\mathrm{H}^+$ with [their] cited errors were calculated using [O II] λ7320,7330 Å lines only if the line [OII] λ3727 Å was not detected in the spectra.

5.2. Morphology and classification

The SHOC catalog contains several large groups of gas-rich HII galaxies and superassociations in the different type of galaxies. To assign SHOC galaxies to some of the morphological types we examined combined g, r, i images from SDSS DR1 and produced visual morphological classifications of five different types: (1) blue compact galaxies (BCGs) – if the luminosity of the bright SF region comprises $\gtrsim$50% of the total galaxy light; (2) irregular and/or dwarf (anemic) spirals (Irr) – if the luminosity of bright SF knots is less than half of the total galaxy light; (3) low surface brightness galaxies (LSBGs) – if the SF region is of very low luminosity; (4) interacting galaxies with a range of separations (Int); (5) various types of spiral galaxies (Sp). In many cases, off- or near-center supergiant HII regions (super-associations, "sa") were clearly observed. This information was added into our classification scheme. In intermediate cases and/or in cases which were unclear, a question mark ("?") was used as a label. A significant number of HII galaxies are found at large radial velocities/distances ($>$ 20000 km s^{-1}) and are poorly resolved. While most of them currently are classified as BCG/BCG?, their classification requires better angular resolution. BCGs are the most common type, making up about 75% (461 galaxies) of the catalog. The catalog contains also 78 Irr, 20 LSBGs, 10 Int and 43 obvious spiral galaxies.

5.3. Objects with truncated strong lines

In total we found 64 SDSS targets with strong emission lines, for which one or more lines were truncated in the processing stage with the SDSS spectroscopic pipeline. All of these spectra are marked in column 7 of Table 1. In five SDSS spectra, the Hβ line was truncated and restored. In 26 SDSS spectra, the Hα line was truncated and restored. In two SDSS spectra, both Hβ and Hα were truncated and restored. In 41 SDSS spectra, either the [OIII] $\lambda\lambda$ 4959 or 5007Å line was truncated, which was subsequently restored.

Of course, it is difficult to exclude the possibility that both the [O III] λ5007 and 4959 Å lines were truncated for some of these spectra, but we found only one object (SHOC 193b) for which intensities of both [OIII] $\lambda\lambda$ 4959 Å and 5007Å were truncated. For this object, intensities of [OIII] $\lambda\lambda$ 4959 Å and 5007Å were restored based on data from Pustilnik et al. (1999). It should be noted here that all truncated and restored spectra were also used for the comparisons shown above to check the quality of oxygen abundance determinations. For example, one spectrum used to check repeatability (Section 4.1) was truncated and restored. Besides, three more truncated and restored spectra were used in Section 4.3 (see Table 5 for details). We performed the analysis similar to that described in detail in Section 4, but excluding all truncated spectra. Since the number of truncated spectra is very small, all our statistics and conclusions for that Section were not changed.

5.4. Narrow Line AGN and LINERs

As mentioned in Section 2.2, in the framework of the applied algorithm in order to create a continuum appropriate for the measurements of narrow lines, we adopted the following parameters: 35 Å smoothing window for Gaussian-smoothing convolution and 30 full iterations for the "smooth-and-cut" algorithm. Due to the selected smoothing window size we strongly suppressed all emission lines with FWHM $\gtrsim$ 15 Å. Galaxies with broad emission lines (FWHM$\gtrsim$ 15 Å, e.g., Sy1) were lost. Therefore, the list of AGNs below is incomplete.

In order to distinguish narrow-line AGN and LINERs from HII galaxies in our sample, we used classification diagrams based on various line flux ratios, and models from Veilleux & Osterbrock (1987) and Baldwin, Phillips, & Terlevich (1981), which describe the regions occupied by different types of ELGs on these diagrams. As an example, we show in Fig. 2 the ratios of the line fluxes [OIII]λ5007/Hβ versus [NII]λ6584/Hα for $\sim$5000 preselected ELGs and the results of the mentioned models. This resulted in the identification of 99 galaxies, which are very probable narrow-line AGN or LINERs. Most of them have rather large luminosities, corresponding to $M_{\rm r} \leq -20$. Finally, we used models from Kewley et al. (2001) (the solid line in Fig. 2) for AGN/LINER separation and found 30 narrow-line AGN in our list. All these AGN and LINERs were not included in the final catalog and do not have SHOC numbers, but are presented in a separate list in Table 6. This includes the SDSS name (column 1), Plate+MJD+Fiber information for spectral data (column 2), Petrosian r magnitude (column 3), redshift (column 4), type (column 5), and comments, which include alternative names, taken from NED (column 6).

5.5. WR galaxies

Altogether, we detected WR blue ($\sim\lambda4650$ Å) and/or red ($\sim\lambda5808$ Å) features in 84 SHOC spectra of 81 SHOC ELGs. Twenty-eight additional WR galaxies were found among galaxies selected at the preliminary step and not included in the catalog. They either have an r.m.s. uncertainty of log(O/H) worse than 0.2 dex, or belong to the AGN/LINER type (4 galaxies). They are listed in Table 7 with the same columns as in Table 1. These additional WR galaxies do not have SHOC numbers. The most recent catalog of 139 WR galaxies was compiled by Schaerer, Contini, & Pindao (1999, SCP99 hereafter). Among the WR galaxies found in this work, only seven were listed in that catalog and two more were listed by SCP99 as suspected WR galaxies. Seven WR galaxies from SCP99 are marked in Column 6 of Table 1 with an asterisk and one of our WR galaxies identified as suspected by SCP99 is marked with a cross in Column 6 of Table 1 and one is in Column 6 of Table 7. The present paper increases the number of known WR galaxies by $\sim70\%$. The most distant known WR galaxy from SCP99 was at redshift of 0.12. The SHOC catalog extends the known population of WR galaxies out to redshift $z = 0.25$ (SHOC 100).

5.6. Extremely metal-poor galaxies

Follow-up spectroscopy of the strongest emisison-line objects from the recent objective-prism based ELG surveys with limiting B-magnitudes of ∼18.0–18.5 (e.g., SBS, HSS-ELG and HSS-LM) indicates that the XMPG surface density is $3-4$ per 1000 square degrees (e.g., Pustilnik et al. 2003a). This implies that the SDSS should have another 30–40 BCGs with $Z < 1/20\ Z_{\odot}$, of which ∼2/3 should be new objects. Accounting for SDSS spectroscopy of a significant number of fainter galaxies, the expected number may even be larger. The first eight new XMPGs from SDSS and four rediscovered well-known XMPGs were identified after an analysis of 250,000 galaxy spectra within an area of ~3000 deg^2 (Kniazev et al. 2003). All reported XMPGs have uncertainty of log(O/H) $\leq$0.10 dex.

Here, we detected from SDSS DR1 in total 10 galaxies with 12+log(O/H) between 7.25 and 7.65 with r.m.s. uncertainties below 0.2 dex. The following four galaxies have log(O/H) uncertainties lower than 0.10 dex and were presented in Kniazev et al. (2003): SDSS J020549.13−094918.0 (SHOC 106), HS 0837+4717 (SHOC 220), I Zw 18 (SHOC 261), and SDSS J120122.32+021108.3 (SHOC 357). The remaining galaxies from the catalog have oxygen abundances near the formal threshold of 12+log(O/H)=7.65, used to assign objects to the XMPG group (Kunth & Östlin 2000). However, due to the lower accuracy of their abundances, all these galaxies from the catalog should be checked more carefully. In particular, one should be aware, that due to the noise fluctuations, about 5% of the catalog

objects with r.m.s. uncertainties of O/H >0.10 dex can appear to have true abundances differing by 0.20–0.40 dex from their catalogued values after higher-quality spectra have been taken. Such objects may augment the number of currently identified XMP galaxies.

6. Discussion

Our aim in the present work was to create an SDSS based ELG catalog with reliable oxygen abundances, which would be useful for various statistical studies related to galaxy chemical evolution. In the current edition of SHOC, we provide only the oxygen abundance. Argon, neon, nitrogen, and sulphur abundances will be available for a large number of ELGs in forthcoming papers.

Galaxies selected in the SDSS for spectroscopy come from two different subsamples. One is selected by the criterion of the total r-filter magnitude to be brighter than $r = 17\overset{\mathrm{m}}{.}77$ (Strauss et al. 2002). The other fainter subsample is a by-product of a color-selected sample of quasars (Richards et al. 2002). The SHOC catalog consists of objects selected from both SDSS galaxy subsamples. The QSO candidate galaxy subsample is, of course, selected with different criteria and its study should take this into account.

To demonstrate the range of key galaxy parameters for catalog objects, we plot them in Fig. 10– 12. First, we show in Fig. 10 the distribution of 12+log(O/H) derived for all 612 SHOC ELGs (in case of observations for multiple knots in a given galaxy, only metallicity for knot "a" is shown). The open histogram outlines the distribution of all ELGs with r.m.s. uncertainties of log(O/H) $\leq$0.20 dex. The hashed histogram shows the same distribution for the subsample with log(O/H) uncertainties $\leq$0.10 dex. Both distributions appear similar and their similar mean values and the standard deviations confirm this impression. Not surprisingly, the subsample with larger uncertainties exhibits somewhat larger scatter. In Figure 11 we show the distributions of apparent r magnitudes, absolute magnitudes M_r, and heliocentric radial velocities for all 612 SHOC ELGs. The median apparent magnitude is m_r^{med}=$17\overset{\mathrm{m}}{.}67$ (top panel on Figure 11), which indicates that more than 50% of SHOC galaxies are in the magnitude range "completely" sampled by SDSS spectroscopy. The median value of the absolute magnitude M_r is $M_r^{\mathrm{med}} = -18\overset{\mathrm{m}}{.}4$. The characteristic r-band luminosity L_r^* for the SDSS-determined luminosity function (for a Hubble constant 75 km s^{-1} Mpc^{-1}) corresponds to $M_r^* = -21\overset{\mathrm{m}}{.}45$ (see, e.g., Blanton et al. 2001). About 90% of the Catalog galaxies are subluminous ($M_r > M_r^* + 1$).

The number distribution of galaxies with radial velocities decreases above V_{hel} ~10,000 km s^{-1} up to V_{hel} ~110,000 km s^{-1}(top panel on Figure 12). About 90% of all ELGs have V_{hel} $\leq$55,000 km s^{-1}.

ELGs with redshifts $z \leq 0.024$, for which [O II]λ3727 is not measurable, are shown by hashed bins on the top panel on Figure 12. They comprise ~30% of the total number of SHOC galaxies. The median radial velocity of ~14,000 km s^{-1} on the top panel on Figure 12 reflects the presence in the catalog of a significant number of rather distant galaxies with H II type spectra. If we limit the subsample of galaxies to those selected for SDSS spectroscopy with r-magnitudes brighter than $17\overset{m}{.}77$, this subsample is about 50% of the total number (hashed histogram on bottom panel of Figure 12). The redshift distribution is more narrow for this subsample: its median radial velocity is ~7000 km s^{-1} with about 90% of all galaxies having V_{hel} ≤17,000 km s^{-1}.

It is interesting to compare this catalog with other samples of BCG/H II galaxies with O/H measured by the classic T_e method. They include the BCG samples from the Second Byurakan Survey (SBS) (Izotov & Thuan 1999), the Tololo and UM surveys (Masegosa, Moles, & Campos-Aguilar 1994), the KISS (Melbourne & Salzer 2002) and the HSS-LM (Ugryumov et al. 2003).

For the SBS BCGs the value of O/H is measured for about 40 objects with r.m.s. uncertainties of log(O/H) in the range of 0.01 to 0.05 dex (Izotov & Thuan 1999). Their published magnitudes are known with moderate to low precision, so it is quite difficult to address the issue of completeness.

For Tololo and UM galaxies (Terlevich et al. 1991), oxygen abundances are presented for 100 galaxies (Masegosa, Moles, & Campos-Aguilar 1994). Their cited r.m.s. uncertainties are between 0.01 and 0.08 dex. However, checks of several objects from that work (e.g., Kniazev et al. 2001; Pustilnik et al. 2002a) showed that the real uncertainties are larger, with some values shifted by about 0.3 dex. For a part of this sample of galaxies, the magnitudes are poorly known.

For the KISS sample the number of ELGs with strong lines is significantly larger. However, only 12 galaxies have been published with oxygen abundances derived with the T_e method (Melbourne & Salzer 2002). No estimates of their uncertainties are presented. These ELGs are on average more distant, since KISS includes galaxies with m_B as faint as 20^m.

For the HSS-LM published List I (Ugryumov et al. 2003) there are 46 strong-lined BCG/H II galaxies with T_e oxygen abundances; the faintest galaxy is about $m_B = 18\overset{m}{.}5$. The uncertainties of log(O/H) for this sample vary between 0.02 and 0.20 dex. List II (Pustilnik et al., in preparation) will augment a comparable number of H II galaxies with similar properties.

For the detected WR galaxies we notice that a majority of the objects have EW(Hβ)

larger than 60 Å (see Figure 13, top panel), with the median of 72 Å for all detected WR galaxies and 86 Å for the WR galaxies in the catalog. This is consistent with expectations from current models of massive star evolution, which predict the presence of an observable number of WR stars for starburst ages between 3 and 6 Myr, for the metallicity range of SHOC objects (Schaerer & Vacca 1998). The maximum of the WR fraction in the catalog galaxies with oxygen abundances 12+log(O/H)$\gtrsim$8.1 (Figure 13, bottom panel) is as well consistent with the model predictions of the dependence of the WR-bump strength and duration on the galaxy metallicity.

Thus, the SHOC catalog of ELGs with measured oxygen abundances presents three key advantages. First, SHOC is by number several times larger than any of the previously published similar samples. Two, almost all SHOC galaxies have potentially good photometry. However, in many cases derived photometry of SDSS data requires additional software (e.g., used in Kniazev et al. 2004) to avoid galaxy shredding. Finally, about 50% of the SHOC galaxies with $m_r < 17\overset{m}{.}7$ have been observed spectroscopically to a high level of completeness ($\sim$0.9; Strauss et al. 2002). The SHOC catalog provides a significant opportunity to improve the statistical study of many issues related to the metallicity of gas-rich galaxies.

7. Conclusions

With respect to the present SHOC catalog and data from Kniazev et al. (2003), we draw the following conclusions:

- SDSS spectra permit accurate oxygen abundance determinations over the range $7.1 \lesssim 12 + \log(\mathrm{O/H}) \lesssim 8.5$.
- The method for calculating O^+/H^+ using intensities of the [O II] λ7320,7330 Å lines appears to yield reliable results over a wide range of oxygen abundances.
- A large number of strong-line ELGs with measurable oxygen abundances and detectable WR populations is selected from the SDSS DR1 database.
- A large majority of strong-line ELGs with detected [O III]λ4363 are HII galaxies with a broad range of r-band luminosities, corresponding to absolute r magnitudes $-22 \lesssim M_r \lesssim -12$.

We plan to produce regular updates of the SHOC catalog of strong-line ELGs with measured oxygen abundances, based on subsequent Data Releases from the SDSS.

The Sloan Digital Sky Survey (SDSS) is a joint project of The University of Chicago, Fermilab, the Institute for Advanced Study, the Japan Participation Group, The Johns Hopkins University, the Max-Planck-Institute for Astronomy (MPIA), the Max-Planck-Institute for Astrophysics (MPA), New Mexico State University, Princeton University, the United States Naval Observatory, and the University of Washington. Apache Point Observatory, site of the SDSS telescopes, is operated by the Astrophysical Research Consortium (ARC).

Funding for the project has been provided by the Alfred P. Sloan Foundation, the SDSS member institutions, the National Aeronautics and Space Administration, the National Science Foundation, the U.S. Department of Energy, the Japanese Monbukagakusho, and the Max Planck Society. The SDSS Web site is http://www.sdss.org/.

This research has made use of the NASA/IPAC Extragalactic Database (NED) which is operated by the Jet Propulsion Laboratory, California Institute of Technology, under contract with the National Aeronautics and Space Administration.

REFERENCES

Abazajian et al. 2003, submitted (astro-ph/0305492)

Aller, H.L., 1984, Physics of Thermal Gaseous Nebulae, Dordreht, Reidel

Baldwin, J.A., Phillips, M.M.,& Terlevich R. 1981, PASP, 93, 5

Bernardi, M. 2003, AJ, 125, 1817

Blanton, M.R., Dalcanton, J., Eisenstein, D., et al. 2001, AJ, 121, 2358

Blanton, M.R., Lupton, R.H., Maley, F.M., Young, N., Zehavi, I., & Loveday, J. 2003, AJ, 125, 2276

Brocklehurst, M. 1971, MNRAS, 153, 471

Dalcanton, J.J., Spergel, D.N., & Summers, F.J. 1997, ApJ, 482, 659

Denicoló, G., Terlevich, R., & Terlevich, E. 2002, MNRAS, 330, 69

Eisenstein, D.J., et al. 2003, AJ, 585, 594

ESO-MIDAS User's Guide, 1998, Volume A

Erukhimov, B.L. 1988, Bulletin SAO, 59, 18

Fillipenko, A.V., 1982, PASP, 94, 715

Fukugita, M., Ichikawa, T., Gunn, J.E., Doi, M., Shimasaku, K., & Schneider, D.P. 1996, AJ, 111, 1748

Grebel, E.K., Gallagher, J.S., & Harbeck, D. 2003, AJ, 125, 1926

Grogin, N.A., & Geller, M.J., 2000, AJ, 119, 32

Goto, T., Nichol, R.C., Miller, C.J., et al. 2003, PASJ, 55, 771

Gunn, J.E., Carr, M.A., Rockosi, C.M., Sekiguchi, M., et al. 1998, AJ, 116, 3040

Guseva, N.G., Izotov, Y.I., & Thuan, T.X. 2000, ApJ, 531, 776

Guseva, N.G., Papaderos, P., Izotov, Y.I., Green, R.F., Fricke, K.J., Thuan, T.X., & Noeske, K.J. 2003, A&A, 407, 105

Heckman, T.M. 1980, A&A, 87, 152

Hogg, D.W., Finkbeiner, D.P., Schlegel, D.J., & Gunn, J.E. 2001, AJ, 122, 2129

Izotov, Y.I., Guseva, N.G., Lipovetsky, V.A., Kniazev, A.Y., & Stepanian, J.A. 1990, Nature, 343, 238

Izotov, Y.I., & Thuan, T.X. 1998, ApJ, 497, 227

Izotov, Y.I., & Thuan, T.X. 1999, ApJ, 511, 639

Izotov Y.I., Guseva N.G., Lipovetsky V.A., Neizvestny S.I., Stepanian J.A., Kniazev A.Y. 1993, Astron.Astropys.Trans., 3, 179

Izotov, Y.I., Thuan, T.X., & Lipovetsky, V.A. 1994, ApJ, 435, 647

Izotov, Y.I., Thuan, T.X., & Lipovetsky, V.A. 1997, ApJS, 108, 1

Kauffmann, G., Heckman, T.M., White, S.D.M. et al. 2003, MNRAS, 341, 33

Kewley, L.J., Dopita, M.A., Sutherland, R.S., Heisler, C.A., & Trevena, J. 2001, ApJ, 556, 121

Kniazev, A.Y. 1997, Ph.D. Thesis, Special Astrophys. Obs., Nizhnij Arkhyz (http://precise.sao.ru)

Kniazev, A.Y., Pustilnik, S.A., Ugryumov, A.V., & Kniazeva, T.F. 2000, Astronomy Letters, 26, 129

Kniazev, A.Y., Pustilnik, S.A., Ugryumov, A.V., & Kniazeva, T.F. 2000, Astronomy Letters, 26, 129

Kniazev, A.Y., Pustilnik, S.A., Ugryumov, A.V., & Pramsky, A.G. 2001, A&A, 371, 404

Kniazev, A.Y., Grebel, E.K., Hao, L., Strauss, M., Brinkmann, J. & Fukugita, M., 2003, ApJ, 593, L73

Kniazev, A.Y., Grebel, E.K., Pustilnik, S.A., Pramskij, A.G., Kniazeva, T.F., Prada, F., & Harbeck, D. 2004, AJ, 127, 704

Korn, G.A., & Korn, T.M. 1968, Mathematical handbook for scientist and engineers, second, enlarged and revised edition, McGraw-Hill Book Company

Kunth, D., & Östlin, G., 2000, A&A Rev., 10, 1

Lee, H., McCall, M.L., & Richer, M.G. 2003, AJ, 125, 2975

Lewis D.W., McAlpine G.M. & Weedman D.W. 1979, ApJ, 233, 787

Lupton, R., Gunn, J.E., Ivezić, Z., Knapp, G.R., Kent, S., & Yasuda, N. 2001, in Astronomical Data Analysis Software and Systems X, ASP Conf. Ser. 238, eds. F. R. Harnden, Jr., F. A. Primini, & H. E. Payne (San Francisco: ASP), 269

Markarian, B.E., Lipovetsky, V.A., & Stepanian, J.A., 1983, Astrofizika, 19, 29

Masegosa, J., Moles, M., & Campos-Aguilar, A. 1994, ApJ, 420, 576

Matteucci, F. The chemical evolution of the Galaxy, Dordrecht, Kluwer Academic Publishers, 2001

McAlpine, G.M., Smith, S.B., & Lewis, D.W. 1977, ApJS, 34, 95

McAlpine, G.M., & Lewis, D.W. 1978, ApJS, 36, 587

McGaugh, S.S. 1991, ApJ, 380, 140

Melbourne, J. & Salzer, J.J., 2002, AJ, 123, 2302

Pagel, B.E.J. Nucleosynthesis and chemical evolution of galaxies, Cambridge Univ. Press, 1997

Pagel, B.E.J., Edmunds, M.G., Blackwell, D.E., Chun, M.S., Smith, G. 1979, MNRAS, 189, 95

Pesch, P., & Sanduleak, N. 1983, ApJS, 51, 171

Pier, J.R., Munn, J.A., Hindsley, R.B, Hennessy, G.S., Kent, S.M., Lupton, R.H., & Ivezic, Z. 2003, AJ, 125, 1559

Pilyugin, L.S. 2001, A&A, 374, 412

Pilyugin, L.S. 2003, A&A, 399, 1003

Popescu, C., Hopp, U., Hagen, H.-J., & Elsasser, H. 1996, A&AS, 116, 43

Pustilnik, S.A., Engels, D., Ugryumov, A.V., Lipovetsky, V.A., Hagen, H.-J., Kniazev, A.Y., Izotov, Y.I., & Richter, G.. 1999, A&AS, 137, 299

Pustilnik, S.A., Kniazev, A.Y., Masegosa, J., Márquez I., Pramsky A.G., & Ugryumov A.V. 2002, A&A, 389, 779

Pustilnik, S.A., Martin, J.-M., Huchtmeier, W., Brosch, N., Lipovetsky V., Richter, G. 2002, A&A, 389, 405

Pustilnik, S.A., Kniazev, A.Y., Pramskij, A.G., & Ugryumov, A.V., 2003a, ApSS, 284, 795

Pustilnik, S.A., Kniazev, A.Y., Pramskij, A.G., Ugryumov, A.V., & Masegosa, J. 2003b, A&A, 409, 917

Richards, G.T., Fan, X., Newberg, H.J., et al. 2002, AJ, 123, 2945

Salzer, J.J., McAlpine, G.M., & Boroson, T.A. 1989, ApJS, 70, 479

Salzer, J.J., Moody, J.W., Rosenberg, J.L., Gregory, S.A., & Newberry, M.V. 1995, AJ, 109, 2376

Salzer, J.J., Gronwall, C., Lipovetsky, V., Kniazev, A., Moody, J.W., Boroson, T., Thuan, T.X., Izotov, Y., Herrero, J., Frattare, L. 2000, AJ, 120, 80

Schaerer, D., & Vacca, W.D. 1998, ApJ, 497, 618

Schaerer, D., Contini, T., & Pindao, M. 1999, A&AS, 136, 35 (SCP99)

Shergin, V.S., Kniazev, A.Y., & Lipovetsky, V.A. 1996, Astronomische Nachrichten, 2, 95

Skillman, E.D., & Kennicutt, R.C. 1993, ApJ, 411, 655

Searle, L., & Sargent, W.L.W., 1972, ApJ, 173, 25

Smith, M.G., Aguirre, C., & Zemelman, M. 1976, ApJS, 32, 217

Smith, J.A., Tucker, D.L., Kent, S. et al. 2002, AJ, 123, 2121

Stasinska, G. 1990, A&AS, 83, 501

Stasinska, G., & Izotov, Y.I. 2003, A&A, 397, 71

Stoughton, C. et al. 2002, AJ, 123, 485

Strauss, M.A., Weinberg, D.H., Lupton, R.H., et al. 2002, AJ, 124, 1810

Terlevich, R., Melnick, J., Masegosa, J., Moles, M., Copetti, M.V.F. 1991, A&A, 91, 285

Thuan, T.X., Izotov, Y.I., & Lipovetsky, V.A. 1995, ApJ, 445, 108

Ugryumov, A.V., Pustilnik, S.A., Lipovetsky V.A., Richter, G., Izotov, Y.I. 1998, A&AS, 131, 285

Ugryumov, A.V., Engels, D., Lipovetsky, V., Hagen, H.-J., Hopp, U., Pustilnik, S.A., Kniazev, A.Y., Richter, G., Izotov, Y., Popescu, C., 1999, A&AS, 135, 511

Ugryumov, A. V., Engels, D., Kniazev, A. Y., et al. 2001, A&A, 374, 907

Ugryumov, A.V., Engels, D., Pustilnik, S.A., Kniazev, A.Y., Pramsky, A.G., & Hagen, H.-J. 2003, A&A, 397, 463

Veilleux, S., & Osterbrock, D.E. 1987, ApJS, 63, 295

Vilchez, J.M., & Iglesias-Páramo,J. 2003, ApJS, 145, 225

Whitford, A.E. 1958, AJ, 63, 201

York, D.G., Adelman, J., Anderson, J.E. et al. 2000, AJ, 120, 1579

This preprint was prepared with the AAS LaTeX macros v5.2.

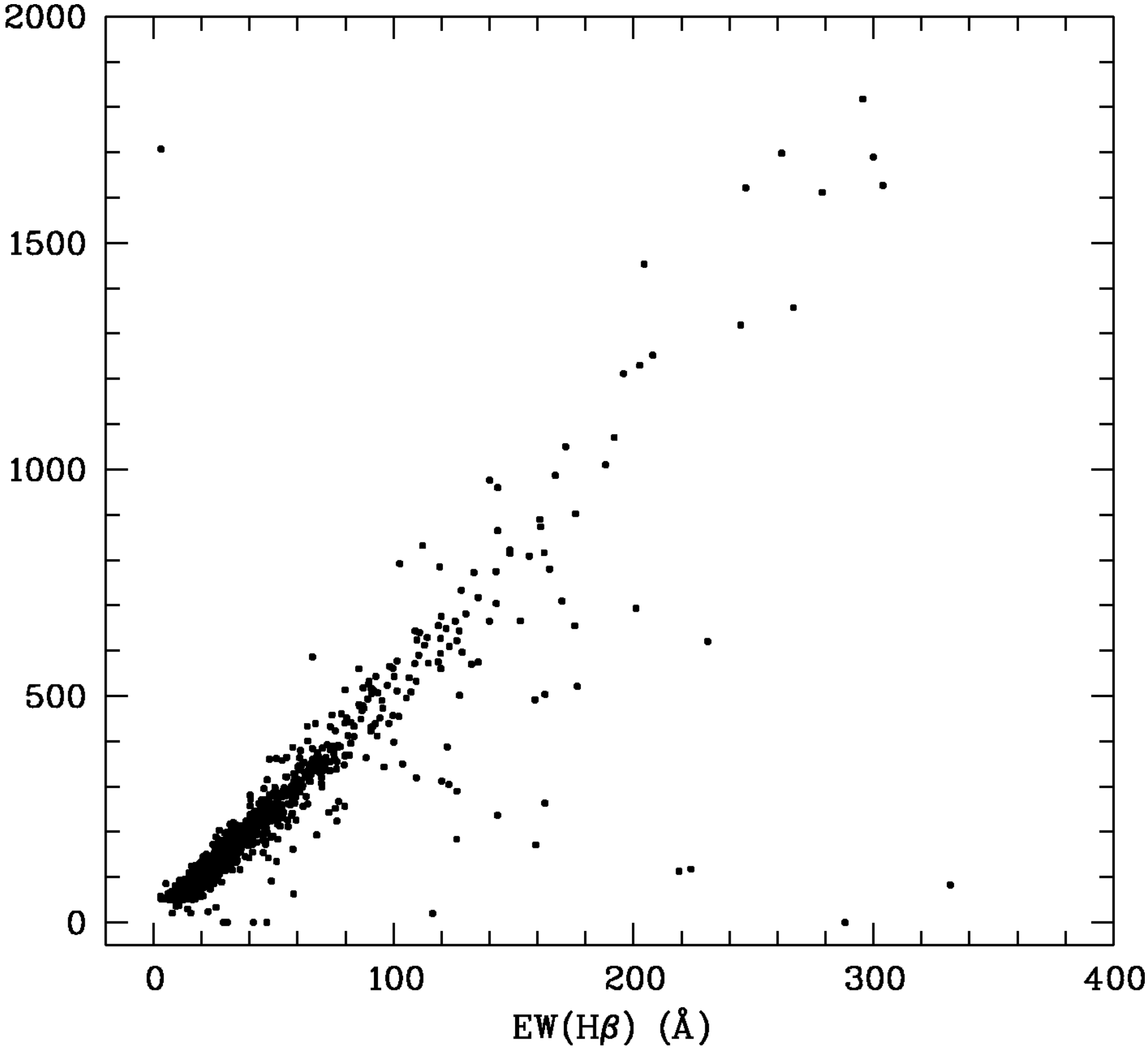

Fig. 1.— The relation between the EWs of the Hβ and Hα lines for all preselected ELGs ($\sim$5000 spectra). The truncation of the Hα line is seen in all spectra whose points are located significantly below the main locus.

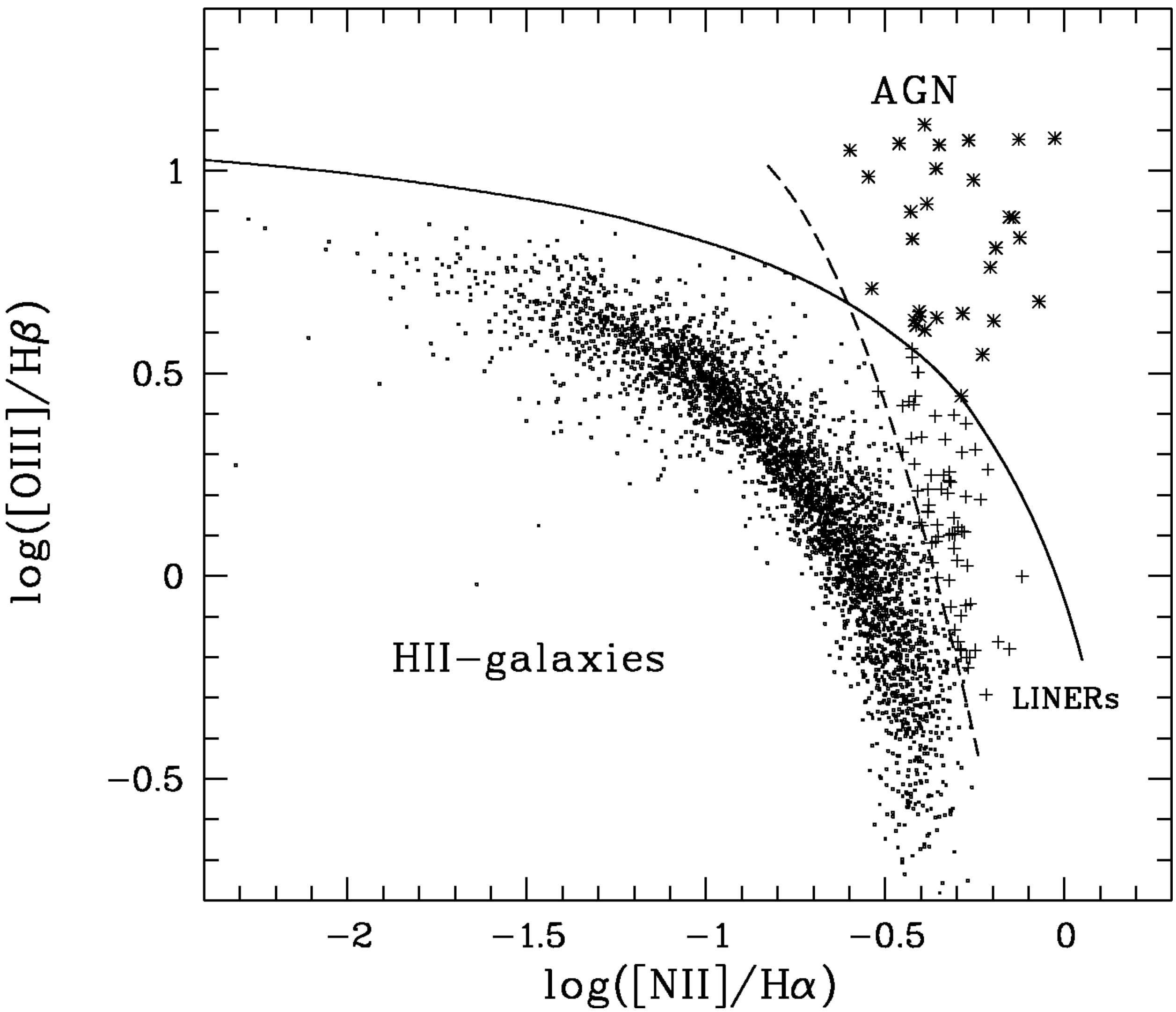

Fig. 2.— Classification diagram for all preselected ELGs ($\sim$ 5000 spectra). Galaxies identified as AGN are shown as asterisks and galaxies identified as LINERs are shown as crosses. The other ELGs are plotted as filled circles. The dashed line separates regions of HII-type and AGN/LINER spectra following Veilleux & Osterbrock (1987) and Baldwin, Phillips, & Terlevich (1981). The solid line shows models from Kewley et al. (2001) that were used for AGN/LINER separation.

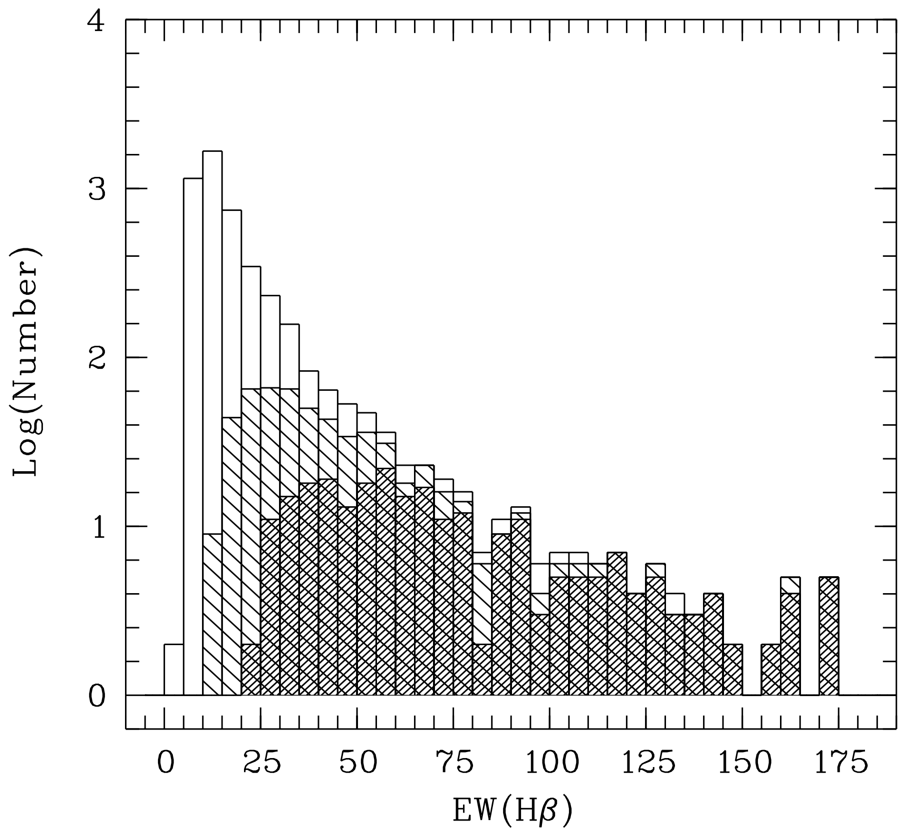

Fig. 3.— Distributions of EW(Hβ): all preselected ELGs (open bins, 4773 spectra), the final selected sample with an accuracy of log(O/H) $\leq$ 0.2 dex (hashed bins, 624 spectra) and the sample with an accuracy of log(O/H) $\leq$ 0.1 dex (double-hashed bins, 272 spectra). 17 galaxies are outside the plot region, having EW(Hβ) up to 356 Å. All of them have an accuracy of log(O/H) $\leq$ 0.1 dex. All AGNs and repeated observations are not shown in the plot.

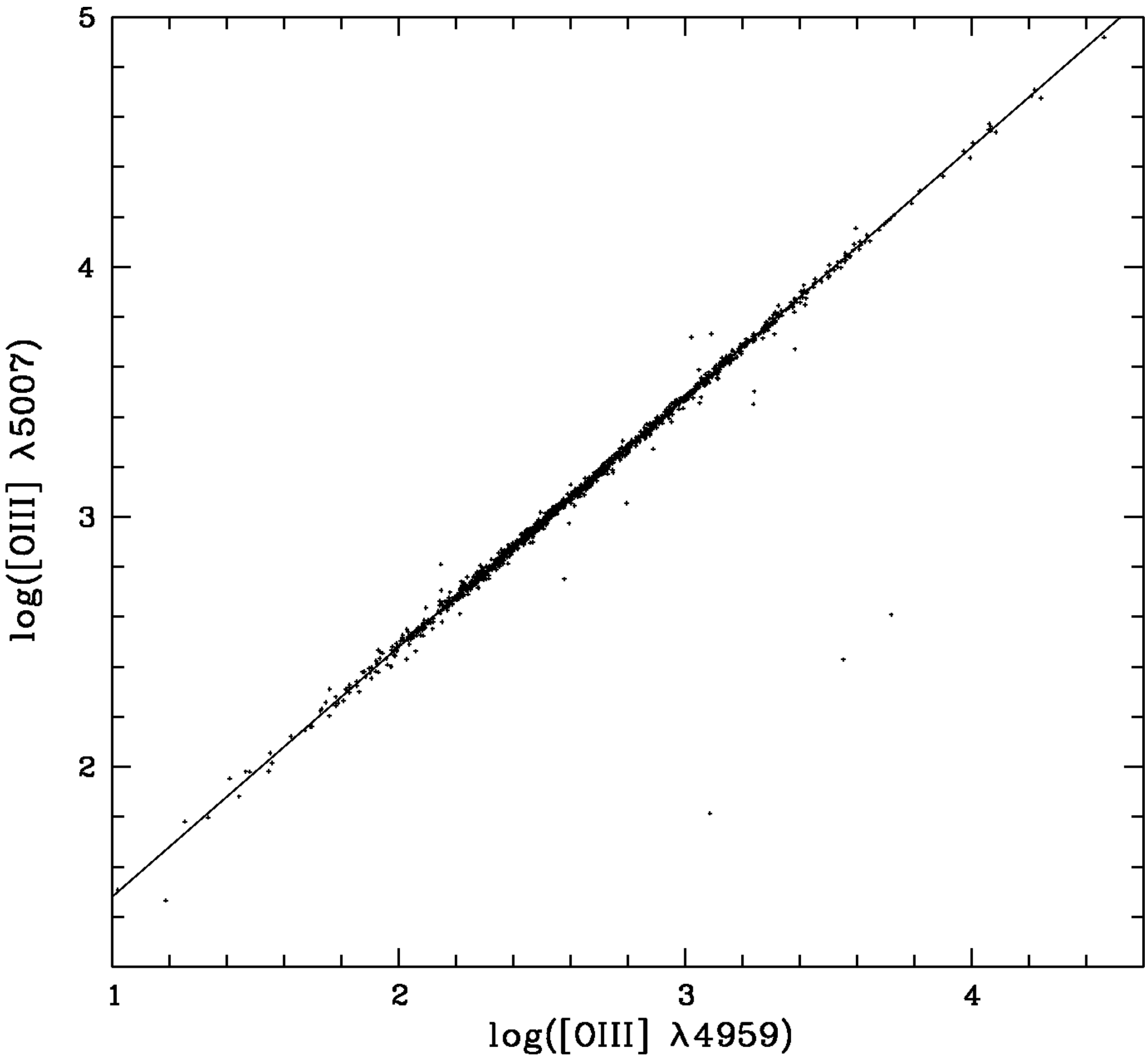

Fig. 4.— Plot of the logarithmic flux of [O III] $\lambda4959$ Å versus logarithmic flux of [O III] $\lambda5007$ Å (fluxes for the presented lines are given in units of 10^{-17} erg s^{-1} sm^{-2} Å^{-1}). The solid line corresponds to the ratio $F(\lambda5007)/F(\lambda4959) = 3$. No systematic trend is visible. Some cases are seen where either the line [O III] $\lambda5007$ Å (points below the line), or [O III] $\lambda4959$ Å (points above the line) are truncated, which indicates problems with the SDSS reduction system and/or saturation.

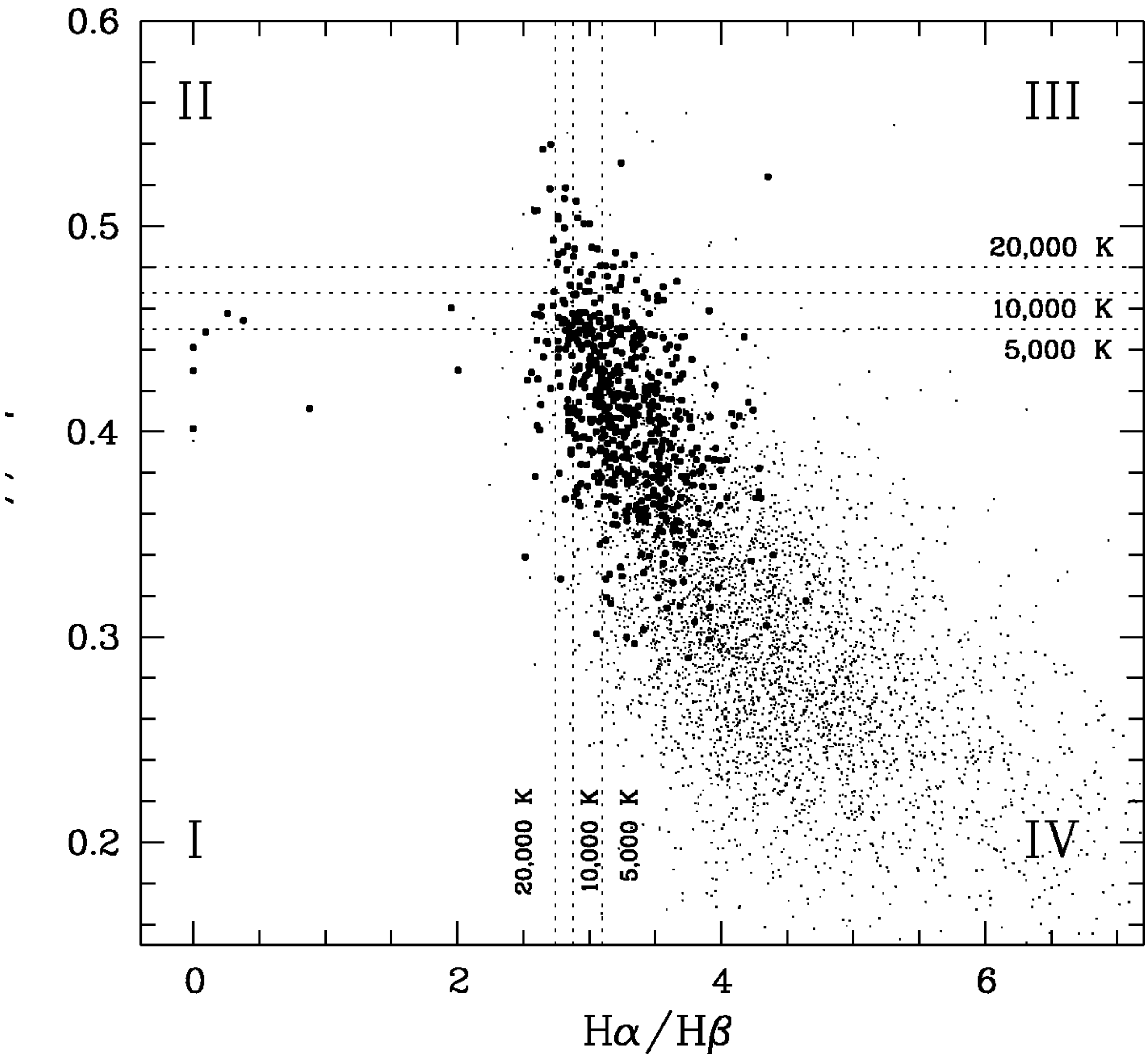

Fig. 5.— Plot of the observed Hγ/Hβ versus Hα/Hβ flux ratios to show truncation problems and distribution of these strong line ratios. The three dotted lines correspond to the theoretical Balmer lines ratios for T_e = 5,000, 10,000 and 20,000 K. Filled circles denote the spectra from the SHOC, while points indicate all other ∼ 5000 preselected ELGs. Only the area marked "IV" is the correct region for the two Balmer line intensity ratios. It should be noted that among spectra located in regions "I","II", and "III", truncated spectra are selected for which the measured line ratios differ from theoretical Balmer lines ratios by more than 5σ (see equation 9).

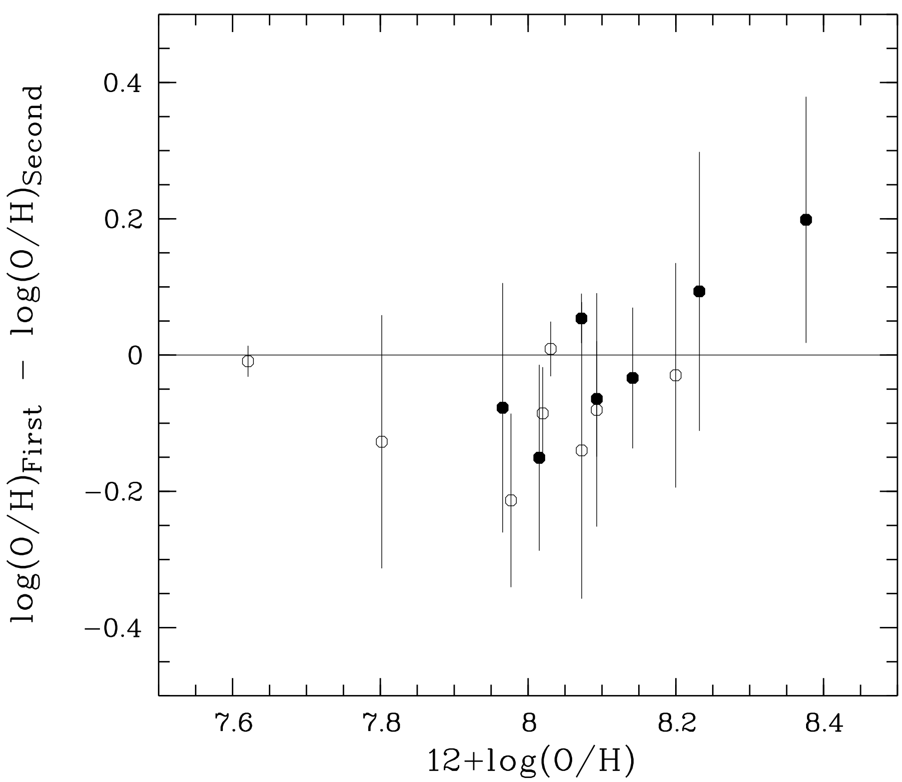

Fig. 6.— Comparison of calculated oxygen abundances for catalog galaxies with two independent observations. The differences Δ (First−Second) = $\log(\mathrm{O/H})_{\mathrm{First}}$–$\log(\mathrm{O/H})_{\mathrm{Second}}$, with their total r.m.s. uncertainties are plotted versus the value 12+log(O/H) for the more accurate ('First') of two measurements. The filled circles denote 7 galaxies without detected [O II] λ3727 Å; the [O II] λλ7320,7330 Å lines were used to compute $\mathrm{O^+/H^+}$.

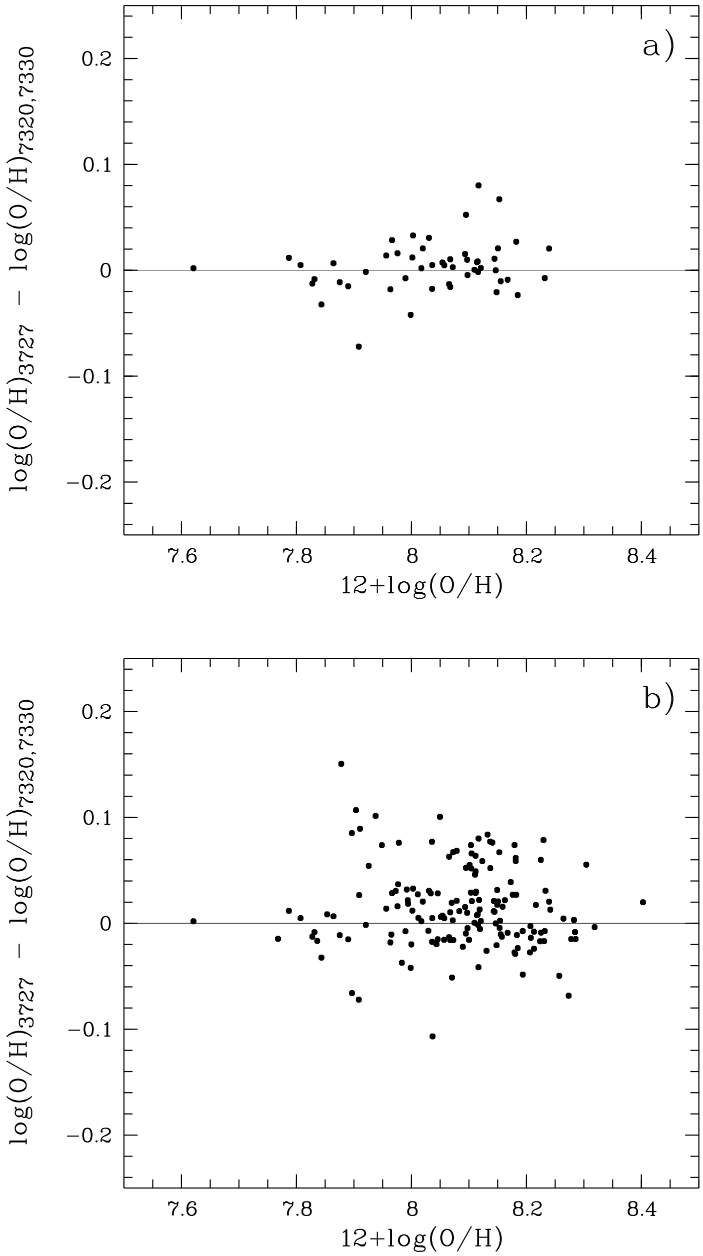

Fig. 7.— Differences of logarithmic total oxygen abundances $\log(\mathrm{O/H})_{3727} - \log(\mathrm{O/H})_{7320,7330}$ (where $\log(\mathrm{O/H})_{3727}$ means 12+log(O/H) with the use of [O II] λ3727 Å, and $\log(\mathrm{O/H})_{7320,7330}$ means 12+log(O/H) with use of [O II] λ7320,7330 Å lines) versus 12+log(O/H), for objects with $z \geq 0.024$: a) SHOC galaxies with an accuracy of log(O/H) $\leq$ 0.05 dex and b) SHOC galaxies with an accuracy of log(O/H) $\leq$ 0.1 dex.

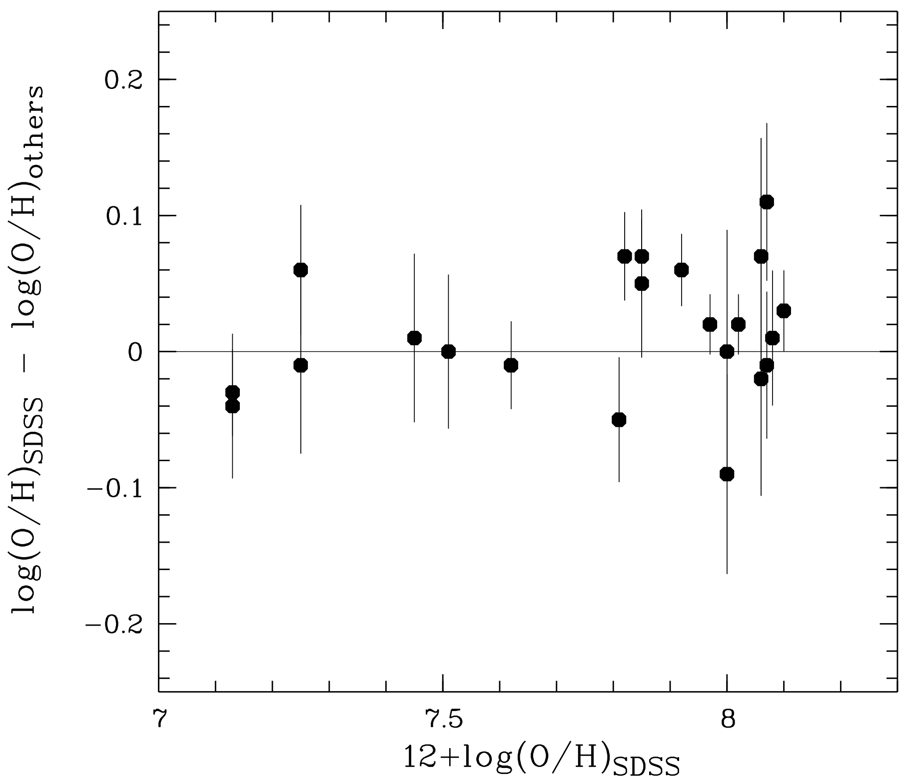

Fig. 8.— A comparison of 22 independent measurements of 15 strong-line ELGs taken from previous works. Plot of differences of logarithmic total oxygen abundances Δ log(O/H) = log(O/H)$_{\rm SDSS}-$log(O/H)$_{\rm others}$ versus 12+log(O/H)$_{\rm SDSS}$, with the error bars corresponding to the total r.m.s. uncertainties of these differences. All presented data are from Table 5.

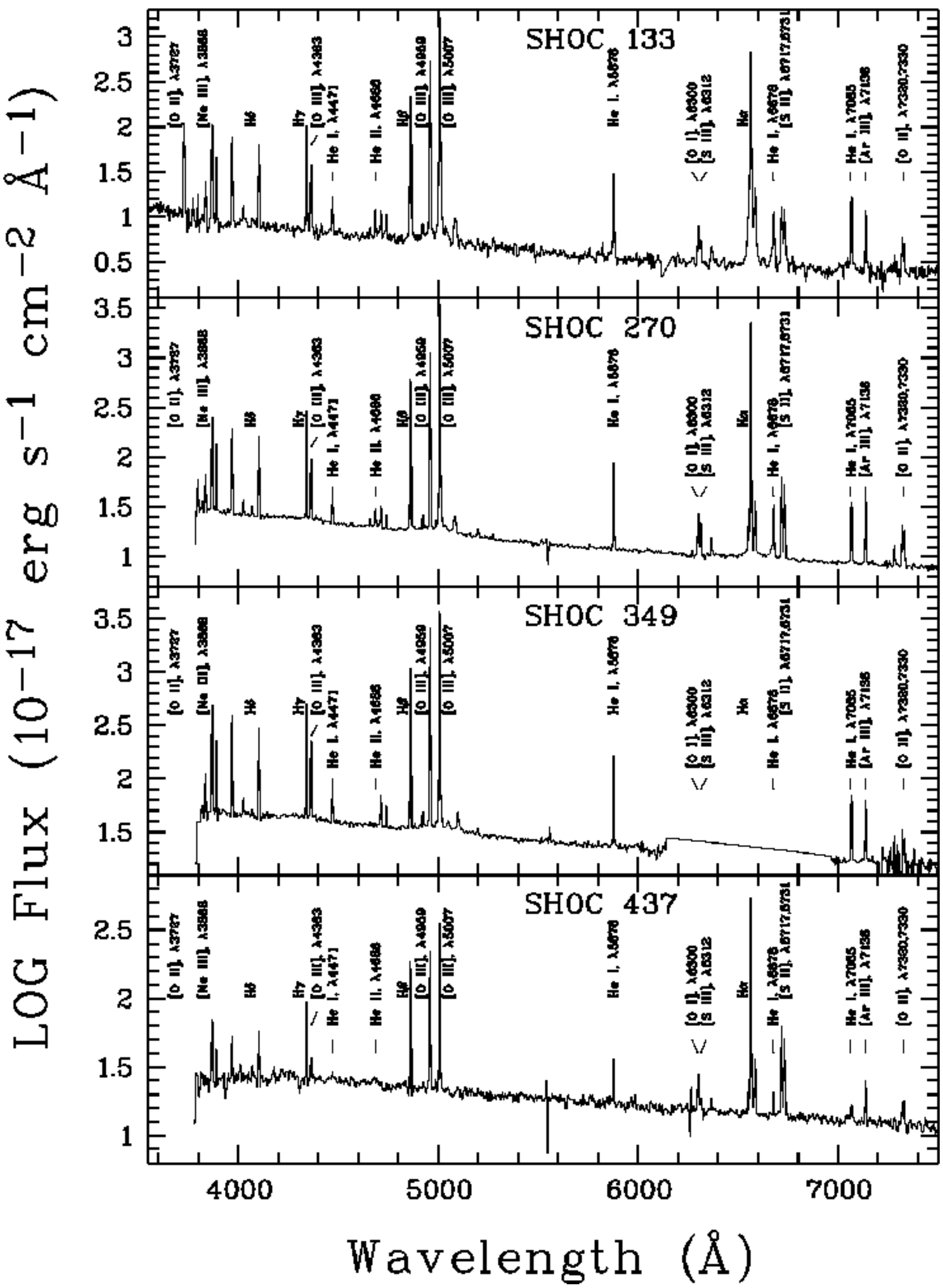

Fig. 9.— Examples of spectra from the catalog over the rest-frame wavelength range of 3600 Å to 7500 Å. All spectra are shown in logarithmic scale to see both strong and weak emission lines simultaneously. Note that of the four galaxies, the line [O II] λ3727 Å is seen only for SHOC 133 (SDSS J024052.20−082827.4) (z=0.08221). In the spectrum of SHOC 349 (SDSS J115133.36−022222.0) all lines are truncated in the spectral region around the Hα line.

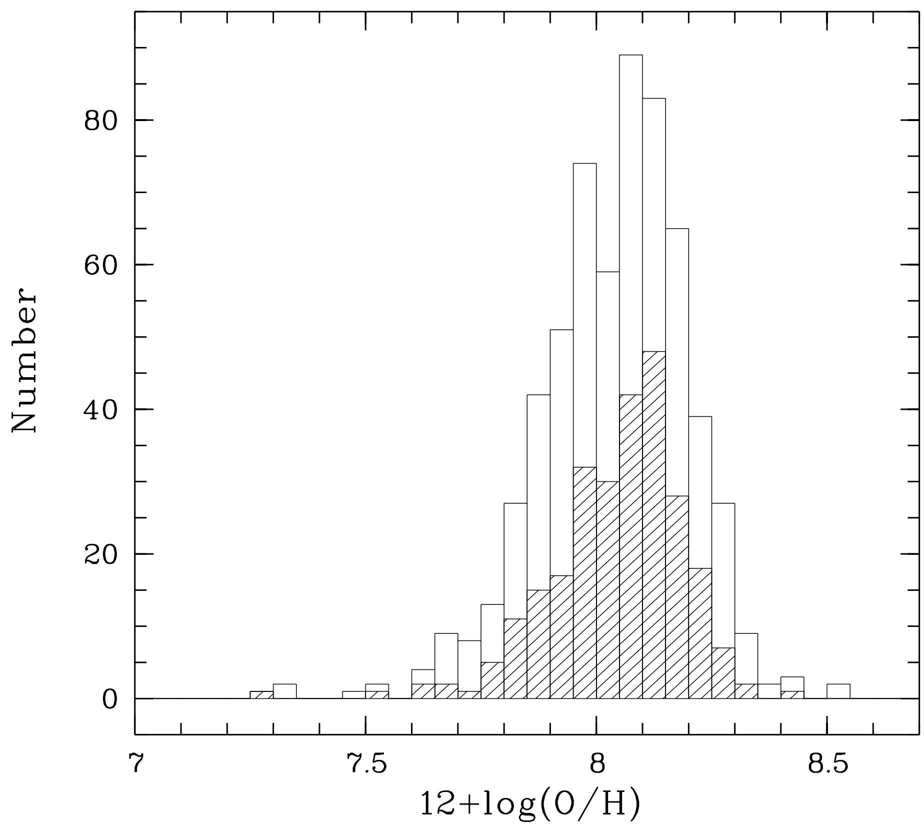

Fig. 10.— The metallicity distribution of all ELGs from our catalog, as measured by their oxygen abundances. Where observations exist for multiple knots in a given galaxy, only metallicity for knot “a” is shown. The open histogram shows the metallicity distribution for 612 galaxies with an accuracy of log(O/H) $\leq$ 0.2 dex (mean = 8.04, σ = 0.16, median = 8.06). The hashed histogram shows the metallicity distribution for 263 galaxies with an accuracy of log(O/H) $\leq$ 0.1 dex (mean = 8.05, σ = 0.14, median = 8.07).

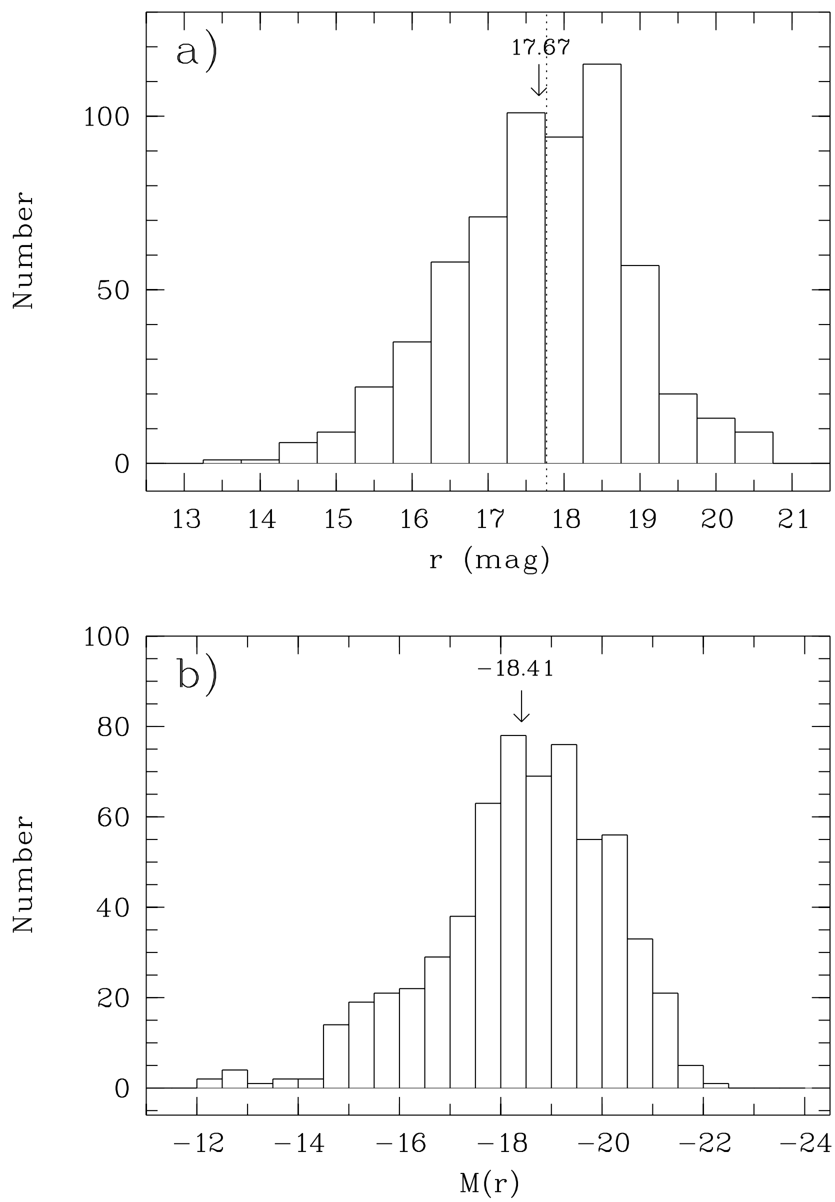

Fig. 11.— Distributions of apparent r-magnitudes (a) and absolute r-magnitudes (b) for SDSS-selected HII galaxies with accuracies of log(O/H) $\leq$ 0.2 dex. The arrows indicate median values. The dotted vertical line in panel (a) marks the SDSS spectroscopic limit r = $17\overset{\mathrm{m}}{.}77$ (Strauss et al. 2002).

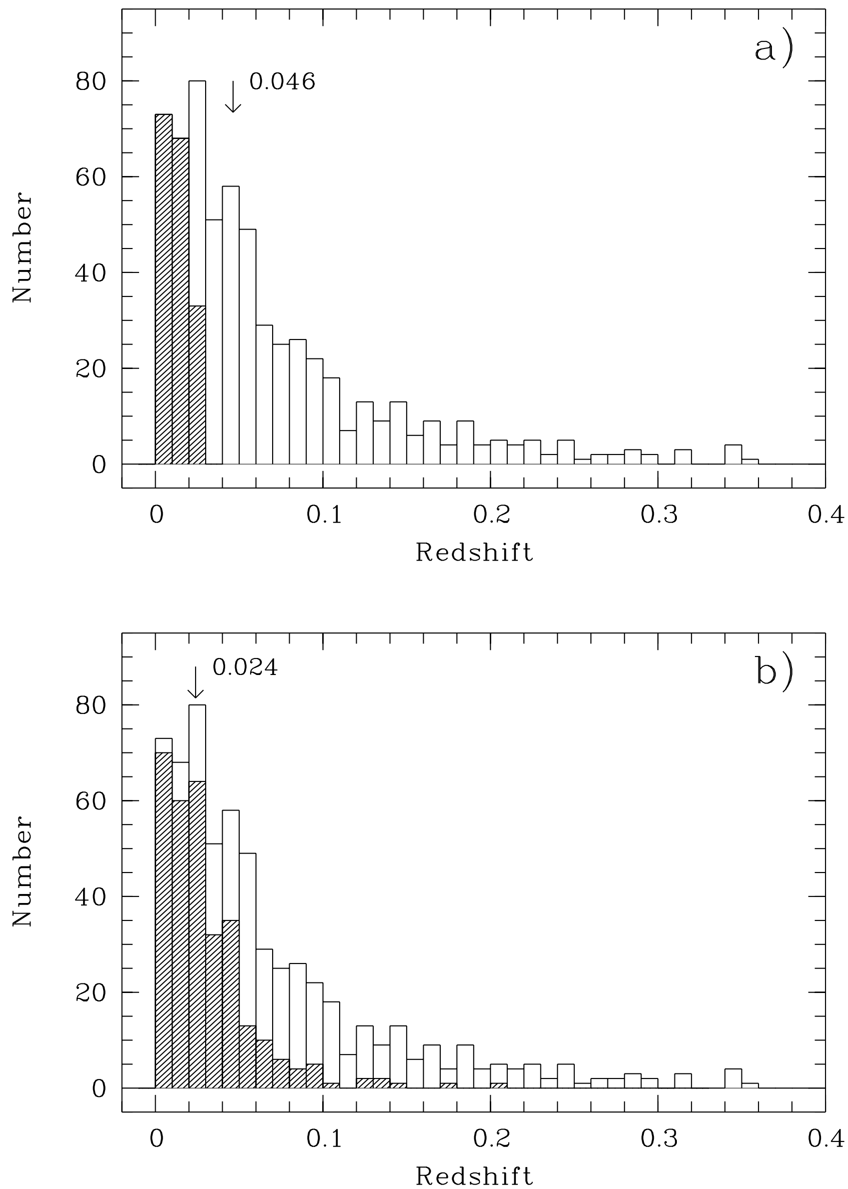

Fig. 12.— Distributions of redshifts for the SHOC galaxies. a) All 612 galaxies (open histogram) and 174 objects (hashed histogram) for which only [O II] λ7320,7330 Å were used for O^+/H^+ calculation. The arrow indicates the median redshift for all galaxies. b) All galaxies (open histogram) and magnitude limited sample of galaxies with r-magnitudes are brighter than $17\overset{m}{.}77$ (hashed histogram). The arrow indicates the median redshift for the magnitude-limited sample.

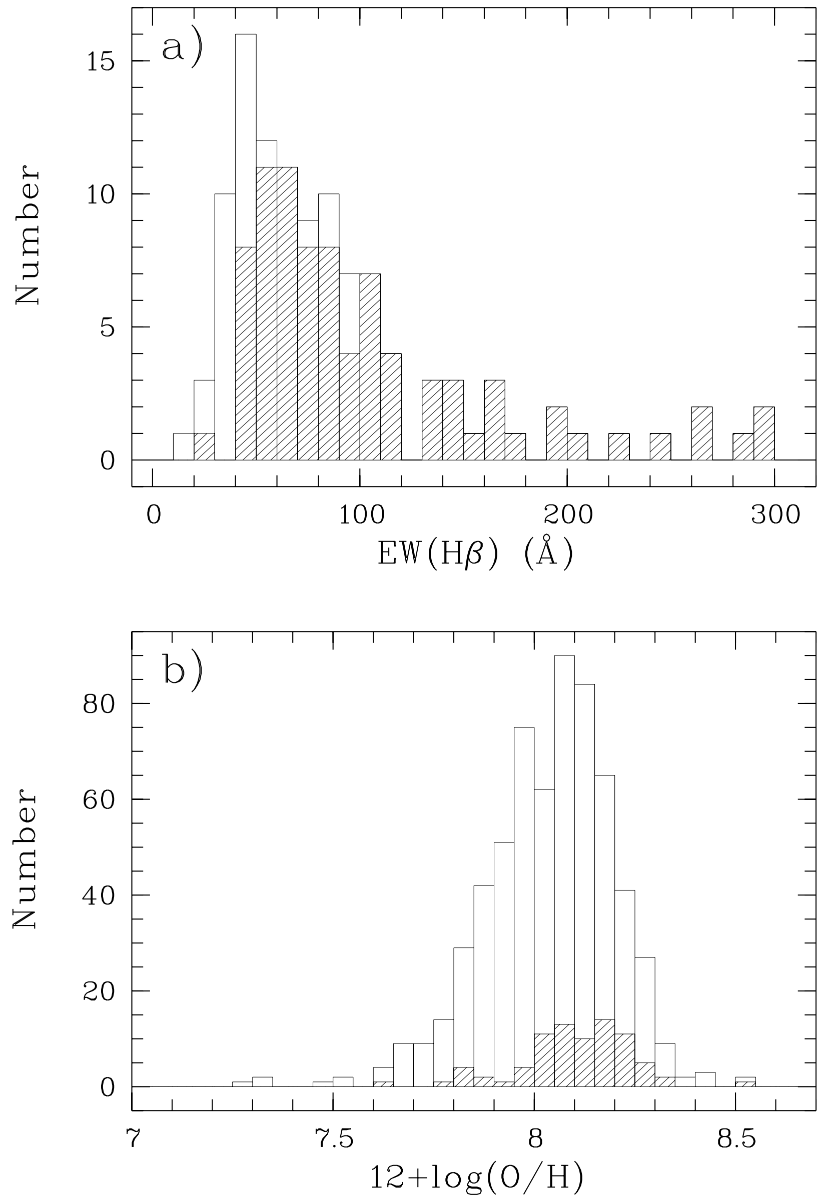

Fig. 13.— a) Distribution of EW(Hβ) for all 109 detected WR-galaxies from this work (open histogram) and 81 WR-galaxies from the catalog (hashed histogram). b) The oxygen abundance distribution (open histogram) of galaxies from the SHOC and similar distribution of WR-galaxies (hashed histogram) in the SHOC (81 galaxies).

Table 1. General parameters of the Strong Emission Line HII galaxies from SDSS DR1 with an oxygen abundance accuracy of ≤0.2 dex

SHOC ID[a] (1)	SDSS name (2)	Plate,MJD,Fiber (3)	r (4)	z (5)	WR[b] (6)	Trun (7)	Class (8)	Comments (9)
1	SDSS J000439.33−100909.3	650 52143 61	17.93	0.10842	0	0000	BCG	
2	SDSS J000657.03+005125.9	388 51793 457	18.81	0.07358	0	0000	BCG	UM 199
3	SDSS J000703.99−003447.5	388 51793 239	18.69	0.12129	0	0000	BCG	
4	SDSS J000706.61−085051.1	651 52141 408	18.04	0.03568	0	0000	BCG	
5	SDSS J000847.56−085905.5	651 52141 452	17.62	0.02662	0	0000	BCG	
6	SDSS J001327.48−001855.9	389 51795 266	18.54	0.04329	0	0000	BCG	UM 214
7	SDSS J001354.80+005427.3	389 51795 405	19.16	0.08466	0	0000	BCG	
8	SDSS J001647.76−104742.3	652 52138 90	16.08	0.02324	0	0000	Irr?	
9	SDSS J001739.96+003022.3	389 51795 544	16.73	0.01732	0	0000	Irr?	UM 225
10	SDSS J002021.62+003021.6	390 51900 430	19.07	0.10560	1	0000	BCG	
11[c]	SDSS J002101.03+005248.0	390 51900 445	17.54	0.09839	3*	0000	BCG	UM 228, LBQS 0018+0036
12	SDSS J002146.52+001902.4	390 51900 463	18.76	0.10699	0	0000	BCG?	
13	SDSS J002335.40−093022.2	653 52145 470	16.45	0.01801	0	0000	BCG	
14	SDSS J002339.62−094848.6	653 52145 462	17.91	0.05301	3	0000	BCG?	
15	SDSS J002501.27−005337.3	390 51900 10	18.48	0.04021	0	0000	BCG	
16	SDSS J002507.43+001845.6	391 51782 394	17.14	0.01089	0	0000	Irr	UM 240
17	SDSS J002519.92+003131.1	390 51900 596	16.14	0.01412	0	0000	BCG	UM 241
18	SDSS J002727.90−105734.2	653 52145 56	17.19	0.07777	0	0000	BCG	
19	SDSS J002735.85+011541.0	391 51782 445	18.89	0.04026	0	0000	BCG	
20	SDSS J003127.55−104032.8	654 52146 219	17.48	0.01181	0	0001	LSBG	
21	SDSS J003145.29−110656.8	654 52146 122	18.28	0.01377	0	0000	Irr	
22	SDSS J003218.59+150014.0	417 51821 513	16.66	0.01787	3	0000	BCG	HS 0029+1443
	SDSS J003218.59+150014.0	418 51817 302	16.66	0.01798	3	0000	BCG	HS 0029+1443
23	SDSS J003520.00+001556.8	392 51793 423	18.23	0.05574	0	0000	BCG	
24	SDSS J003748.48+145558.0	418 51817 173	17.76	0.01801	0	0000	Irr	
25	SDSS J003927.31+140828.3	418 51817 97	18.61	0.09384	0	0000	BCG	
26	SDSS J004054.31+153409.8	419 51879 335	20.03	0.28330	0	0000	BCG	
27	SDSS J004100.55+003951.4	393 51794 348	18.08	0.06139	0	0000	BCG	
28	SDSS J004236.94+160202.7	419 51879 364	19.40	0.24731	0	0000	BCG	
29	SDSS J004529.16+133908.6	419 51879 137	20.54	0.29522	0	0000	BCG?	
30	SDSS J004608.81−102430.9	656 52148 176	17.93	0.01304	0	0000	BCG	
31	SDSS J004633.12+160312.2	419 51879 568	18.34	0.05621	0	0000	BCG	
32	SDSS J004645.72−105410.4	656 52148 140	17.76	0.03647	0	0000	BCG	
33	SDSS J004651.19+010022.7	393 51794 605	18.17	0.05657	0	0001	BCG	
34	SDSS J004958.70+155247.2	420 51871 328	18.78	0.04984	0	0000	BCG	
35	SDSS J005105.28+004600.1	394 51913 402	18.85	0.05573	0	0000	BCG	

Table 1—Continued

SHOC ID[a] (1)	SDSS name (2)	Plate,MJD,Fiber (3)	r (4)	z (5)	WR[b] (6)	Trun (7)	Class (8)	Comments (9)
36	SDSS J005147.30+000940.0	394 51913 472	18.51	0.03758	1	0000	BCG	UM 282, HS 0049-0006, UCM 0049-0006
37	SDSS J005149.42+003353.2	394 51913 461	16.40	0.01553	2	0000	Irr?	UM 283, HARO 0049.3+00, UCM 0049+0017
38	SDSS J005249.80−084133.9	657 52177 405	18.96	0.05274	0	0000	BCG	
39	SDSS J005300.53+150129.6	420 51871 474	17.73	0.03818	0	0000	BCG	
40	SDSS J005319.63−102411.8	657 52177 193	15.84	0.01471	0	0000	BCG	
41	SDSS J005425.68+144852.2	420 51871 156	17.97	0.04051	0	0000	BCG	
42	SDSS J005527.46−002148.7	394 51913 75	18.10	0.16745	3	0000	BCG	LBQS 0052-0038
43	SDSS J005602.26−101009.4	658 52146 312	18.31	0.05817	0	0000	BCG	
44	SDSS J005855.46+010017.4	395 51783 451	16.49	0.01784	0	0010	Irr	UM 295, UCM 0056+0044
45	SDSS J005904.10+010004.1	395 51783 525	15.99	0.01783	0	0000	BCG	UM 296, HARO 0056.5+00
46	SDSS J010005.93−011058.9	395 51783 58	17.78	0.05140	0	0000	BCG	
47	SDSS J010040.08−092817.2	658 52146 509	17.91	0.07696	0	0000	BCG	
48	SDSS J010059.66+011228.1	395 51783 570	17.00	0.04171	0	0000	BCG	UM 298, HARO 0058.4+00
49	SDSS J010409.91−095346.8	659 52199 307	18.81	0.06727	0	0000	BCG	
50	SDSS J010513.49−103740.8	658 52146 17	18.81	0.06234	0	0000	BCG	
51	SDSS J010526.30+000942.1	396 51816 498	19.07	0.06739	0	0000	BCG	
52	SDSS J010643.32−092223.2	659 52199 435	18.88	0.06733	0	0000	BCG	
53	SDSS J010907.97+010715.5	397 51794 336	16.43	0.00395	0	0000	LSBG	
54	SDSS J011354.58+153947.8	423 51821 402	18.05	0.07298	0	0000	BCG	
55	SDSS J011500.55−100217.1	659 52199 33	15.98	0.02277	0	0000	BCG	MBG 01125-1018
56[d]	SDSS J011534.39−005146.0	398 51789 294	16.74	0.00559	3	0100	Sp(sa)	NGC 04050
57	SDSS J011616.82−085021.4	660 52177 414	17.86	0.06247	0	0000	BCG	
58	SDSS J011633.94−002043.1	398 51789 223	18.14	0.04098	0	0001	BCG	
59	SDSS J011729.09−084403.7	660 52177 450	17.94	0.16650	0	0000	BCG	
60	SDSS J011833.24−091258.2	660 52177 543	17.49	0.03397	0	0000	BCG?	
61	SDSS J011914.28−093546.2	660 52177 591	18.15	0.00644	0	0000	Irr	
62	SDSS J012213.87+005731.4	399 51817 324	19.58	0.00744	0	0000	Sp(sa)	NGC 0493, UGC 00914
63	SDSS J012223.90+152031.9	424 51893 368	18.63	0.15288	0	0000	BCG	
64	SDSS J012402.40−091617.2	661 52163 497	18.90	0.04943	0	0000	BCG	
65	SDSS J012542.89−091710.7	661 52163 542	17.83	0.03156	0	0010	BCG	
66	SDSS J012646.58−003845.9	399 51817 140	15.64	0.00638	0	0010	BCG?	UM 323
67	SDSS J012947.98+134944.7	425 51898 181	18.30	0.03848	0	0000	BCG	
68	SDSS J013010.66−085250.9	662 52147 333	17.75	0.14410	0	0000	BCG	
69	SDSS J013048.22+144349.8	425 51898 500	17.53	0.02319	0	0000	LSBG	
70	SDSS J013111.95+153240.2	425 51898 537	18.52	0.05474	0	0000	BCG	
71	SDSS J013126.59+140615.1	425 51898 173	16.73	0.01392	0	0000	BCG	

Table 1—Continued

SHOC ID[a] (1)	SDSS name (2)	Plate,MJD,Fiber (3)	r (4)	z (5)	WR[b] (6)	Trun (7)	Class (8)	Comments (9)
72	SDSS J013258.54−085337.6	662 52147 466	18.43	0.09517	0	0000	BCG	
73	SDSS J013344.64+005711.2	400 51820 441	17.84	0.01916	0	0101	BCG	UM 336, SCHG 0131+007
74	SDSS J013526.02−101818.7	663 52145 282	17.34	0.04132	0	0000	BCG	
75	SDSS J013700.31+144157.1	425 51898 634	17.37	0.04475	0	0000	BCG	
76	SDSS J013706.41−103153.7	663 52145 288	17.52	0.02657	0	0000	BCG	
77	SDSS J013711.14+005256.7	400 51820 568	17.21	0.01896	0	0000	BCG	UM 345
78	SDSS J013844.90−083540.7	663 52145 406	18.49	0.05356	0	0000	BCG	
79a	SDSS J014137.22−091435.2	664 52174 355	16.82	0.01807	0	0000	BCG	
79b	SDSS J014137.39−091437.0	663 52145 588	17.53	0.01798	0	0000	BCG	
80	SDSS J014357.12−100954.3	663 52145 29	18.49	0.14370	0	0000	BCG	
81	SDSS J014540.58−003341.6	401 51788 66	18.16	0.08318	0	0000	BCG	
82	SDSS J014637.06+144121.4	429 51820 456	16.81	0.02442	0	0000	Sp(sa)	UGC 01242, CGCG 437-024
83	SDSS J014652.37−090812.3	664 52174 541	18.52	0.05112	0	0000	BCG	
84	SDSS J014707.03+135629.4	429 51820 495	18.57	0.05665	3	0000	BCG	
85	SDSS J014713.82−080702.8	664 52174 447	18.34	0.03925	0	0000	BCG	
86	SDSS J014721.67−091646.2	664 52174 112	19.11	0.13564	0	0000	BCG	
87	SDSS J015103.02+010830.9	402 51793 407	18.32	0.04249	0	0000	BCG	
88	SDSS J015256.74−081902.9	665 52168 402	18.52	0.13583	0	0000	BCG	
89	SDSS J015346.92−004901.7	402 51793 49	18.73	0.11552	0	0000	BCG?	
90	SDSS J015400.50−004509.8	402 51793 59	20.17	0.01573	0	0000	Sp(sa)	UGC 01365, KUG 0151-009, CGCG 386-050
91	SDSS J015408.47−094615.3	665 52168 159	17.54	0.01805	0	0000	BCG	
92	SDSS J015453.90+130721.7	430 51877 97	19.12	0.11887	0	0010	BCG	
93	SDSS J015507.37+135925.4	430 51877 560	17.50	0.05059	0	0000	Sp?	
94	SDSS J015550.59+145830.3	430 51877 522	17.41	0.06251	0	0000	BCG	
95	SDSS J015559.78−002641.4	402 51793 23	17.82	0.02718	0	0000	BCG	
96	SDSS J015606.19+003911.1	403 51871 468	17.55	0.02744	0	0010	BCG	UM 379
97	SDSS J015726.93−093212.4	666 52149 320	17.43	0.04307	0	0000	BCG?	
98	SDSS J015928.44−082104.6	666 52149 429	17.68	0.03401	0	0000	Irr?	
99	SDSS J015953.06−081348.9	666 52149 331	18.92	0.15166	0	0000	BCG	
100	SDSS J020038.66−005954.4	403 51871 48	17.97	0.25306	1	0000	BCG	
101	SDSS J020051.60−084542.9	666 52149 492	19.16	0.08670	0	0000	BCG?	
102	SDSS J020108.28+132660.0	427 51900 161	17.63	0.05175	0	0000	BCG	
103	SDSS J020332.59−095547.4	666 52149 87	17.08	0.01282	0	0000	Sp(sa)	NGC 0806, KUG 0201-101
104	SDSS J020356.90−080758.4	666 52149 532	18.65	0.18855	0	0000	BCG	
105	SDSS J020513.90+131427.9	428 51883 316	17.91	0.05859	0	0000	BCG	
106	SDSS J020549.13−094918.0	667 52163 289	17.83	0.00650	0	0000	LSBG	KUG 0203-100

Table 1—Continued

SHOC ID[a] (1)	SDSS name (2)	Plate,MJD,Fiber (3)	r (4)	z (5)	WR[b] (6)	Trun (7)	Class (8)	Comments (9)
107	SDSS J020656.64−011317.6	404 51812 86	17.80	0.04081	0	0000	BCG	
108	SDSS J020848.48−010804.4	404 51812 53	18.04	0.03558	0	0000	BCG	
109	SDSS J020905.16−094201.3	667 52163 188	16.54	0.01280	0	0000	BCG	KUG 0206-099A, KUV 02066-0956
110	SDSS J021159.98+011302.8	405 51816 365	16.99	0.02317	0	0000	Sp	UM 410, UM 410S, KUG 0209+009A
111	SDSS J021513.99−084624.3	667 52163 634	17.40	0.00495	0	0000	LSBG	
112	SDSS J021623.38−085842.4	668 52162 224	17.68	0.03306	0	0000	BCG	
113	SDSS J021852.92−091218.7	668 52162 152	18.46	0.01274	0	0000	BCG	
114	SDSS J021934.94−002432.1	405 51816 29	17.61	0.02593	0	0000	BCG	
115	SDSS J022037.66−092907.3	668 52162 89	18.95	0.11300	0	0000	BCG	
116	SDSS J022110.25−074544.3	668 52162 576	18.13	0.06745	0	0000	BCG	
117	SDSS J022237.82+002907.9	406 51869 478	19.51	0.02480	0	0000	Irr	
118	SDSS J022250.40−074709.4	454 51908 338	17.71	0.20295	0	0000	BCG	
119	SDSS J022407.68+003226.3	406 51869 484	18.26	0.07349	0	0000	BCG	
120	SDSS J022417.21+000625.9	406 51869 160	17.88	0.06761	0	0000	BCG	
121	SDSS J022658.03+003437.2	406 51869 589	16.79	0.02544	0	0000	BCG	
122	SDSS J022907.37−085726.1	454 51908 111	18.69	0.18270	0	0000	BCG	
123	SDSS J023132.23−004339.4	407 51820 176	19.27	0.00892	0	0000	Irr	
124	SDSS J023146.01−090847.6	454 51908 62	16.37	0.00541	3	0000	LSBG	
125	SDSS J023224.96+005750.8	407 51820 540	18.13	0.02334	0	0000	BCG	
126	SDSS J023238.11+003539.3	407 51820 509	15.51	0.02186	0	0000	BCG	KUG 0230+003A, CGCG 388-045
127	SDSS J023247.42+004041.1	407 51820 542	15.67	0.02285	0	0000	BCG	MRK 1047, KUG 0230+004
128	SDSS J023426.93−072807.7	455 51909 369	18.14	0.05331	0	0000	BCG	
129	SDSS J023628.78−005829.8	408 51821 296	17.68	0.00837	0	0000	Irr	
130	SDSS J023749.54−092556.1	455 51909 47	15.58	0.04463	0	0000	BCG	I Zw 007
131	SDSS J023900.79+001835.8	408 51821 472	19.81	0.21656	0	0000	BCG	
132	SDSS J023903.17−074825.2	455 51909 549	16.65	0.02413	0	0001	Irr?	
133	SDSS J024052.20−082827.4	456 51910 306	19.61	0.08221	0	0000	BCG	
134	SDSS J024453.66−082137.9	456 51910 195	19.08	0.07753	0	0000	BCG	
135	SDSS J024529.54−081637.8	456 51910 191	18.52	0.19553	0	0000	BCG	
136	SDSS J024736.53+002704.1	409 51871 465	17.41	0.07519	0	0000	BCG?	
137	SDSS J024815.94−081716.5	456 51910 76	16.65	0.00459	3	0010	Irr?	
138a	SDSS J024909.31−075027.3	457 51901 304	14.25	0.00430	0	0000	Sp(sa)	NGC 1110, UGCA 043
138b	SDSS J024910.78−074924.4	457 51901 309	15.21	0.00458	1	0010	Sp(sa)	NGC 1110, UGCA 043
139	SDSS J024914.59−085809.7	456 51910 17	17.95	0.05634	0	0000	BCG	
140	SDSS J024939.72−011151.3	409 51871 50	19.10	0.06720	0	0000	BCG	[CLA95] 024706.93-012415.1
141	SDSS J025325.30−001357.0	409 51871 33	17.01	0.02731	0	0000	Irr	KUG 0250-004

Table 1—Continued

SHOC ID[a] (1)	SDSS name (2)	Plate,MJD,Fiber (3)	r (4)	z (5)	WR[b] (6)	Trun (7)	Class (8)	Comments (9)
142	SDSS J025346.70−072343.9	457 51901 465	17.84	0.00452	0	0000	Irr	
143	SDSS J025426.11−004122.7	410 51816 220	17.17	0.01470	2	0000	BCG	US 3320, [CLA95] 025152.97-005332.3
144	SDSS J025436.12−000137.8	410 51816 181	18.76	0.02596	0	0000	BCG	
145	SDSS J025437.85−075157.6	457 51901 159	18.65	0.14740	0	0000	BCG	
146	SDSS J025536.26+005609.4	410 51816 538	18.61	0.06722	0	0000	BCG	
147	SDSS J030214.59−070940.0	458 51929 461	17.19	0.03837	0	0000	BCG	
148	SDSS J030321.41−075923.2	458 51929 185	18.74	0.16495	0	0000	BCG	
149	SDSS J030434.75−002830.8	411 51817 159	16.56	0.00565	0	0000	Irr	
150	SDSS J030457.96+005714.0	411 51817 578	17.57	0.01215	0	0000	LSBG?	US 3620
151	SDSS J030501.49+002304.4	411 51817 556	17.73	0.01956	0	0000	Int	
152	SDSS J030539.70−083905.2	458 51929 42	19.24	0.06501	0	0000	BCG	
153	SDSS J031023.95−083432.8	459 51924 253	19.00	0.05155	1	0000	BCG	
154	SDSS J031100.38−081504.3	459 51924 255	18.21	0.02970	0	0000	BCG	
155	SDSS J031133.14−000509.2	412 51931 513	17.58	0.02645	0	0000	BCG	
156	SDSS J031606.31−002618.0	412 51931 38	17.86	0.02296	0	0000	Irr	KUG 0313-006
157	SDSS J031623.98+000912.2	413 51929 391	19.53	0.20257	0	0000	BCG	
158	SDSS J032101.01−080150.3	460 51924 128	18.16	0.03396	0	0000	BCG	
159	SDSS J032343.37+003620.3	414 51901 399	16.90	0.02099	0	0000	BCG	
160	SDSS J032454.55+010609.1	414 51901 393	16.98	0.03037	0	0000	Sp	
161	SDSS J032613.63−063512.5	460 51924 592	18.93	0.16208	0	0000	BCG	
162	SDSS J032750.16+010134.8	414 51901 546	18.26	0.10882	0	0100	BCG	
163	SDSS J032853.35+003104.2	414 51901 526	17.68	0.08582	0	0000	BCG	
164	SDSS J033031.22−005846.7	415 51810 285	19.14	0.05155	0	0000	BCG	
165	SDSS J033144.26−055609.3	461 51910 445	18.72	0.24668	0	0000	BCG?	
166	SDSS J033314.45+002437.3	415 51810 486	16.33	0.04892	0	0000	BCG	
167	SDSS J033352.32−060605.5	461 51910 569	18.62	0.18253	0	0000	BCG	
168	SDSS J033526.64−003811.3	415 51810 141	18.04	0.02320	2	0000	BCG	
169	SDSS J033812.96−053225.4	462 51909 363	16.29	0.02218	0	0000	BCG	SBS 0335-057A
170	SDSS J033947.81−072541.2	462 51909 220	18.73	0.26076	0	0000	BCG	
171	SDSS J034543.94−065446.0	463 51908 299	16.91	0.03318	0	0000	Sp	
172	SDSS J034905.74−053324.8	463 51908 470	18.61	0.07329	0	0000	BCG	
173	SDSS J035257.79−050446.7	463 51908 563	17.67	0.01743	0	0010	Irr?	
174	SDSS J040937.63−051805.8	465 51910 524	19.42	0.07472	0	0000	BCG	
175	SDSS J073256.64+370449.4	431 51877 191	17.88	0.13947	3	0000	BCG?	
176	SDSS J073536.24+370628.8	431 51877 104	18.64	0.09530	0	0001	BCG	
177	SDSS J073805.76+403947.5	432 51884 332	19.56	0.06126	0	0000	Irr	

Table 1—Continued

SHOC ID[a] (1)	SDSS name (2)	Plate,MJD,Fiber (3)	r (4)	z (5)	WR[b] (6)	Trun (7)	Class (8)	Comments (9)
178	SDSS J073845.84+392736.7	432 51884 201	19.11	0.08605	0	0000	BCG	
179	SDSS J074115.84+343309.0	542 51993 269	18.85	0.14979	0	0000	BCG	
180	SDSS J074428.32+352417.6	542 51993 326	18.74	0.18628	0	0000	BCG	
181	SDSS J074724.24+404327.4	435 51882 356	17.60	0.02837	0	0000	BCG	
182	SDSS J075237.68+442202.2	436 51883 267	18.45	0.10476	0	0000	BCG	
183	SDSS J075315.84+401449.9	435 51882 145	20.16	0.15694	0	0000	BCG	
184	SDSS J075446.32+450502.7	436 51883 391	18.61	0.18359	2	0000	BCG	
185	SDSS J075715.84+452137.8	436 51883 488	20.29	0.28780	0	0000	BCG	
186	SDSS J075726.40+370443.3	543 52017 5	17.69	0.08314	0	0000	BCG	
187	SDSS J080131.44+440244.5	436 51883 20	17.61	0.01564	0	0000	Irr	
188	SDSS J080143.68+445458.3	436 51883 600	16.90	0.04909	0	0000	BCG	
189	SDSS J080147.04+435302.0	437 51869 456	19.32	0.08425	2	0000	BCG	
190	SDSS J080718.24+433647.1	439 51877 260	18.80	0.19071	0	0010	BCG	
191	SDSS J081016.56+432329.4	439 51877 86	18.41	0.06666	0	0000	BCG	
192	SDSS J081358.80+454442.3	441 51868 315	20.57	0.00192	0	0000	Sp(sa)	IC 2233, UGC 04278, CGCG 236-036
193a	SDSS J081437.20+490260.0	440 51885 151	17.60	0.00207	3	0000	Sp(sa)	NGC 2541, UGC 04284, CGCG 236-037
193b[e]	SDSS J081447.52+490400.8	440 51885 158	17.85	0.00195	1	0110	Sp(sa)	HS 0811+4913 in NGC 2541
194	SDSS J081523.76+453504.2	439 51877 613	17.24	0.01989	0	0010	BCG	HS 0811+4544
195	SDSS J081722.56+464459.6	441 51868 179	18.48	0.27966	0	0000	BCG	
196	SDSS J081829.76+453309.3	441 51868 187	17.22	0.04025	0	0000	Irr	
	SDSS J081829.76+453309.3	548 51986 324	17.22	0.04023	0	0000	Irr	
197	SDSS J081919.68+500020.5	440 51885 608	15.21	0.00179	0	1100	Sp(sa)	NGC 2552, UGC 04325, CGCG 236-042
198	SDSS J082001.68+505039.1	442 51882 223	18.66	0.21734	0	0000	BCG	
199	SDSS J082059.28+461823.4	548 51986 347	18.77	0.04864	0	0000	BCG	
	SDSS J082059.28+461823.4	441 51868 100	18.77	0.04871	0	0000	BCG	
200	SDSS J082234.56+502626.8	442 51882 168	17.54	0.02426	0	0000	Sp	
201	SDSS J082303.12+522334.4	442 51882 413	16.75	0.03392	0	0000	BCG	
202	SDSS J082353.52+484650.5	443 51873 217	18.40	0.09373	0	0000	BCG	
203	SDSS J082530.72+504804.3	442 51882 156	18.80	0.09691	2	0000	BCG	
204	SDSS J082604.80+455807.3	548 51986 503	14.84	0.00718	0	0010	Sp(sa)	UGC 04393, KUG 0822+461, CGCG 237-001
205	SDSS J082621.12+472812.3	441 51868 634	16.91	0.03784	0	0000	BCG	
206a	SDSS J082718.00+460157.3	549 51981 281	16.46	0.00734	0	0000	BCG	
206b	SDSS J082718.00+460203.1	548 51986 517	15.60	0.00719	0	0000	BCG	
207	SDSS J082922.08+462445.7	548 51986 546	18.51	0.01500	0	0000	BCG	
	SDSS J082922.08+462445.7	549 51981 270	18.51	0.01502	0	0000	BCG	
208	SDSS J083108.16+493159.1	443 51873 542	18.20	0.05212	0	1001	BCG	

Table 1—Continued

SHOC ID[a] (1)	SDSS name (2)	Plate,MJD,Fiber (3)	r (4)	z (5)	WR[b] (6)	Trun (7)	Class (8)	Comments (9)
209	SDSS J083216.56+493943.2	443 51873 591	18.50	0.08017	0	0000	BCG	
210	SDSS J083240.08+515946.6	444 51883 209	18.53	0.20918	0	0000	BCG	
211	SDSS J083313.20+542222.8	446 51899 352	19.29	0.10386	0	0000	BCG	
212	SDSS J083327.36+464349.4	549 51981 512	18.38	0.04682	0	0000	BCG	
213	SDSS J083350.16+454933.6	549 51981 90	18.91	0.18826	2	0000	BCG	
214	SDSS J083440.08+480540.9	549 51981 447	19.63	0.34259	0	0000	BCG?	
215	SDSS J083511.04+480314.7	550 51959 240	16.08	0.04127	0	0000	BCG	
216	SDSS J083517.04+533211.0	446 51899 283	17.49	0.06813	0	0000	BCG	
217a	SDSS J083743.44+513830.1	445 51873 404	17.55	0.00244	3	0000	Sp(sa)	MRK 0094, SBS 0834+518 in UGC 04499
217b	SDSS J083747.76+513838.0	444 51883 41	19.24	0.00226	0	0000	Sp(sa)	UGC 04499
218	SDSS J083914.88+481518.3	550 51959 485	18.24	0.03842	0	0000	BCG	
219	SDSS J083937.68+532723.4	446 51899 249	13.93	0.00228	0	0000	Sp(sa)	UGC 04514, CGCG 263-066
220	SDSS J084030.00+470710.2	549 51981 621	18.48	0.04219	1	0000	BCG	PC 0837+4717, HS 0837+4717, US 1442
221	SDSS J084526.64+530916.2	446 51899 86	16.89	0.03066	0	0000	Irr	CGCG 264-011
222	SDSS J084527.60+530852.8	447 51877 361	17.50	0.03107	1	0010	BCG	CGCG 264-011
223	SDSS J084702.88+545039.4	446 51899 541	18.93	0.12307	0	0000	BCG	
224	SDSS J084852.56+514532.7	447 51877 172	18.33	0.05010	0	0000	BCG	
225	SDSS J084936.24+545810.5	448 51900 241	17.62	0.02613	0	0000	BCG	
226	SDSS J085201.92+010459.6	467 51901 628	18.55	0.10777	1	0010	BCG	
227	SDSS J085207.68−001117.9	468 51912 250	18.86	0.15614	0	0000	BCG	
228	SDSS J085208.40+534200.3	449 51900 356	17.13	0.04971	0	0000	Sp	
229	SDSS J085754.00+524941.1	449 51900 139	18.45	0.13514	0	0000	BCG	
230	SDSS J085756.88+013728.3	469 51913 421	18.22	0.04076	0	0000	BCG	
231	SDSS J085907.44+533759.8	449 51900 151	18.90	0.01614	0	0000	Sp(sa)	UGC 04696, CGCG 264-044
232	SDSS J085920.88+005142.2	469 51913 154	16.78	0.01312	0	0000	Irr	
233	SDSS J090047.52+574255.0	483 51924 495	18.45	0.08923	0	0000	BCG	
234	SDSS J090106.48+005418.1	469 51913 110	19.09	0.11065	0	0000	BCG	
235	SDSS J090122.80−002818.8	470 51929 246	20.40	0.18749	0	1001	BCG?	
236	SDSS J090139.84+575945.9	483 51924 594	19.13	0.08603	0	0000	Int?	
237	SDSS J090223.04+000221.3	470 51929 239	17.90	0.04056	0	0000	BCG	
	SDSS J090223.04+000221.3	469 51913 9	17.90	0.04054	0	0000	BCG	
238	SDSS J090503.60+502834.3	552 51992 181	17.72	0.09914	0	0000	BCG	
239	SDSS J090539.12+534631.0	449 51900 631	17.60	0.01359	0	0000	BCG?	
240	SDSS J090704.80+532656.7	553 51999 342	16.74	0.02985	1	0000	BCG	
241	SDSS J090760.00+503910.0	552 51992 27	17.16	0.04495	0	0000	BCG	
242	SDSS J090806.24+540007.2	450 51908 125	18.66	0.08127	0	0000	BCG	

Table 1—Continued

SHOC ID[a] (1)	SDSS name (2)	Plate,MJD,Fiber (3)	r (4)	z (5)	WR[b] (6)	Trun (7)	Class (8)	Comments (9)
243	SDSS J090850.64+552244.7	450 51908 520	17.31	0.05705	0	0000	BCG	
244	SDSS J091052.56+522756.5	553 51999 134	17.88	0.06139	2	0000	BCG	
245	SDSS J091644.16+594628.5	485 51909 306	15.51	0.01378	0	0000	BCG	MRK 0019, SBS 0912+599, CGCG 288-028
246	SDSS J091645.60+532628.6	554 52000 205	17.07	0.00742	2	0000	BCG	UGCA 154, MRK 0104, SBS 0913+536, CGCG 264-090
247	SDSS J091652.32+003114.0	472 51955 546	18.75	0.05699	3	0000	BCG	
248	SDSS J091701.92+564700.6	451 51908 428	18.53	0.08961	0	0000	BCG	
249	SDSS J091747.28+531737.3	554 52000 203	15.82	0.00763	0	0010	Irr	
250	SDSS J091759.52+015751.0	473 51929 422	17.56	0.09344	0	0000	BCG	
251	SDSS J091856.16+521339.3	553 51999 4	17.14	0.00770	0	0000	Irr	
252	SDSS J091901.92+522841.1	554 52000 114	17.45	0.03265	0	0000	BCG	
253	SDSS J092030.00+015055.5	473 51929 518	18.48	0.01677	0	0000	Irr?	
254a	SDSS J092055.92+523407.3	554 52000 190	16.02	0.00783	1	0000	BCG	MRK 1416, SBS 0917+527, KUG 0917+527
254b	SDSS J092056.16+523404.4	553 51999 602	17.63	0.00780	0	0000	BCG	MRK 1416, SBS 0917+527, KUG 0917+527
255	SDSS J092242.24+590946.0	485 51909 247	17.24	0.03009	0	0000	BCG	
256	SDSS J092635.28+582047.4	452 51911 387	20.04	0.22704	0	0000	BCG?	
257	SDSS J092918.48+002813.2	474 52000 610	19.53	0.09383	0	0000	BCG	
258	SDSS J093006.48+602653.5	485 51909 550	17.22	0.01364	3*	0000	BCG	SBS 0926+606A, KUG 0926+606A
259	SDSS J093248.72+582530.7	452 51911 487	17.86	0.04747	1	0000	BCG	SBS 0929+586
260	SDSS J093345.84+595054.9	485 51909 72	18.85	0.23096	0	0000	BCG	
261	SDSS J093402.40+551423.2	556 51991 312	17.45	0.00267	0	0000	BCG	MRK 0116, I Zw 018, I Zw 018 (SE component)
262	SDSS J093719.20+603407.3	486 51910 213	18.70	0.09509	0	0000	BCG	
263	SDSS J093813.44+542824.9	556 51991 224	17.60	0.10212	2	0000	BCG	SBS 0934+546, SBS 0934+547
264	SDSS J094137.44+020545.0	480 51989 341	21.58	0.04642	0	0001	Irr	
265	SDSS J094214.64+554336.8	556 51991 131	18.15	0.10999	0	0000	BCG	
266	SDSS J094223.04−011219.1	266 51630 209	18.92	0.14737	0	0001	BCG	
267	SDSS J094306.00+001912.7	266 51630 438	17.42	0.02490	0	0000	Irr	
268	SDSS J094330.24+020843.8	477 52026 588	17.64	0.05999	0	0000	Int	
269	SDSS J094333.84+010659.4	266 51630 407	17.50	0.05159	0	0000	BCG	
	SDSS J094333.84+010659.3	477 52026 16	17.50	0.05155	0	0000	Irr	
270	SDSS J094401.92−003832.1	266 51630 100	15.85	0.00483	3	0000	Irr	CGCG 007-025
271	SDSS J094410.80+001047.3	266 51630 474	16.59	0.01117	0	0000	Irr	
	SDSS J094410.80+001047.3	480 51989 250	16.59	0.01116	2	0000	Irr	
272	SDSS J094517.52−000147.9	480 51989 128	17.19	0.02176	0	0000	Irr	
	SDSS J094517.52−000147.9	266 51630 155	17.19	0.02171	0	0000	Irr	
273	SDSS J094630.72+553542.0	556 51991 56	17.60	0.04500	0	0000	BCG	
274	SDSS J094712.96+560607.2	556 51991 611	16.90	0.02531	0	0010	BCG	SBS 0943+563, KUG 0943+563, CGCG 265-038

Table 1—Continued

SHOC ID[a] (1)	SDSS name (2)	Plate,MJD,Fiber (3)	r (4)	z (5)	WR[b] (6)	Trun (7)	Class (8)	Comments (9)
275	SDSS J094745.36+023737.0	480 51989 578	14.23	0.00616	3	0000	Sp(sa)	UGC 05249, CGCG 035-058
	SDSS J094745.36+023737.0	481 51908 335	14.23	0.00615	0	1100	Sp(sa)	UGC 05249, CGCG 035-058
276	SDSS J094809.60+023143.9	480 51989 579	16.82	0.02054	0	0000	Int	CGCG 035-059
277	SDSS J094824.48+613956.8	486 51910 597	18.70	0.17258	0	0000	BCG	
278	SDSS J094850.88+553716.3	556 51991 7	20.19	0.26968	0	0000	BCG?	
279	SDSS J094920.88+014303.1	480 51989 552	17.72	0.17491	1	0000	BCG	
280	SDSS J094930.24+553446.9	556 51991 11	15.66	0.00535	3*	0000	BCG	UGCA 184, MRK 0022, SBS 0946+558, KUG 0946+558
281a	SDSS J094954.24+003659.7	481 51908 289	16.67	0.00656	3*	0000	Sp(sa)	VV 620, MRK 1236
281b	SDSS J094954.24+003658.6	267 51608 384	15.19	0.00632	3	0000	Sp(sa)	VV 620, MRK 1236
282	SDSS J095023.28+004229.2	480 51989 4	18.76	0.09776	0	0000	BCG	
	SDSS J095023.28+004229.2	267 51608 421	18.76	0.09767	2	0000	BCG	
283	SDSS J095226.88+021759.8	481 51908 483	18.19	0.11911	3	0000	BCG	
284	SDSS J095241.52+020758.1	481 51908 518	17.53	0.01171	0	0001	LSBG	
285	SDSS J095245.12+004505.9	267 51608 485	17.26	0.02618	0	0000	BCG	
286	SDSS J095334.80+013524.5	481 51908 180	14.82	0.00386	0	0000	Sp(sa)	NGC 3044, UGC 05311, CGCG 007-056
287	SDSS J095620.88−002429.1	268 51633 319	19.19	0.14967	0	0000	BCG?	2QZ J095620.7-002430
288	SDSS J095721.60+640220.7	487 51943 410	17.74	0.04472	0	0000	Irr?	
289	SDSS J095830.24+000242.9	268 51633 200	17.55	0.00654	0	0000	LSBG	
290	SDSS J100122.32+633630.2	487 51943 574	18.21	0.07625	0	0000	BCG	
291	SDSS J100453.76+632120.8	487 51943 583	17.56	0.06769	0	0000	BCG	
292	SDSS J100836.00−004036.6	270 51909 306	17.30	0.02129	0	0000	Irr?	
293	SDSS J101430.96+004755.0	502 51957 7	18.30	0.14692	0	0000	BCG	2QZ J101430.9+004754
	SDSS J101430.96+004755.0	270 51909 617	18.30	0.14688	1	0000	BCG	2QZ J101430.9+004754
294	SDSS J101701.92+020046.0	503 51999 273	17.76	0.05296	1	0000	BCG	
295	SDSS J101704.08+025515.4	503 51999 369	18.64	0.09128	0	0000	BCG	
296	SDSS J102004.80+011601.3	503 51999 123	16.65	0.03345	0	0000	BCG	
297	SDSS J102007.92+021903.1	503 51999 490	18.16	0.09865	1	0000	BCG	
298	SDSS J102134.08+000427.6	271 51883 595	18.19	0.05690	0	0000	BCG	
299	SDSS J102256.64−002303.2	272 51941 231	18.96	0.06364	0	0001	BCG	
300	SDSS J102319.44+024941.5	503 51999 619	18.68	0.07306	0	0000	BCG	
301	SDSS J103007.44+654756.0	489 51930 434	17.80	0.03546	0	0000	BCG	
302	SDSS J103058.80+002955.8	273 51957 428	16.93	0.02843	0	0000	Sp?	
303	SDSS J103201.68+010240.9	273 51957 442	18.98	0.10356	0	0000	BCG	
304	SDSS J103227.36+003003.1	273 51957 500	18.63	0.12841	0	0000	Int	
305	SDSS J103344.16+635317.1	489 51930 122	19.43	0.34668	0	0000	BCG?	
306	SDSS J104324.72+661538.8	489 51930 567	16.92	0.01168	0	0000	Irr	

Table 1—Continued

SHOC ID[a] (1)	SDSS name (2)	Plate,MJD,Fiber (3)	r (4)	z (5)	WR[b] (6)	Trun (7)	Class (8)	Comments (9)
307	SDSS J104455.92+004433.4	275 51910 429	18.19	0.00547	0	0000	Irr	
308	SDSS J104554.72+010405.8	275 51910 445	17.10	0.02623	3	0100	BCG	
309	SDSS J104604.32+031057.7	506 52022 563	17.76	0.12002	0	0000	Int	
310	SDSS J104642.48+022930.0	506 52022 626	17.90	0.08687	0	0000	BCG	
311	SDSS J105032.40+661654.1	490 51929 396	19.08	0.08025	0	0000	BCG	
312	SDSS J105248.72+000204.1	276 51909 197	15.15	0.00604	0	0000	BCG?	CGCG 010-041
313	SDSS J105342.48+000945.1	276 51909 490	18.62	0.10965	0	0000	BCG	
314	SDSS J105506.00+670918.3	490 51929 363	17.71	0.03286	0	0000	Irr	
315	SDSS J105639.12+671049.0	490 51929 401	16.49	0.03305	0	0000	BCG	
316	SDSS J105742.00+653539.8	490 51929 128	16.08	0.01147	3	0000	BCG	
317	SDSS J111256.16−005435.4	279 51984 293	16.78	0.03962	0	0000	BCG	
318	SDSS J112145.12−000121.0	280 51612 192	18.06	0.09903	0	0000	BCG	
319	SDSS J112335.28−011337.0	280 51612 46	17.80	0.04797	0	0000	BCG	
320	SDSS J112337.20+005854.6	281 51614 323	18.42	0.02364	0	0000	BCG	
321	SDSS J112415.60+025731.3	512 51992 334	16.49	0.02326	3	0000	BCG	
322	SDSS J112502.64−004525.4	281 51614 291	19.22	0.35848	0	0000	BCG?	
323	SDSS J112526.64+654606.9	491 51942 47	17.30	0.00370	0	0000	Irr?	
324	SDSS J112552.08−003941.7	281 51614 221	17.11	0.01875	0	0100	BCG	
325	SDSS J112742.96+641001.5	597 52059 235	16.92	0.00795	0	0000	BCG	
326	SDSS J112800.72−010736.1	281 51614 129	18.22	0.07467	0	0000	BCG	
327	SDSS J112803.60+002537.6	281 51614 499	17.66	0.02999	0	0000	BCG	
328	SDSS J112816.08+023802.9	512 51992 516	16.94	0.02280	0	0000	Irr	
329	SDSS J112938.16+031504.1	512 51992 524	16.92	0.05631	0	0000	Int	
330	SDSS J112959.28+631324.2	597 52059 210	16.69	0.00346	0	0000	LSBG(sa)	
331	SDSS J113024.48+631758.5	597 52059 207	17.51	0.04235	0	0000	Irr(sa)	
332	SDSS J113025.68−005014.5	282 51658 296	17.49	0.07588	0	0000	BCG	
333	SDSS J113303.84+651341.1	597 52059 460	19.65	0.24136	0	0000	BCG?	
334	SDSS J113341.28+634926.0	597 52059 136	17.43	0.00695	2	0000	BCG	
335	SDSS J113459.52−000104.1	282 51658 493	20.14	0.24094	0	0000	BCG?	
336	SDSS J113624.00−002948.5	282 51658 155	17.68	0.02219	0	0000	Sp	
337	SDSS J113636.96+004900.7	282 51658 532	14.78	0.00369	0	0100	Irr	UGC 06578, UM 439, CGCG 012-040
338	SDSS J113655.68+033333.4	513 51989 521	18.84	0.17477	0	0000	BCG?	
339	SDSS J113703.84+002817.2	282 51658 543	18.66	0.10587	0	0000	BCG?	
340	SDSS J114013.20−002442.0	282 51658 29	15.95	0.02201	0	0000	BCG	MRK 1303, UM 444
341	SDSS J114047.52+644710.3	597 52059 586	17.64	0.03839	0	0000	BCG	
342	SDSS J114143.44+024339.9	514 51994 391	17.36	0.02562	0	0001	Irr	

Table 1—Continued

SHOC ID[a] (1)	SDSS name (2)	Plate,MJD,Fiber (3)	r (4)	z (5)	WR[b] (6)	Trun (7)	Class (8)	Comments (9)
343	SDSS J114212.48+002002.6	283 51959 389	14.65	0.01856	3*	0000	Int	UGC 06665, MRK 1304, ARP 161, ARK 312, UM 448
344	SDSS J114306.48+680717.7	492 51955 449	17.55	0.04889	3	0000	BCG	
345	SDSS J114649.44+005345.9	283 51959 572	20.13	0.05651	0	0011	BCG	
346	SDSS J114818.24−013823.8	329 52056 529	16.13	0.01305	0	0000	BCG	UM 454, CGCG 012-085
348	SDSS J115117.04+010917.7	284 51943 408	17.26	0.04680	0	0000	BCG	UM 459
347	SDSS J115117.04+032655.9	515 52051 378	18.48	0.04636	0	0001	BCG	
349	SDSS J115133.36−022222.0	329 52056 640	16.69	0.00353	1*	0011	Irr	UM 461, SCHG 1148-020
350	SDSS J115237.20−022809.9	329 52056 633	14.70	0.00350	3*	1000	BCG?	UGC 06850, MRK 1307, UM 462
351	SDSS J115247.52−004007.6	284 51943 170	17.40	0.00464	0	0000	BCG	UM 463
352	SDSS J115411.76−010754.3	284 51943 92	17.05	0.01100	0	0000	Irr?	
353	SDSS J115559.28−010001.1	284 51943 7	16.05	0.03646	0	0000	BCG	UM 468
354	SDSS J115712.48+022827.8	516 52017 315	17.25	0.05815	3	0000	BCG?	UM 469, TOLOLO 1154+027
355	SDSS J120047.04−003612.0	285 51930 154	18.59	0.08286	0	0000	BCG	
356	SDSS J120055.68+032403.9	516 52017 403	19.69	0.08491	0	0000	BCG?	
357	SDSS J120122.32+021108.3	516 52017 178	17.45	0.00337	0	0000	LSBG	
358	SDSS J120219.68+663319.8	493 51957 284	17.87	0.03199	0	0000	BCG	
359	SDSS J120340.08+023828.2	517 52024 356	13.89	0.00418	0	0000	Sp(sa)	UGC 07035, CGCG 041-031
360	SDSS J120505.04+024329.3	517 52024 422	17.82	0.07616	0	0000	BCG	
361	SDSS J120514.64+661657.7	493 51957 254	18.86	0.16551	0	0000	BCG	
362	SDSS J120628.56+672926.5	493 51957 474	16.98	0.00775	0	0000	BCG	
363	SDSS J120821.84+661905.8	493 51957 219	17.03	0.04031	0	0000	BCG	
364	SDSS J121004.80+015540.1	517 52024 30	18.50	0.07616	0	0000	BCG	
365	SDSS J121101.44+034227.2	517 52024 603	18.81	0.04739	0	0000	BCG	
366	SDSS J121135.28−004158.4	287 52023 230	17.38	0.03503	0	0000	BCG	
367	SDSS J121203.36−003621.7	287 52023 236	15.97	0.03518	0	0000	Sp(sa)	UM 482, CGCG 013-101
368	SDSS J121214.64+000420.3	287 52023 466	15.64	0.00782	2+	0000	BCG	UM 483, MRK 1313
369	SDSS J121333.60+665053.8	493 51957 144	18.73	0.06306	0	0000	BCG	
370	SDSS J121412.48−002702.3	288 52000 303	18.08	0.03613	0	0000	BCG	
371	SDSS J122417.04+672624.0	493 51957 636	14.37	0.00439	0	0000	BCG	UGCA 280, MRK 0206, CGCG 315-036
372	SDSS J122419.68+010559.5	289 51990 369	18.43	0.03986	0	0000	BCG	UM 496
373a	SDSS J122622.56−011518.0	334 51993 365	16.70	0.00669	0	0000	Irr	UM 501
373b	SDSS J122622.80−011512.3	289 51990 210	16.74	0.00665	2	0000	Irr	UM 501
374	SDSS J122754.48−021902.3	334 51993 467	17.40	0.03098	0	0000	BCG	
375	SDSS J123436.24−020721.9	335 52000 385	17.78	0.02080	0	0000	BCG	UM 507
376	SDSS J123747.04−023159.4	335 52000 198	16.68	0.00795	0	0000	BCG?	
377	SDSS J123859.76+011507.3	290 51941 567	17.67	0.04581	0	0000	BCG	

Table 1—Continued

SHOC ID[a] (1)	SDSS name (2)	Plate,MJD,Fiber (3)	r (4)	z (5)	WR[b] (6)	Trun (7)	Class (8)	Comments (9)
378	SDSS J124035.04−011702.4	335 52000 604	18.01	0.09015	0	0000	BCG	
379	SDSS J124049.92+662420.1	494 51915 7	18.35	0.08772	0	0000	BCG	
380	SDSS J124159.28−034002.4	336 51999 289	18.20	0.00931	0	0000	BCG	
381	SDSS J124318.48−012802.5	336 51999 414	15.68	0.00562	0	0000	Irr	
382	SDSS J124450.88−021304.5	336 51999 198	17.57	0.01094	0	0000	BCG	
383	SDSS J124715.36+003806.8	292 51609 372	17.79	0.07281	0	0000	BCG	
384	SDSS J124738.88−015350.7	336 51999 559	18.66	0.08484	0	0000	BCG	
385	SDSS J124802.64+665603.1	495 51988 279	18.79	0.04932	0	0001	BCG	
386	SDSS J124832.88+032904.3	522 52024 566	18.58	0.02337	0	0010	BCG	
387	SDSS J124948.96−022756.5	336 51999 33	17.89	0.04775	0	0000	BCG	
388	SDSS J125105.76−005656.2	292 51609 84	18.35	0.19376	0	0000	BCG	
389	SDSS J125214.40+005158.3	292 51609 566	18.02	0.12651	3	0000	BCG	
390	SDSS J125236.48−020345.2	338 51694 345	16.89	0.00941	0	0000	BCG	
391	SDSS J125306.00−031258.9	337 51997 97	15.84	0.02280	3	0011	BCG	
392	SDSS J125451.12+023914.7	523 52026 480	14.48	0.00322	0	0000	Irr(sa)	NGC 4809, UGC 08034, ARP 277, VV 313a
393	SDSS J125502.88+672846.9	495 51988 466	17.41	0.02801	0	0000	BCG	
394	SDSS J125526.16−021334.1	337 51997 593	20.30	0.05186	0	0010	BCG	
395	SDSS J125544.16−005902.1	293 51689 247	17.14	0.04678	0	0000	BCG	CGCG 015-041
396	SDSS J125558.08−012057.5	338 51694 325	16.48	0.00989	0	0000	Irr(sa)	CGCG 015-042
397	SDSS J125636.72+030211.6	523 52026 501	16.80	0.06305	0	0000	BCG	
398	SDSS J125718.72−004626.3	293 51689 218	17.36	0.04669	0	0000	BCG	
399	SDSS J125808.40+015144.5	523 52026 114	16.24	0.06678	0	0000	BCG	UM 530
400	SDSS J130029.28+021502.9	523 52026 65	20.49	0.27186	0	0000	BCG?	
401	SDSS J130054.72−004152.9	293 51689 64	18.44	0.08212	0	0000	BCG	
402	SDSS J130129.76+652810.5	602 52072 324	17.23	0.02064	0	0000	BCG	
403	SDSS J130148.00+013718.6	524 52027 260	18.32	0.08543	0	0000	BCG	
404	SDSS J130211.04−000516.4	293 51689 68	20.14	0.22559	0	0000	BCG?	
405	SDSS J130240.80+010426.9	294 51986 334	16.91	0.00310	0	0010	Irr	UM 538
406	SDSS J130249.20+653449.4	602 52072 369	17.66	0.02765	0	0000	BCG	
407	SDSS J130252.08+002425.1	293 51689 625	18.25	0.02096	0	0000	BCG	UM 539
408	SDSS J130324.24−021046.9	339 51692 437	17.59	0.04675	0	0001	BCG	
409a	SDSS J130431.92−033518.0	339 51692 89	16.29	0.00460	0	0000	Sp(sa)	UGCA 322, CGCG 015-060
409b	SDSS J130432.16−033322.1	339 51692 83	17.17	0.00453	3	0000	Sp(sa)	
409c	SDSS J130437.92−033357.8	339 51692 53	17.25	0.00445	0	0000	Sp(sa)	UGCA 322, CGCG 015-060
410	SDSS J130746.80+025803.5	524 52027 600	18.25	0.05018	0	0000	BCG	
411	SDSS J130831.68+012208.0	524 52027 16	18.79	0.09589	0	0000	BCG	

Table 1—Continued

SHOC ID[a] (1)	SDSS name (2)	Plate,MJD,Fiber (3)	r (4)	z (5)	WR[b] (6)	Trun (7)	Class (8)	Comments (9)
412	SDSS J130932.88−020618.2	339 51692 622	18.02	0.13808	0	0000	BCG	
413	SDSS J131213.20+003554.8	295 51985 333	18.59	0.04811	0	0000	Sp(sa)?	
414	SDSS J131226.64−024728.9	340 51990 181	15.76	0.01332	0	0000	Sp(sa)	CGCG 016-021
415	SDSS J131412.00+010741.3	295 51985 564	17.96	0.05394	0	0000	BCG	
416	SDSS J131426.64+633311.5	602 52072 19	17.37	0.03669	0	0000	BCG	
417	SDSS J131601.44+644000.8	603 52056 346	17.57	0.03123	0	0000	Irr?	
418	SDSS J131654.48−024930.4	340 51990 67	20.29	0.18659	0	0000	BCG?	
419	SDSS J131824.96−032507.6	341 51690 256	18.40	0.12878	1	0000	BCG	
420	SDSS J131937.20+005043.9	296 51984 416	18.53	0.04766	0	0000	BCG	UM 564
421	SDSS J132139.12−013953.8	341 51690 498	17.74	0.13985	0	0000	BCG	
422	SDSS J132215.60−003754.9	296 51984 101	18.13	0.02326	0	0000	BCG	
423	SDSS J132236.96−030114.5	341 51690 141	18.54	0.04574	0	0000	BCG	
424	SDSS J132347.52−013251.9	341 51690 606	18.86	0.02254	0	0000	BCG	UM 570
425	SDSS J132627.36+642800.4	603 52056 486	17.66	0.09172	0	0000	BCG	
426	SDSS J132654.72+011346.6	297 51959 442	18.54	0.17969	0	0000	BCG	
427	SDSS J132837.44−000400.1	298 51955 307	17.77	0.01736	0	0000	BCG	
428	SDSS J132921.36−005639.1	297 51959 19	17.24	0.01356	0	0000	BCG	
429	SDSS J132947.76+003038.2	297 51959 587	17.71	0.01801	0	0000	Irr?	
430	SDSS J133303.84+624603.7	603 52056 49	20.13	0.31817	0	0001	BCG?	
431	SDSS J133649.44−001158.9	299 51671 311	18.11	0.05405	1	0000	BCG	UM 591
432	SDSS J133815.36−002354.7	299 51671 222	15.88	0.02199	0	0000	Irr	UM 595
433	SDSS J134008.88+654304.8	497 51989 198	16.18	0.04801	0	0000	BCG	
434	SDSS J134242.72+625756.1	604 52079 179	17.57	0.03183	0	0000	BCG	
435	SDSS J134404.32−010724.8	299 51671 50	18.15	0.07719	0	0000	BCG	
436	SDSS J134521.60+022544.1	530 52026 360	18.19	0.03287	0	0010	BCG	
437	SDSS J135030.72+622649.2	604 52079 7	16.82	0.00632	0	0010	Irr	
438	SDSS J135153.52+642222.4	604 52079 604	16.14	0.00588	0	0000	Irr(sa)	UGCA 375, MRK 0277, VII Zw 528
439	SDSS J135155.92+032524.3	530 52026 525	18.61	0.12954	3	0000	BCG	
440	SDSS J135236.96+000120.9	301 51942 360	17.45	0.01506	0	0000	BCG	UM 618
441	SDSS J135244.64+000753.1	301 51942 345	19.44	0.01536	0	0000	Sp(sa)	UM 619, CGCG 017-086
442	SDSS J135517.76+642625.8	498 51984 294	19.27	0.14117	0	0000	BCG	
443	SDSS J135930.48−010322.2	301 51942 81	18.42	0.02432	3	0000	BCG	
444	SDSS J135954.24+643234.0	498 51984 236	18.75	0.10200	1	0000	BCG	
445	SDSS J140018.96+010453.9	301 51942 531	18.96	0.12117	2	0000	BCG	
446	SDSS J140423.52+044304.4	582 52045 440	15.73	0.02964	0	0000	Irr?	CGCG 046-046, TOLOLO 1402+049
447	SDSS J140501.20+043126.1	582 52045 199	18.33	0.03316	0	0000	BCG	

Table 1—Continued

SHOC ID[a] (1)	SDSS name (2)	Plate,MJD,Fiber (3)	r (4)	z (5)	WR[b] (6)	Trun (7)	Class (8)	Comments (9)
448	SDSS J140655.44+655456.5	498 51984 521	17.43	0.05988	0	0000	BCG	
449	SDSS J140725.20+052837.8	582 52045 445	19.63	0.08501	0	0000	BCG	
450	SDSS J140846.80+045435.2	582 52045 547	16.16	0.01765	0	0000	BCG	TOLOLO 1406+051
451	SDSS J141012.24−005224.9	302 51688 19	17.77	0.02530	0	0000	BCG	
452	SDSS J141212.72−003645.7	302 51688 25	16.92	0.02498	0	0000	Irr	
453	SDSS J141252.32−002243.9	303 51615 310	18.43	0.09618	0	0000	BCG	
454	SDSS J141621.60+020009.1	533 51994 156	18.36	0.05454	0	0000	BCG	
455	SDSS J141808.88+011319.9	304 51957 380	19.77	0.02587	0	0000	Irr	
456	SDSS J141838.16+051817.9	583 52055 611	19.12	0.22209	0	0000	BCG?	
457	SDSS J141940.32+050906.7	584 52049 375	18.65	0.05708	0	0001	BCG	TOLOLO 1417+053
458	SDSS J142112.00+044717.2	584 52049 421	17.14	0.02642	0	0000	BCG	TOLOLO 1418+049
459	SDSS J142200.24+010213.3	304 51957 568	18.30	0.13318	0	0000	BCG	
460	SDSS J142214.40−003919.6	304 51957 12	19.40	0.10588	0	0000	BCG	
461	SDSS J142656.16+630046.0	499 51988 84	17.01	0.02098	2	0000	BCG	
462	SDSS J142714.64+005925.2	305 51613 594	16.47	0.05227	0	0000	BCG	
463	SDSS J142722.32+032508.1	585 52027 255	18.33	0.07674	0	0000	BCG	
464	SDSS J142801.92+011505.8	535 51999 297	18.49	0.02831	0	0000	BCG	
	SDSS J142801.92+011505.8	305 51613 585	18.49	0.02830	0	0000	BCG	
465	SDSS J142840.32+624449.2	499 51988 44	18.79	0.08401	0	0000	BCG	
466	SDSS J142843.20+031434.6	585 52027 241	16.90	0.02779	0	0001	Irr	
467	SDSS J143053.52+002746.3	305 51613 604	16.62	0.01335	2	0100	Irr	
468	SDSS J143124.48+011208.9	306 51637 402	17.72	0.03046	0	0001	Irr	
469	SDSS J143210.08+012551.8	535 51999 52	18.99	0.13650	0	0000	BCG	
470	SDSS J143244.88+025447.7	585 52027 49	16.45	0.00520	0	0010	Sp(sa)	TOLOLO 1430+031, CGCG 047-085
471	SDSS J143439.12+041550.5	586 52023 433	15.87	0.00573	0	0000	LSBG(sa)	UGC 09380, VIII Zw 436, CGCG 047-104
472	SDSS J143447.28+024921.0	536 52024 326	16.63	0.02840	0	0000	BCG	TOLOLO 1432+030, [BFW78] 76
473	SDSS J143553.04+043701.6	586 52023 369	18.91	0.15647	0	0000	BCG	
474	SDSS J143708.88+030249.6	536 52024 402	16.46	0.00590	0	0000	Irr	TOLOLO 1434+032
475	SDSS J143804.32+013333.5	536 52024 167	19.40	0.31232	0	0000	BCG?	
476	SDSS J143949.92−004222.9	307 51663 99	17.75	0.00603	1	0000	Sp(sa)	NGC 5705, UGC 09447, CGCG 019-076
477	SDSS J144148.48+004128.1	308 51662 326	16.55	0.00630	3	0100	Sp(sa)	UGC 09470, CGCG 019-082
478	SDSS J144205.52−005248.6	308 51662 275	19.41	0.28232	0	0000	BCG?	
479	SDSS J144246.32−002055.7	308 51662 314	16.11	0.00564	0	0000	Sp(sa)	NGC 5733, CGCG 020-002
480	SDSS J144329.04+585543.6	608 52081 255	18.00	0.03925	0	0000	BCG	
481	SDSS J144441.28+040941.7	587 52026 495	20.45	0.03876	0	0101	BCG	
482	SDSS J144458.56+004618.8	308 51662 412	19.01	0.20614	0	0000	BCG	

Table 1—Continued

SHOC ID[a] (1)	SDSS name (2)	Plate,MJD,Fiber (3)	r (4)	z (5)	WR[b] (6)	Trun (7)	Class (8)	Comments (9)
483	SDSS J144610.32+033921.5	587 52026 155	18.15	0.16732	0	0000	BCG?	
484	SDSS J144620.64−010520.1	308 51662 130	18.64	0.02893	0	0000	Irr(sa)	
485	SDSS J144709.36−004425.8	308 51662 175	18.50	0.04281	0	0000	BCG	
486	SDSS J144805.28−011057.7	308 51662 81	16.91	0.02743	3	0000	BCG	
487	SDSS J145147.04−005643.7	309 51994 288	18.36	0.04322	1	0001	BCG?	
488	SDSS J145424.48+035925.1	588 52045 483	18.78	0.22202	0	0000	BCG?	
489	SDSS J145533.60+003657.3	309 51994 489	18.25	0.07533	0	0000	BCG	
490	SDSS J145700.48+600947.8	611 52055 289	18.84	0.09454	0	0000	BCG	
491	SDSS J145814.64+020652.1	539 52017 356	16.81	0.03443	0	0000	Irr(sa)	
492	SDSS J145917.76+025221.0	589 52055 250	18.95	0.12103	0	0000	BCG	
493	SDSS J150046.08+033449.0	589 52055 221	18.78	0.10202	0	0000	BCG	
494	SDSS J150311.76+013430.4	539 52017 155	17.57	0.02924	0	0000	BCG	
495	SDSS J150339.36+035051.6	589 52055 483	18.05	0.05487	0	0000	BCG	
496a	SDSS J150355.68+002555.6	311 51665 352	16.55	0.00533	0	0000	LSBG(sa)	
496b	SDSS J150356.16+002546.6	310 51990 487	16.89	0.00535	0	0000	LSBG(sa)	
497	SDSS J150356.88−004200.2	310 51990 136	18.97	0.14130	0	0000	BCG	
498	SDSS J151045.36+033038.4	590 52057 200	17.29	0.04253	0	0000	BCG	
499	SDSS J151047.28−002054.0	311 51665 230	15.98	0.00724	0	0000	Sp(sa)	CGCG 021-030
500	SDSS J151320.64−002551.8	311 51665 8	18.50	0.21804	0	0000	BCG	
501	SDSS J151625.20+582421.6	612 52079 527	19.47	0.10273	0	0000	BCG	
502	SDSS J151725.92−000805.4	312 51689 508	17.06	0.05293	3	0000	Irr	
503	SDSS J152228.80+033431.2	592 52025 412	18.32	0.10526	0	0000	BCG	
504	SDSS J152446.56+030142.1	592 52025 161	18.46	0.09023	0	0000	BCG	
505	SDSS J152450.16+030453.2	592 52025 177	16.99	0.00589	0	0000	BCG	
506	SDSS J152542.96+001406.2	313 51673 516	18.46	0.08186	0	0000	BCG	
507	SDSS J152721.84−002347.3	313 51673 147	17.95	0.05420	0	0000	BCG	
508	SDSS J152830.72+001740.1	313 51673 638	18.90	0.11364	0	0000	BCG	
509	SDSS J153258.32+004100.1	363 51989 532	18.40	0.07368	0	0000	BCG	
510	SDSS J153335.76+035230.4	593 52026 505	17.88	0.01871	0	0000	BCG	
511	SDSS J153647.28+035216.5	593 52026 589	16.46	0.03408	0	0000	Sp	
512	SDSS J153905.04+033817.8	593 52026 569	16.82	0.01276	0	0000	BCG	
513	SDSS J154054.24+565139.2	617 52072 464	16.81	0.01140	3	0000	Irr(sa)	
514	SDSS J154108.40+032029.4	594 52045 364	19.80	0.31013	0	0000	BCG?	
515	SDSS J154218.72+002838.4	342 51691 352	16.55	0.00653	2	0000	Irr(sa)	UGC 09979, DDO 201, CGCG 022-031
	SDSS J154218.72+002838.4	315 51663 594	16.55	0.00656	0	0000	Irr(sa)	UGC 09979, DDO 201, CGCG 022-031
516	SDSS J154337.20−000608.1	342 51691 319	20.20	0.34903	0	0000	BCG?	

Table 1—Continued

SHOC ID[a] (1)	SDSS name (2)	Plate,MJD,Fiber (3)	r (4)	z (5)	WR[b] (6)	Trun (7)	Class (8)	Comments (9)
517	SDSS J154348.72+571359.5	617 52072 409	15.43	0.01352	0	0000	Sp(sa)	UGC 10002, SBS 1542+573B
518	SDSS J154654.48+030902.2	594 52045 493	18.87	0.20884	0	0010	BCG	
519	SDSS J155434.56+540220.4	619 52056 320	17.45	0.02230	0	0000	BCG	
520	SDSS J155644.40+540328.8	619 52056 278	19.36	0.06312	0	0000	BCG	
521	SDSS J155833.84+524243.5	618 52049 14	18.14	0.05299	0	0000	BCG	
522	SDSS J155957.36+004741.1	344 51693 321	19.67	0.24688	0	0000	BCG?	
523	SDSS J160131.68+491440.9	622 52054 337	17.69	0.02076	0	0000	LSBG	
524	SDSS J160429.76+000605.6	344 51693 495	18.08	0.05090	0	0000	BCG	
525	SDSS J160819.68+515039.1	623 52051 337	17.40	0.04337	0	0000	BCG	
526	SDSS J160842.48+491049.4	622 52054 445	16.87	0.04319	1	0000	BCG	SBS 1607+493, HS 1607+4918
527	SDSS J160951.84+535035.5	621 52055 624	18.85	0.06408	0	0000	BCG	
528	SDSS J161031.44+522306.0	623 52051 396	18.72	0.03911	0	0000	BCG	
529	SDSS J161111.52+482003.8	622 52054 135	14.98	0.00949	0	0000	BCG	HS 1609+4827
530	SDSS J161156.40+532630.1	621 52055 618	18.20	0.10195	0	0000	BCG	
531	SDSS J161243.44−002427.7	346 51693 270	17.50	0.07617	0	0000	BCG	
532	SDSS J161633.84−003519.9	346 51693 254	15.79	0.01643	0	0000	BCG?	CGCG 023-030
533	SDSS J162150.64+003509.3	364 52000 384	18.27	0.09805	0	0000	BCG	
534	SDSS J162215.84+003913.5	346 51693 624	17.46	0.04820	0	0000	Irr?	
535	SDSS J162249.92+450417.0	626 52057 340	18.06	0.01047	0	0000	Irr	
536	SDSS J162410.08−002202.5	364 52000 187	16.89	0.03133	3	0000	BCG	
537	SDSS J162535.52−010116.6	364 52000 129	18.63	0.05020	0	0000	BCG	
538	SDSS J163006.96−001810.8	364 52000 66	18.76	0.05416	0	0000	BCG	
539	SDSS J163012.72−005408.6	348 51671 297	18.67	0.16212	0	0000	BCG	
540	SDSS J163046.32+002444.5	364 52000 627	18.34	0.16249	0	0000	BCG	
541	SDSS J163107.20+005324.6	348 51671 331	17.65	0.03314	0	0000	Irr	
542	SDSS J163644.88+430729.6	628 52083 371	17.42	0.03098	0	0000	LSBG	
543	SDSS J163843.44+435202.6	629 52051 261	18.12	0.01541	0	0000	Irr	
544	SDSS J163854.00+421127.2	628 52083 195	21.46	0.02738	0	0000	Irr	
545	SDSS J164235.52+422349.5	628 52083 555	18.00	0.15106	0	0000	BCG	
546	SDSS J164359.28+443632.7	629 52051 497	18.12	0.05247	0	0000	BCG	
547	SDSS J164421.36+423042.4	628 52083 594	18.50	0.12840	0	0000	BCG	
548	SDSS J164519.44+400945.0	630 52050 395	17.08	0.03879	0	0000	Int	HS 1643+4015
549	SDSS J164645.12+413208.8	631 52079 307	17.59	0.03235	0	0000	LSBG	HS 1645+4137
550	SDSS J164734.32+402004.2	630 52050 463	17.16	0.02841	0	0000	BCG	HS 1645+4025
551	SDSS J165241.52+630134.6	349 51699 226	17.29	0.01007	0	0000	LSBG	
552	SDSS J165711.28+401915.6	633 52079 336	17.66	0.04077	0	0000	Sp	

Table 1—Continued

SHOC ID[a] (1)	SDSS name (2)	Plate,MJD,Fiber (3)	r (4)	z (5)	WR[b] (6)	Trun (7)	Class (8)	Comments (9)
553	SDSS J165730.00+384123.2	633 52079 300	16.56	0.00686	0	0000	BCG	HS 1655+3845
554	SDSS J165757.36+383414.1	633 52079 288	17.54	0.06122	0	0000	BCG	
555	SDSS J170022.08+595333.7	353 51703 345	18.76	0.05710	0	0000	BCG	
556	SDSS J170201.44+604746.3	351 51780 212	17.22	0.12568	0	0000	BCG	
557	SDSS J170309.60+612737.4	351 51780 178	16.93	0.01984	2	0100	Irr	CGCG 299-048
558	SDSS J170328.08+594326.0	353 51703 430	17.88	0.01762	0	0010	Sp(sa)	UGC 10687, CGCG 299-049
559	SDSS J170517.76+593546.6	353 51703 479	18.55	0.10896	0	0000	BCG	
560	SDSS J170613.92+644917.0	350 51691 396	18.69	0.07932	0	0000	BCG	
561	SDSS J170649.20+594629.2	353 51703 486	17.95	0.07889	0	0000	BCG	
562	SDSS J170911.04+632940.2	352 51694 347	18.34	0.07946	0	0000	BCG	
563	SDSS J170912.72+604950.1	351 51780 47	16.52	0.04714	0	0000	Irr	SBS 1708+608, SBS 1708+609, KAZ 453
564	SDSS J170922.56+614851.1	351 51780 600	18.58	0.18057	0	0000	BCG	
565	SDSS J171212.00+650248.4	350 51691 500	18.59	0.14530	0	0000	BCG	
566	SDSS J171554.24+612139.9	351 51780 37	16.72	0.01290	0	0000	Sp(sa)	
567	SDSS J171941.04+611831.3	354 51792 437	16.51	0.01174	0	0000	Sp(sa)	
568	SDSS J171942.72+632300.9	352 51694 515	17.75	0.06965	0	0000	BCG	
569	SDSS J172000.96+602931.5	354 51792 275	16.93	0.02148	0	0000	Irr?	
570	SDSS J172009.84+542133.1	367 51997 125	20.32	0.29382	0	0000	BCG?	
571a	SDSS J172437.44+562837.9	367 51997 561	16.76	0.02831	0	0000	BCG	HS 1723+5631A
571b	SDSS J172438.16+562838.6	358 51818 311	17.22	0.02853	0	0000	BCG	HS 1723+5631B
572	SDSS J172524.96+603744.0	354 51792 177	18.29	0.02081	0	0000	BCG	
573	SDSS J172706.24+594902.2	354 51792 85	19.74	0.34708	0	0000	BCG?	
574	SDSS J172716.08+600030.2	354 51792 98	16.53	0.01047	3	0000	Sp(sa)	NGC 6381, UGC 10871, KUG 1726+600B
575	SDSS J172906.48+565319.3	358 51818 472	17.28	0.01577	3	0000	BCG	HS 1728+5655
576	SDSS J173021.84+571531.6	358 51818 403	18.83	0.14502	0	0000	BCG?	
577	SDSS J173126.64+591150.2	366 52017 541	20.23	0.23283	0	0000	BCG?	
578	SDSS J173316.32+601241.0	354 51792 63	19.09	0.09319	0	0000	BCG	
579	SDSS J173501.20+570308.6	358 51818 504	17.61	0.04733	3	0000	BCG	HS 1734+5704
580	SDSS J173548.72+575734.5	366 52017 3	18.74	0.14289	0	0000	BCG?	
581	SDSS J174327.60+544320.2	360 51780 622	20.27	0.21405	0	0000	BCG?	
582	SDSS J203559.76−060233.9	634 52164 308	17.09	0.02807	0	0000	BCG	
583	SDSS J205430.96−061739.6	636 52176 439	17.38	0.04233	0	0000	Sp	
584	SDSS J210114.40−055510.3	637 52174 399	18.89	0.19620	0	0000	BCG?	
585	SDSS J210415.60−060517.4	637 52174 526	16.36	0.02619	0	0000	Irr	
586	SDSS J210501.44−062238.8	637 52174 523	18.47	0.14273	0	0000	BCG?	
587	SDSS J210632.40−073050.0	637 52174 31	18.75	0.13571	0	0000	BCG?	

Table 1—Continued

SHOC ID[a] (1)	SDSS name (2)	Plate,MJD,Fiber (3)	r (4)	z (5)	WR[b] (6)	Trun (7)	Class (8)	Comments (9)
588	SDSS J211527.12−075951.3	639 52146 242	18.66	0.02832	0	0000	Irr(sa)	
589	SDSS J211720.88−074641.5	639 52146 182	18.43	0.04819	0	0000	BCG	
590	SDSS J211902.16−074226.8	639 52146 143	18.26	0.08954	0	0000	BCG	
591	SDSS J211942.48−073224.4	640 52178 320	17.25	0.00956	0	0000	LSBG	
592	SDSS J212332.64−074831.1	640 52178 267	17.94	0.02799	0	0000	BCG	
593	SDSS J212340.56−074904.7	640 52178 261	16.63	0.02806	0	0000	BCG	
594	SDSS J213236.24−082914.9	641 52199 213	17.57	0.06531	0	0000	BCG	
595	SDSS J230703.84+011311.2	381 51811 370	18.14	0.12592	1	0000	BCG?	
596	SDSS J230805.52+003423.2	381 51811 428	18.04	0.06996	0	0000	BCG	
597	SDSS J231042.00−010948.4	381 51811 86	17.52	0.01239	0	0000	Irr	
598	SDSS J231329.52−004807.2	381 51811 12	17.93	0.05483	0	0000	BCG	
599	SDSS J231330.00−004823.6	382 51816 286	18.85	0.05488	0	0000	BCG	
600	SDSS J231729.52−005104.1	382 51816 134	17.43	0.02986	0	0000	Irr	
601	SDSS J232035.28−005251.2	383 51818 290	16.41	0.01457	0	0100	BCG?	UM 158
	SDSS J232035.28−005251.2	382 51816 1	16.41	0.01459	0	0000	BCG?	UM 158
602	SDSS J232207.92−000314.2	383 51818 266	16.87	0.05677	0	0001	Int	
603	SDSS J232255.92−101518.3	645 52203 106	17.74	0.08166	0	0000	BCG	
604	SDSS J232812.24−010345.7	383 51818 11	17.42	0.00862	0	0010	LSBG	
605	SDSS J232936.48−011056.9	384 51821 281	18.42	0.06601	0	0000	BCG	UM 162
606	SDSS J233245.36−003906.8	384 51821 189	17.44	0.04344	0	0000	BCG	
607	SDSS J233414.88+002907.2	384 51821 488	17.94	0.02387	0	0000	BCG	
608	SDSS J233646.80+003724.4	385 51877 341	16.19	0.00884	0	0000	LSBG	
609	SDSS J234910.56+010558.8	386 51788 409	19.32	0.07292	0	0100	BCG	
610	SDSS J235347.76+005402.2	386 51788 573	19.24	0.22353	0	0000	BCG?	
611	SDSS J235449.44−105842.2	649 52201 117	17.95	0.12081	0	0000	BCG	
612	SDSS J235604.80−085423.4	649 52201 637	18.83	0.16848	0	0000	BCG?	

[a]The number of individual galaxy in the SHOC catalog. Letters 'a' and 'b' indicate separate regions within the same galaxy

[b]The Wolf-Rayet galaxy flag. "1", "2", or "3" mean that either only the "blue" bump, or only the "red" bump, or both bumps are detected. Asterisks identify WR galaxies from SCP99. Crosses identify WR galaxies from the list of suspected WR galaxies in SCP99.

[c]SHOC 11 was selected as a Sy 2 galaxy (LBQS 0018+0036) by Lewis, McAlpine, & Weedman (1979), and is assigned

as an AGN in NED. However, from both Terlevich et al. (1991) (UM 228) and from SDSS data this is classified as an H II galaxy.

[d] SHOC 56 is not UM 311 as identified in NED, but is another superassociation in the spiral galaxy NGC 0450 as seen by comparing SDSS images with those in McAlpine & Lewis (1978).

[e] SHOC 193b (SDSS J081447.52+490400.8) has very strong lines. This is a giant H II region on the periphery of a nearby SA(s)cd galaxy NGC 2541, also known as HS 0811+4913 (Pustilnik et al. 1999). For this object, both [O III] $\lambda\lambda$ 4959 and 5007Å were truncated, while Hα and Hβ are not. To correct an oxygen abundance the intensity ratio [O III] λ 5007 Å/Hβ = 7.37 was taken from Pustilnik et al. (1999).

Table 2. Observed Relative Emission Line Fluxes and Errors[a] .

SHOC[b] ID (1)	[O II] 3727 Å (2)	H10 3798 Å (3)	H9 3835 Å (4)	Hδ 4101 Å (5)	Hγ 4340 Å (6)	[O III] 4363 Å (7)	Hβ 4861 Å (8)	[O III] 4959 Å (9)	[O III] 5007 Å (10)	Hα 6563 Å (11)	[S II] 6716 Å (12)	[S II] 6731 Å (13)	[O III] 7320+7330 Å (14)	W(Hβ)[c] 4861 Å (15)	F(Hβ)[d] 4861 Å (16)
1	191.3± 3.7	···	1.5±1.0	17.4±1.3	38.2±1.2	2.4±0.8	100.0±1.3	113.0± 1.8	341.5± 4.7	428.4± 5.8	43.8± 1.4	31.7± 1.3	6.1±2.0	50.6	3.93
2	174.7± 2.9	2.1±0.7	2.5±0.8	21.1±1.4	43.2±0.7	7.2±0.5	100.0±0.6	181.4± 1.3	556.1± 3.6	305.3± 2.0	17.7± 0.8	13.7± 0.8	5.1±1.1	87.6	9.05
3	234.0± 5.3	1.4±0.8	4.4±1.1	27.7±1.2	48.9±1.1	7.6±0.9	100.0±1.1	188.0± 2.6	560.3± 7.0	289.0± 3.4	17.3± 1.0	12.8± 1.0	3.8±1.1	67.4	6.32
4	278.0± 9.1	···	···	14.2±3.4	38.0±1.9	3.9±1.5	100.0±2.3	99.8± 2.8	304.7± 7.3	307.0± 7.2	35.6± 1.4	24.7± 1.1	9.7±2.8	22.8	4.36
5	262.8± 6.0	···	···	19.3±1.6	41.7±1.3	3.8±0.9	100.0±1.3	150.7± 2.2	460.7± 6.4	304.2± 4.1	28.5± 0.7	18.8± 0.6	5.6±0.7	41.8	10.85
6	262.1± 6.0	···	2.9±1.5	23.3±2.3	46.7±1.3	1.7±0.9	100.0±1.3	137.1± 1.9	411.1± 5.5	288.0± 3.8	23.3± 0.7	17.3± 0.7	2.8±0.6	51.4	5.02
7	238.5± 6.3	···	3.5±2.0	24.3±2.9	45.8±2.1	3.2±1.6	100.0±1.6	84.4± 1.7	247.9± 4.2	345.6± 5.9	41.1± 1.7	30.1± 1.6	2.5±1.2	50.3	3.73
8	···	1.8±0.7	1.7±0.8	16.8±1.3	40.5±0.7	3.8±0.5	100.0±0.8	140.3± 1.3	434.5± 3.9	346.4± 2.9	32.5± 0.4	23.6± 0.4	6.2±0.4	55.9	14.78
9	···	···	···	14.5±2.4	37.5±1.5	2.9±1.1	100.0±1.4	110.2± 1.7	340.3± 4.9	332.3± 4.7	36.7± 0.8	25.6± 0.7	4.9±0.8	29.7	6.93

[a]Observed flux ratios $100 \cdot I(\lambda)/I(H\beta)$ are shown.

[b]The number of individual galaxy in the SHOC catalog. Letters ‘a’ and ‘b’ indicate separate regions within the same galaxy.

[c]Equivalent width for the Hβ line in emission.

[d]Flux for the Hβ line is in units of 10^{-15} erg $s^{-1}cm^{-2}$.

Note. — The complete version of this table is in the electronic edition of the Journal. The printed edition contains only a sample.

Table 3. Corrected Relative Emission Line Fluxes and Errors[a] .

SHOC[b] ID (1)	[O II] 3727 Å (2)	H10 3798 Å (3)	H9 3835 Å (4)	Hδ 4101 Å (5)	Hγ 4340 Å (6)	[O III] 4363 Å (7)	Hβ 4861 Å (8)	[O III] 4959 Å (9)	[O III] 5007 Å (10)	Hα 6563 Å (11)	[S II] 6716 Å (12)	[S II] 6731 Å (13)	[O III] 7320+7330 Å (14)	C(Hβ)[c] (15)	EW(abs)[d] Å (16)
1	263.4± 5.5	···	6.8± 5.9	25.7± 2.5	46.9±1.9	2.7±1.0	100.0±2.1	107.2± 1.8	319.9± 4.5	288.1± 4.5	28.5± 1.0	20.6± 0.9	3.6±1.2	0.490±0.018	1.400±0.397
2	175.7± 3.1	7.6± 3.5	8.2± 3.5	26.5± 2.0	46.9±1.0	7.0±0.5	100.0±1.0	174.3± 1.2	533.4± 3.5	282.9± 2.3	16.2± 0.8	12.5± 0.8	4.6±1.0	0.060±0.009	3.300±0.439
3	239.0± 5.5	1.4± 1.1	4.5± 1.4	28.1± 1.3	49.4±1.2	7.6±0.9	100.0±1.6	187.7± 2.6	559.0± 7.0	282.5± 3.7	16.9± 1.0	12.5± 0.9	3.7±1.0	0.030±0.015	0.000±0.278
4	249.5± 9.5	···	···	24.7± 8.2	44.6±3.9	3.5±1.5	100.0±4.7	89.6± 2.8	273.5± 7.3	282.9± 8.3	32.0± 1.4	22.2± 1.2	8.7±2.8	0.000±0.030	2.600±0.667
5	251.4± 6.2	···	···	25.9± 2.9	46.6±2.2	3.6±0.9	100.0±2.3	142.1± 2.2	434.0± 6.4	286.1± 4.5	26.4± 0.7	17.5± 0.6	5.2±0.7	0.020±0.018	2.500±0.499
6	259.6± 6.2	···	4.2± 2.7	24.5± 3.0	47.4±1.9	1.7±0.9	100.0±2.1	135.8± 1.9	407.2± 5.5	285.9± 4.2	23.0± 0.8	17.2± 0.7	2.8±0.6	0.000±0.017	0.500±0.577
7	286.8± 7.8	···	4.1± 3.3	27.4± 3.9	49.5±2.9	3.4±1.7	100.0±2.7	83.2± 1.7	242.9± 4.2	283.3± 5.4	33.2± 1.4	24.3± 1.3	1.9±0.9	0.260±0.022	0.000±0.697
8	···	8.8± 4.8	8.9± 5.8	24.9± 2.4	47.5±1.2	3.8±0.5	100.0±1.4	131.1± 1.3	404.3± 3.8	286.1± 2.8	26.2± 0.4	19.1± 0.3	4.8±0.3	0.190±0.011	3.300±0.379
9	···	···	···	26.3± 6.0	46.7±3.2	2.7±1.1	100.0±3.0	98.1± 1.7	302.1± 4.9	286.0± 5.1	30.7± 0.8	21.4± 0.7	4.0±0.7	0.080±0.019	3.550±0.608

[a]Corrected intensity ratios 100·I(λ)/I(Hβ) are shown.

[b]The number of individual galaxy in the SHOC catalog. Letters 'a' and 'b' indicate separate regions within the same galaxy.

[c]Extinction coefficient.

[d]Equivalent width of underlying absorption in Balmer hydrogen lines.

Note. — The complete version of this table is in the electronic edition of the Journal. The printed edition contains only a sample.

Table 4. Oxygen Abundances in SHOC galaxies

SHOC ID (1)	T_e(**O** III) **K (2)**	T_e(**O** II) **K (3)**	N_e(**S** II) **cm^{-3} (5)**	**O$^+$/H$^+$ $\times10^5$ (6)**	**O^{++}/H$^+$ $\times10^5$ (7)**	**12+log(O/H) (8)**
1	**10900±1300**	**11500±1400**	**37± 48**	**5.57± 2.02**	**8.47± 3.18**	**8.15± 0.12**
2	**12800± 400**	**12600± 400**	**127± 110**	**2.68± 0.23**	**8.72± 0.73**	**8.06± 0.03**
3	**13000± 600**	**12700± 700**	**64± 97**	**3.54± 0.46**	**8.90± 1.13**	**8.09± 0.04**
4	**12700±2000**	**12600±2300**	**<10**	**3.81± 1.76**	**4.57± 2.09**	**7.92± 0.14**
5	**10900±1000**	**11500±1100**	**<10**	**5.32± 1.42**	**11.49± 3.17**	**8.23± 0.09**
6	**8800±1300**	**10100±1400**	**75± 62**	**9.25± 4.48**	**22.64± 12.34**	**8.50± 0.18**
7	**13100±2600**	**12800±3000**	**55± 70**	**4.15± 2.35**	**3.76± 2.09**	**7.90± 0.17**
8	**11300± 500**	**11800± 600**	**47± 28**	**4.28± 0.63**	**9.47± 1.34**	**8.14± 0.05**
9	**11100±1600**	**11600±1800**	**<10**	**4.08± 1.86**	**7.52± 3.34**	**8.06± 0.14**
10	**12700±1500**	**12500±1700**	**242± 97**	**5.14± 1.74**	**5.48± 1.84**	**8.03± 0.10**

Note. — The complete version of this table is in the electronic edition of the Journal. The printed edition contains only a sample.

Table 5. 12+log(O/H) from SDSS data and from other sources

SHOC ID (1)	Name (2)	SDSS (3)	Others (4)	References (5)	Comment[a] (6)
22	**HS 0029+1443**	**8.07±0.02**	**7.96±0.07**	**9**	**N**
220	**HS 0837+4717**	**7.62±0.01**	**7.63±0.03**	**6**	**Y**
254a	**MRK 1416**	**7.92±0.02**	**7.86±0.02**	**5**	**N**
254b	**MRK 1416**	**7.81±0.04**	**7.86±0.02**	**5**	**N**
261	**MRK 0116 (SE)**	**7.25±0.04**	**7.19±0.02**	**4**	**N**
261	**MRK 0116 (SE)**	**7.25±0.04**	**7.26±0.05**	**9**	**N**
280	**MRK 0022**	**8.02±0.02**	**8.00±0.01**	**5**	**N**
281a	**MRK 1236**	**8.10±0.01**	**8.07±0.03**	**2**	**N**
282b	**MRK 1236**	**8.08±0.04**	**8.07±0.03**	**2**	**N**
337	**UM 439**	**8.07±0.05**	**8.08±0.02**	**7**	**N,0100**
343	**UM 448, MRK 1304**	**8.06±0.08**	**7.99±0.04**	**5**	**N**
343	**UM 448, MRK 1304**	**8.06±0.08**	**8.08±0.03**	**7**	**N**
349	**UM 461**	**7.85±0.01**	**7.78±0.03**	**5**	**N**
349	**UM 461**	**7.85±0.01**	**7.80±0.06**	**1**	**N,0011**
350	**UM 462**	**7.97±0.02**	**7.95±0.01**	**5**	**N,1000**
351	**UM 463**	**7.82±0.02**	**7.75±0.03**	**7**	**N**
354	**UM 469**	**8.00±0.04**	**8.00±0.08**	**1**	**N**
354	**UM 469**	**8.00±0.04**	**8.09±0.05**	**7**	**N**
	HS 0822+3542	**7.45±0.02**[b]	**7.44±0.06**	**8**	**N**
	A1116+517	**7.51±0.04**[b]	**7.51±0.04**	**3**	**N**
	MRK 0116 (NW)	**7.13±0.03**[b]	**7.16±0.01**	**4**	**N**
	MRK 0116 (NW)	**7.13±0.03**[b]	**7.17±0.04**	**9**	**N**

[a]**Oxygen abundances calculated with (Y) or without (N) [O II] λ3727 Å; the set of numbers correspond to the truncation flag from column 7 in Table 1.**

[b]**Abundances were taken from Kniazev et al. (2003).**

References. — (1) Denicoló, Terlevich, & Terlevich (2002); (2) Guseva, Izotov, &

Thuan (2000); (3) Guseva et al. (2003); (4) Izotov & Thuan (1998); (5) Izotov & Thuan (1999); (6) Kniazev et al. (2000); (7) Masegosa, Moles, & Campos-Aguilar (1994); (8) Pustilnik et al. (2003b); (9) Skillman & Kennicutt (1993).

Table 6. General Parameters of Strong Narrow-Line AGN and LINERs from SDSS DR1

#	SDSS name (1)	Plate,MJD,Fiber (2)	r (3)	z (4)	Type (5)	Comments (6)
1	SDSS J002119.69+003801.7	390 51900 454	18.84	0.23382	LINER	
2	SDSS J002531.46−104022.0	653 52145 149	18.26	0.30349	AGN	
3	SDSS J002837.83−095953.7	654 52146 353	16.48	0.04961	LINER	
4	SDSS J002916.68+151101.6	417 51821 396	19.29	0.21595	LINER	
5	SDSS J003356.44−004521.6	392 51793 251	17.47	0.17380	AGN	
6	SDSS J004759.78+134433.7	419 51879 8	15.87	0.05657	AGN	
7	SDSS J005051.46−084100.0	657 52177 327	17.37	0.09654	AGN	
8	SDSS J005800.82+002845.2	395 51783 469	16.65	0.08018	LINER	
9	SDSS J010119.78−004647.9	395 51783 65	19.05	0.19916	LINER	
10	SDSS J010448.84−005341.7	396 51816 217	16.51	0.06487	LINER	
11	SDSS J011147.42+002020.9	397 51794 484	18.43	0.25399	LINER	
12	SDSS J012055.92−084945.4	661 52163 337	19.25	0.12464	AGN	
13	SDSS J012454.14+005935.5	399 51817 441	19.49	0.23181	LINER	
14	SDSS J015343.82+001101.8	402 51793 637	16.06	0.08208	LINER	
15	SDSS J015344.33−085714.9	665 52168 507	17.44	0.16277	AGN	
16	SDSS J015643.85−100047.1	665 52168 54	19.51	0.15746	LINER	
17	SDSS J020017.90+001429.8	403 51871 599	18.44	0.07698	LINER	
18	SDSS J020225.63−010215.9	404 51812 286	18.88	0.19129	LINER	
19	SDSS J020422.32−093757.2	666 52149 93	17.70	0.19191	LINER	
20	SDSS J023414.09−002736.3	408 51821 315	17.32	0.11143	LINER	
21	SDSS J025057.46+002209.8	409 51871 548	16.17	0.04423	LINER	
22	SDSS J030257.14−082942.6	458 51929 211	16.90	0.10558	LINER	
23	SDSS J030430.41−074008.3	458 51929 179	18.03	0.15146	LINER	
24	SDSS J031428.27−072517.8	459 51924 511	17.71	0.20758	AGN	
25	SDSS J031532.54+011255.1	413 51929 325	18.91	0.20350	LINER	
26	SDSS J031752.92−005417.5	413 51929 220	16.63	0.11731	AGN	
27	SDSS J033923.16−054841.6	462 51909 444	17.22	0.08478	AGN	
28	SDSS J035440.32−063539.8	464 51908 303	19.25	0.25107	LINER	
29	SDSS J040759.86−061950.1	465 51910 185	16.77	0.12075	LINER	
30	SDSS J080339.60+441357.0	436 51883 22	18.76	0.19358	LINER	
31	SDSS J083206.24+490230.8	443 51873 537	17.27	0.09096	LINER	
32	SDSS J083354.24+514141.2	445 51873 324	16.76	0.06545	LINER	
33	SDSS J083645.12+530235.8	444 51883 558	17.97	0.13819	LINER	
34	SDSS J084135.04+010156.3	467 51901 358	17.25	0.11065	AGN	
35	SDSS J084715.60+511444.8	447 51877 134	15.11	0.02766	LINER	
36	SDSS J085114.40+004339.5	467 51901 633	20.41	0.27005	LINER	

Table 6—Continued

#	SDSS name (1)	Plate,MJD,Fiber (2)	r (3)	z (4)	Type (5)	Comments (6)
37	SDSS J085449.20+574012.7	483 51924 409	14.60	0.01427	LINER	CGCG 288-011
38	SDSS J085946.80+010812.7	469 51913 517	17.91	0.19853	LINER	
39	SDSS J091326.16+580148.3	484 51907 142	19.42	0.17089	AGN	
40	SDSS J092635.04−002603.7	474 52000 142	17.80	0.07083	AGN	
41	SDSS J092907.68+002637.1	475 51965 205	17.50	0.11731	AGN	
42	SDSS J093716.80+595308.1	485 51909 34	17.49	0.14399	AGN	
43	SDSS J094830.00+553822.5	556 51991 20	16.44	0.04524	LINER	
44	SDSS J095138.64+025911.3	481 51908 402	19.30	0.21166	AGN	
45	SDSS J095642.72+024943.3	500 51994 403	19.08	0.22951	AGN	
46	SDSS J095958.80+030223.7	500 51994 565	17.09	0.09044	LINER	
47	SDSS J101536.24+005459.4	271 51883 372	17.17	0.12031	AGN	
48	SDSS J101653.76+002857.1	271 51883 439	16.55	0.11639	AGN	
49	SDSS J102311.04−002810.8	272 51941 238	17.63	0.11263	AGN	
50	SDSS J103317.52−003754.9	273 51957 93	19.94	0.21851	AGN	
51	SDSS J105823.52−010525.8	277 51908 290	17.71	0.18702	LINER	
52	SDSS J110940.56−010118.0	278 51900 81	17.64	0.10886	LINER	
53	SDSS J111006.24−010116.5	278 51900 96	18.11	0.10951	AGN	
54	SDSS J111753.28−000026.8	279 51984 520	17.11	0.09617	LINER	
55	SDSS J113446.32+025515.7	513 51989 378	15.02	0.02867	LINER	CGCG 040-007
56	SDSS J114203.36+005135.8	283 51959 420	17.95	0.24504	LINER	
57	SDSS J115535.04−010615.7	285 51930 300	17.60	0.08572	LINER	
58	SDSS J115547.76+004852.0	284 51943 613	18.00	0.20886	AGN	
59	SDSS J122357.36−023313.1	334 51993 346	17.47	0.19861	AGN	
60	SDSS J123152.80+001033.6	289 51990 625	19.92	0.19165	LINER	
61	SDSS J123840.32−000744.0	290 51941 119	18.98	0.20463	LINER	
62	SDSS J125246.32+001454.4	292 51609 593	19.84	0.32886	LINER	
63	SDSS J130600.72+000125.0	294 51986 438	17.66	0.13813	AGN	
64	SDSS J131920.40−022535.6	341 51690 275	17.08	0.09744	LINER	
65	SDSS J134003.84+001707.0	299 51671 429	18.37	0.23520	LINER	
66	SDSS J134602.88+001649.8	299 51671 625	17.41	0.17977	AGN	
67	SDSS J135713.68−003011.6	301 51942 182	20.20	0.28056	LINER	
68	SDSS J140418.24+033716.5	582 52045 210	18.81	0.23209	LINER	
69	SDSS J140434.56−000800.4	302 51688 268	19.04	0.30341	LINER	2QZ J140434.6-000801
70	SDSS J142456.16−002233.7	305 51613 202	16.78	0.07898	LINER	
71	SDSS J142638.88+012134.1	535 51999 300	18.45	0.32882	LINER	
72	SDSS J143112.48+021036.1	535 51999 491	16.70	0.11044	LINER	
73	SDSS J144012.72+024743.5	536 52024 575	16.40	0.02975	AGN	TOLOLO 1437+030

Table 6—Continued

#	SDSS name (1)	Plate,MJD,Fiber (2)	r (3)	z (4)	Type (5)	Comments (6)
74	SDSS J144623.76+043939.9	587 52026 575	17.56	0.15722	LINER	
75	SDSS J145322.80−001642.3	309 51994 239	17.56	0.07559	AGN	
76	SDSS J145447.76+010551.4	538 52029 140	17.63	0.16350	LINER	
77	SDSS J151530.72+024503.6	591 52022 261	16.06	0.03811	LINER	
78	SDSS J151732.88+002804.9	312 51689 505	17.55	0.05216	LINER	
79	SDSS J151754.96+571158.9	612 52079 118	18.73	0.31445	LINER	
80	SDSS J154832.40−010811.6	342 51691 81	17.88	0.12155	AGN	
81	SDSS J155250.40+534108.1	618 52049 548	18.05	0.28673	LINER	
82	SDSS J160915.12+490449.4	622 52054 460	17.11	0.11113	LINER	
83	SDSS J161244.16+521954.1	621 52055 21	18.35	0.18168	LINER	
84	SDSS J161325.68+523412.0	623 52051 557	18.72	0.29833	LINER	
85	SDSS J161732.16−001701.5	346 51693 171	16.98	0.05737	LINER	
86	SDSS J163620.40−000828.4	348 51671 176	17.46	0.08748	LINER	
87	SDSS J164450.88+415546.9	628 52083 65	17.64	0.09682	LINER	
88	SDSS J165102.64+421314.1	631 52079 432	18.37	0.25374	LINER	
89	SDSS J165352.08+621149.5	351 51780 332	16.14	0.10607	LINER	
90	SDSS J170437.20+603512.4	351 51780 139	17.13	0.09744	LINER	
91	SDSS J170437.68+603506.3	353 51703 365	16.56	0.09691	AGN	
92	SDSS J170918.48+621731.5	352 51694 289	18.57	0.19112	LINER	
93	SDSS J171218.00+645906.7	350 51691 496	18.63	0.18375	LINER	
94	SDSS J205436.72−053700.3	636 52176 410	17.33	0.12502	AGN	
95	SDSS J210219.92−061109.5	637 52174 447	18.60	0.09703	LINER	
96	SDSS J213532.40−074744.4	641 52199 120	19.83	0.31100	LINER	
97	SDSS J232053.76+010559.2	382 51816 620	19.27	0.26053	LINER	
98	SDSS J234929.76−001600.5	386 51788 225	18.28	0.21991	LINER	
99	SDSS J235641.28−010456.1	387 51791 242	18.98	0.29157	LINER	

Table 7. General Parameters of Additional Strong Narrow-Line Galaxies with WR-features from SDSS DR1

# (1)	SDSS name (2)	Plate,MJD,Fiber (3)	r (4)	z (5)	WR[a] (6)	Comments (7)
1	SDSS J002837.83−095953.7	654 52146 353	16.48	0.04961	3	LINER
2	SDSS J003650.43+000201.9	392 51793 471	17.71	0.11169	3	
3	SDSS J003837.62−095217.9	655 52162 271	18.45	0.06532	3	
4	SDSS J014249.30−093626.8	664 52174 276	18.16	0.16094	1	
5	SDSS J023533.89−092147.3	455 51909 132	21.94	0.00458	3	
6	SDSS J024630.36−001431.5	409 51871 225	17.20	0.00970	1	
7	SDSS J032046.10−005100.0	413 51929 47	19.56	0.02172	2	
8	SDSS J085258.32+492733.8	551 51993 279	16.12	0.00957	3	
9	SDSS J085906.00+534537.0	449 51900 556	18.58	0.00760	3	
10	SDSS J085946.80+010812.7	469 51913 517	17.91	0.19853	3	LINER
11	SDSS J090347.76+014007.1	471 51924 239	18.41	0.24389	1	
12	SDSS J092655.92+545712.2	554 52000 599	18.06	0.04850	1	
13	SDSS J095804.80+001027.2	268 51633 475	17.64	0.16857	2	
14	SDSS J103924.48−002321.4	274 51913 187	14.88	0.01854	3	
15	SDSS J105100.72+655940.5	490 51929 279	16.85	0.03238	3	
16	SDSS J112040.56+674644.0	491 51942 456	19.45	0.05396	1	
17	SDSS J112136.24+003249.4	280 51612 440	18.35	0.22921	2	
18	SDSS J120026.16−010607.8	285 51930 42	15.87	0.00504	3	
19	SDSS J123228.08+002326.4	289 51990 627	14.24	0.00503	3	
20	SDSS J130431.20−033420.6	339 51692 84	14.72	0.00458	2	
21	SDSS J134049.20+654926.0	497 51989 184	15.41	0.04726	2	
22	SDSS J144010.80−001738.3	307 51663 111	18.24	0.00654	1	
23	SDSS J154832.40−010811.6	342 51691 81	17.88	0.12155	3	AGN
24	SDSS J161140.80+522727.0	623 52051 435	14.13	0.02946	3+	NGC 06090
25	SDSS J172715.60+600037.8	366 52017 451	17.38	0.01047	3	
26	SDSS J210219.92−061109.5	637 52174 447	18.60	0.09703	3	LINER
27	SDSS J215130.48−075557.5	644 52173 154	17.92	0.12253	3	
28	SDSS J234227.36+003757.5	385 51877 508	16.97	0.05952	2	

[a]The Wolf-Rayet galaxy flag. “1”, “2”, or “3” means that either only the “blue” bump, or only the “red” bump, or both bumps are detected. A cross identifies the WR galaxy from the list of suspected WR galaxies by SCP99.